Modelling Mass Transfer Inside Scott's Hut, Cape Evans, Antarctica

by
Glen W Mason
BE(Hons)

A thesis submitted in fulfillment
of the requirements for the
Degree of
Master of Engineering
in the
Department of Mechanical Engineering
University of Canterbury
Christchurch, New Zealand

September, 1999

ABSTRACT

Recurring moisture problems inside the historic huts, Ross Sea region, Antarctica, have been recorded over the past few decades. Particularly serious problems have been experienced at Scott's Terra Nova hut at Cape Evans, Ross Island, the focus of this study.

Logged temperature and relative humidity data were analysed for patterns and for correlation with the external weather conditions. A field trip was carried out where physical parameters of the hut were measured to enable accurate modelling of the indoor air state, along with side projects to determine pollutant infiltration. The model provided individual component mass transfers of the four main mechanisms involved, and allowed 'What if?' analysis to be performed. The model was used to determine the effects of current policy on the use of the hut and determine the sensitivity to change.

Periods of high relative humidity inside the hut were found to coincide with moisture-laden, northerly weather patterns. Visitor thoroughfare in the hut was not seen to have any lasting effect on the moisture state of the hut, although some local condensation may appear. Ice removal from under the building would remove a source of bulk moisture that has a role in many moisture transactions to the air state of the building. Some small policy changes that would help offset some human-related conditions and improve information gathered in the future have been recommended.

To Mum and Dad

who made me who I am

–

who made me!

ACKNOWLEDGEMENTS

I would like to express my great appreciation for the support and guidance offered by Dr. Alan Tucker, my academic supervisor. Special thanks go to Mr. Paul Chaplin, *Executive Officer,* and Ms. Sheridan Easdale, *Conservator/Curator*, of the Antarctic Heritage Trust for inspiring the project and providing assistance in all things Antarctic. This project would not have been possible but for the legacy of the late Dr. Trevor Hatherton, *OBE, Polar Medal, BSc, PhD, DIC, DSc, FRSNZ (1924-1992)*, whose kind bequest funded the scholarship and research.

I would also like to thank the following people for assistance offered during the course of the research:

1998/99 K282 Event Team

Mr. Lawrence Smith, *Field Leader*
Mr Chris Jacomb, *Archaeologist*
Prof. David Harrowfield, *Historian*
Ms. Sarah Clayton, *Textile Conservator*

Assistance from the Building Research Association of New Zealand (BRANZ);

Mr. Mark Bassett, *Manager, Building Physics*
Dr. Malcolm Cunningham, *Principle Scientist*
Mr. Peter Haberecht, *Senior Materials Scientist*
Mr. Paul Roberts, *Building Physicist*

And general help in many guises from;

Mr. Julian Phillips and Julian Murphy, *Electronics Technicians*
Mr. Otto Bolt, Ken Brown, and Geoff Leathwick, *Mechanical Technicians*
Mr. Murray Drake, *Christchurch City Council Building Inspector*
Mr. & Mrs. Roger and Lynda Lavers
The staff of Antarctica New Zealand, Christchurch and Scott Base, Antarctica.

TABLE OF CONTENTS

LIST OF FIGURES

LIST OF TABLES

NOMENCLATURE

Symbol	*Description*	*Unit*
A	Infiltration, air changes per hour	hr^{-1}
C	Concentration of mass	kg/m^3
c_p	Specific heat	J/kgK
D	Diffusion coefficient	m^2/s
h_c	Heat transfer coefficient	W/m^2K
h_m	Mass transfer coefficient for concentration gradient driving force	m/s
h_{mc}	Mass transfer coefficient for humidity ratio driving force	kg/m^2s
L	Effective leakage area	cm^2
μ	Degree of saturation	$0 < \mu < 1$
N	Current discrete time step	-
ϕ	Relative humidity	$0 < \phi < 1$
Δp_v	Indoor – Outdoor vapour pressure differential	kPa
p_v	Vapour pressure	kPa
Q	Airflow rate	m^3/hr
q_x	Heat flow in the x-direction	W
ρ	Density	kg/m^3
R_m	Vapour resistivity of a material	GNs/kgm
t	Temperature	ºC
T	Absolute temperature	K
τ	Time	s
Δt	Average indoor - outdoor temperature difference for the time interval of the calculation	ºC
v	Average wind speed for the time interval of interest	m/s
V	Volume of the building	m^3
W	Humidity ratio, or absolute humidity	kg_{water}/kg_{air}
$W(n)$	Time weighting coefficient	$0< W(n) <1$
Δx	Thickness of material	m

Subscript Nomenclature

Symbol	*Description*
a	Room Air
dry	Dry basis measurement
i	inside air state
m	Material
$room$	Indoor, room air state
s	Surface of material
sat	Saturated condition
τ	Current time period
twa	Time weighted average
v	Water vapour
w	Water or moisture in a liquid or solid form

Amendments to Chapter One:

Specific detail for introduction (George's second M)

1.3.1 Objectives

Some deviation from the original research proposal was made in the course of the study, as more important areas were examined in greater detail and some areas were found to be insignificant or irrelevant. The main area of study was to examine the existing situation and produce a model for the mass transfer processes occurring within the building. Specifically, the main areas that were intended to be investigated were as follows:

Observation Based (Chapter Two)

- Subterranean water
- Underfloor ice
- Infiltrating air
- Visitor throughput effects

Data analysis – Logger and weather-station data (Chapter Three)

- Data verification
- Climate study
- Indoor/Outdoor climate comparison
- Temperature stratification indoors
- Occupancy effects

Experimental - Building shell investigation (Chapter Four)

- Construction
- Air infiltration
- Moisture contents
- Aerosol salt infiltration

Modelling (Chapters Five, Six and Seven)

- Develop a mass transfer model, including all major mass transfer mechanisms
- Relative contribution of each psychrometric mechanism at Cape Evans
- Effect of removing underfloor moisture source
- Investigation of visitor effects
- Ventilation requirements
- Investigate means of reducing moisture within building

Conclusions and recommendations based on the above findings have been discussed in the final chapter (Chapter Eight).

Amendments to Chapter Three:

1st M: Detail in introduction – added to end of 3.1

This chapter specifically targets the analysis of this data, initially presenting a critical assessment of the past use of the loggers covering the instruments, and extent and quality of the data (§3.1 – 3.4). A comparison of the difference in indoor and outdoor trends is provided (§3.5), highlighting notable exceptions to the general pattern. The existence of temperature stratification and the effects of occupancy are searched for (§3.6 – 3.7) before rounding out the chapter with a look at the wind patterns existing in the area (§3.8).

2nd M and 1st O: Added in plan and elevation of hut with logger positions noted.

3rd 'M': reasonably consistent *changed to* reasonably continuous
Five day gap: (22/9/97 – 27/9/97) *added after mention*

2nd O: excessively *instead of* rapidly and spuriously
Prove *changed to* strongly indicate

4th M: All relevant chart legends changed to A0, A1 B0, B1 etc. format.

5th M: Added note to Figure 3.3, serving to explain purpose of figure in more detail: While the individual trends are difficult to determine from this chart, it serves to show the similar trend for all but the B0 probe.

6th M: added 'outdoor'

*3rd O: line changed to read: …*the **reduction** of the **fluctuations in** relative humidity becomes…

4th O: The upward trend seen in Fig. 3.8 from the 6500 hour point onward demonstrates the natural rise of room relative humidity during spring, as the

temperatures rise and the frequency of northerly weather patterns increases. This occurrence is discussed in more detail in the following Section 3.5.3.

In the context, ‘reasonably airtight’ *is justifiable because the comment was made from an intuitive feel from the data. This was not a quantitative estimate. (GB only commented here anyway).*

Additional sub-chapter at end:

3.9 Chapter Summary

The data from the loggers that were installed in the hut was shown to be in good order, with the exceptions highlighted. The influence of the building shell in damping the temperature and relative humidity has been shown to cause the internal micro-climate inside the building to differ substantially to the external climate - the sorption mechanism was seen to be effective in this manner. Northerly storms have been shown to influence the relative humidity inside the building to a great degree, especially heading into summer when the frequency of such storms appears to increase. The visitors to the hut do not appear to make a huge impact on the temperature and relative humidity inside the hut, but a better documentation system would be necessary to track the effect of visitors more accurately.

Following naturally from the examination of existing data, Chapter Four sets out to describe the experimental phase, where the collection of information specific to the hut was carried out. This information was necessary to cater the model to the hut.

Amendments to Chapter Four:

1st M: Modifications to the introduction:

4.1 Introduction

The loggers, as described in Chapter Three, provided a good history of the psychrometric state of the interior. A base of knowledge about the shell of the building was also needed so that a prediction of the water mass passing in and out of the control volume could be calculated with the indoor humidity model. **The experiments included:**

- **Physical measurements; hygroscopic area, occupied volume (§4.2)**
- **Moisture content survey of the walls and floor (§4.3)**
- **Insulation resistance of the walls and roof (§4.4)**
- **CO_2 decay infiltration testing (§4.9)**
- **Blower door infiltration testing (§4.10)**

The amount of salt deposition occurring in the huts was measured **(§4.11)**, **along with the analysis of the seagrass insulation (§4.5 – 4.7)** to provide data of possible value in the corrosion prevention work. The general construction survey conducted during the time in the field, **was not deemed to be particularly insightful in this thesis but** is covered in the Antarctic Heritage Trust Field Report [Mason 1999].

This last bit about the construction relates to the only bit of the field report that doesn't appear in this document in one form or another. Included for completeness and to also explain why the document wasn't appended.

2nd M: Hygroscopic material other than the wooden hut lining and contents was neglected **due to the vast area of the walls, floor and ceiling outweighing the minor surface area presented by the artefacts**.

3rd M: Calibration status of MC meter:

MC meters are not known for their high accuracy, but provide good indicative results using a non-destructive technique. **A calibration standard is included with the device (an accurate, single-point resistance comparison) with which the meter was periodically checked during use and found to agree well with.** The instrument was kindly lent by Mr. Murray Drake, of the Christchurch City Council, Building Inspectors Team.

Comment: Cape Royds?

I agree it does jump out of nowhere, but I think I will leave it in. I think that this reference to cape royds is helpful for the AHT personnel to compare and understand better the scale of what I am talking about.

4th M: Implications of the blower door failure, added to

The information that this test would have provided was estimated from the four CO_2 decay infiltration tests that were carried out. The number of CO_2 tests in different conditions allowed the model to be adjusted to best reproduce the infiltration rates with similar input conditions. Put simply, rather than have a single well-defined parameter, the model was fitted to a set of lesser data. This was found to be quite sufficient given the poor nominal accuracy (±25%) of the model.

5th M: Positive reasons into 4.11.3

The four candles were located outside, on either side of the hut and inside, by the door and further into the building. **These locations were chosen to provide data for the more or less exposed external environment which could be compared to that entering the hut near the door and deep within the building.** The exact locations and sample codes were:…

missing dwg…

Whoops! Forgot the drawing! I have pasted an Acad dwg straight in as Fig. 4.6.

6th M: Summary and lead to next chapter

4.14 Chapter Summary

Information regarding the physical construction of the hut has been gathered, along with tests to establish the air-exchange between the inside and outside air states. This will allow essential parameters to be determined for the models. Side experiments of salt infiltration and seagrass insulation analysis were carried out as well during the time in Antarctica. The intended blower door and airfield direction tests were not carried out for technical reasons.

With the data and information gathering phases completed in the previous two chapters, the modelling phase begins in Chapter Five with a detailed review of the published literature related to indoor humidity modelling.

Amendments to Chapter Five:

Added to 5.1 introduction, justification and content

This chapter sets out to provide a chronological history of indoor humidity modelling and related research in sub-models and mechanisms. **The papers summarised here have been learnt or borrowed from in reaching the goals of the author's own modelling and it is intended that this chapter will provide a summarised reference source for future work in this area.**

The papers cover the period from 1976 to the latest relevant work in 1995 and approach the problem using various mathematical tools from pure analytical to simple numerical and more complex finite element methods. Early works focussed on individual mechanisms - particularly infiltration – but later models were combined, coinciding with the reducing cost of computational power.

also chapter summary, although not specified:

5.4 Chapter Summary

The research leading to the formulation of the model developed in this thesis has been summarised and referenced. The modelling practice used in the author's work was of the simple numerical following the foundation work of Tsuchiya, Kusuda and TenWolde.

Chapter Six follows to define the theoretical detail behind the author's model.

Amendments to Chapter Six:

typo's corrected
Amended to the end of the chapter:

6.11 Chapter Summary

The individual model elements; infiltration, sorption, condensation/evaporation and occupancy, have been discussed in terms of practical representation, theoretical approach, and the formulation and flow of computer code. The assumptions made in each model have been highlighted and justified in terms of the required outcome. Psychrometric calculation routines used in determining states from the basic data have also been described. The vapour diffusion model was neglected as being insignificant.

Chapter Seven proves the accuracy of the model and presents the results of the analysis that was carried out on a variety of different scenarios.

Amendments to Chapter Seven:

Additional detail in intro.

be created within Scott's hut. **These scenarios include:**

- **Examining individual component contributions**
- **Removing underfloor ice**
- **Altering the visitor group size, with open and closed doors**
- **Increasing the ventilation**
- **Determining the active layer depth in the timber of the walls**
- **Calculating the moisture load for a potential hygroscopic damping scheme**
- **Calculating the total summer condensate**

2nd M: I have a real problem with this one! The key in figures 7.2/4/6/8 IS in identical format as odd numbered graphs! I can understand that the 's'-prefix might put him off, but it was a unfortunate oversight when I wrote the code. All I would do would be to remove the 's' from the front anyway. Maybe I could paste a text-box over each key?

With regard to the x-axis (I assume this was what he meant) numbering, does he mean to renumber in hours of the year or do you think he missed the x-axis in the plot area (not in the white like the others)? The start-from-1 hourly step is used as a reference in the code, and would require rewriting the software to change away from the fixed reference. The references to the charts have been made in terms of the system depicted, (which he has highlighted as not corresponding) so I think he may have not seen this axis.

Either change would force me to rerun the model for each scenario in order to regenerate the original chart, of which I only have a metafile copy now. What do you think about this? I am firmly in the camp that an 's'-prefix is not a significant impedance to the reading of the thesis, as you can well imagine!

3rd M: Identified and labelled on chart: See §7.4.1 (d) with an arrow.

4th M: comment of effect of overdriving rh added to part (e)

This over-driving of the room relative humidity is caused by the heavy influence of the infiltration model during the very windy conditions present at the time. The model has calculated a higher infiltration rate than actually present at the time. This is an unfortunate result of the lack of adaptability in the model that prevents it from predicting infiltration rates under all conditions. In addition, catering shielding coefficients for every wind angle was not possible and in this particular circumstance the wind may have been more sheltered than actually modelled.

5th M: Definitions in context

attributable to the fact that the model is only replicative **(where the model can only reproduce a given scenario from full input data)**, not predictive **(where the external data and hut parameters are all that are required to determine the indoor conditions)**, so that the…

…assessed by running 'What if?' scenarios**, where changes can be made to the input data, such as increasing the ventilation of the hut, then running through the model again to see the relative effect of the changes.**

6th M: Labels added directly to charts with arrows pointing to individual lines.

Amendments to Chapter Eight:

1st M:

8.1 Introduction

This final chapter serves to finish the thesis by collating all the main findings from throughout the previous chapters and presenting the conclusions drawn from them. The main objectives of the thesis are answered in terms of the determined outcome.

Several recommendations are made as a result of these conclusions, including ideas for future research or development of ideas that have stemmed from this work.

2nd M:

The **continuity** of the **logger** data was found to be sufficient for **the needs of this project**, but large…

I didn't feel the need to go into the optional area here

3rd M: Relating to objectives more closely: Note: with addition of intro, the header numbers have changed, but are shown here the same as the original document.

8.1.2 Groundwater and Ice Heave

The observation-based work showed that the beach location had a propensity to attract…

8.1.3 Visitor Impact

One of the main objectives of the study was to examine the effects of the visitors on the hut micro-climate and then be able to extrapolate the numbers to obtain an indication of the effects that any variation in the policy might cause.

Mod to ***8.1.7 The Experimental Programme***

The field work generally went to plan, **achieving most of the objectives** with the exception…

Added to end of ***8.1.8 The Model***

Overall, the model performed well in accordance with the original objectives of the thesis in that it was adaptable and covered all the major mass transfer mechanisms.

Mod to ***8.3.2 Ice Removal***

The early objective to study the underfloor ice was not fully resolved in that the complete study would involve more structural and soil study than the author was qualified for. Investigation by a geotechnical…

Amendments to Chapter Four:

1st M: Modifications to the introduction:

4.1 Introduction

The loggers, as described in Chapter Three, provided a good history of the psychrometric state of the interior. A base of knowledge about the shell of the building was also needed so that a prediction of the water mass passing in and out of the control volume could be calculated with the indoor humidity model. **The experiments included:**

- **Physical measurements; hygroscopic area, occupied volume (§4.2)**
- **Moisture content survey of the walls and floor (§4.3)**
- **Insulation resistance of the walls and roof (§4.4)**
- **CO_2 decay infiltration testing (§4.9)**
- **Blower door infiltration testing (§4.10)**

The amount of salt deposition occurring in the huts was measured **(§4.11)**, **along with the analysis of the seagrass insulation (§4.5 – 4.7)** to provide data of possible value in the corrosion prevention work. The general construction survey conducted during the time in the field, **was not deemed to be particularly insightful in this thesis but** is covered in the Antarctic Heritage Trust Field Report [Mason 1999].

This last bit about the construction relates to the only bit of the field report that doesn't appear in this document in one form or another. Included for completeness and to also explain why the document wasn't appended.

2nd M: Hygroscopic material other than the wooden hut lining and contents was neglected **due to the vast area of the walls, floor and ceiling outweighing the minor surface area presented by the artefacts**.

3rd M: Calibration status of MC meter:

MC meters are not known for their high accuracy, but provide good indicative results using a non-destructive technique. **A calibration standard is included with the device (an accurate, single-point resistance comparison) with which the meter was periodically checked during use and found to agree well with.** The instrument was kindly lent by Mr. Murray Drake, of the Christchurch City Council, Building Inspectors Team.

Comment: Cape Royds?

I agree it does jump out of nowhere, but I think I will leave it in. I think that this reference to cape royds is helpful for the AHT personnel to compare and understand better the scale of what I am talking about.

4th M: Implications of the blower door failure, added to

The information that this test would have provided was estimated **instead** from the four CO_2 decay infiltration tests that were carried out. The number of CO_2 tests in different conditions allowed the model to be adjusted to best reproduce the infiltration rates with similar input conditions. Put simply, rather than have a single well-defined parameter, the model was fitted to a set of lesser data. This was found to be quite sufficient given the poor nominal accuracy (±25%) of the model.

5th M: Positive reasons into 4.11.3

The four candles were located outside, on either side of the hut and inside, by the door and further into the building. **These locations were chosen to provide data for the more or less exposed external environment which could be compared to that entering the hut near the door and deep within the building.** The exact locations and sample codes were:…

missing dwg…

Whoops! Forgot the drawing! I have pasted an Acad dwg straight in as Fig. 4.6.

6th M: Summary and lead to next chapter

4.14 Chapter Summary

Information regarding the physical construction of the hut ~~has been~~ **was** gathered, along with tests **completed** to establish the air-exchange between the inside and outside air states. This ~~will~~ allow**ed** essential parameters to be determined for the models. Side experiments of salt infiltration and seagrass insulation analysis were carried out as well during the time in Antarctica. The intended blower door and airfield direction tests were not carried out for technical reasons.

With the data and information gathering phases completed in the previous two chapters, **a description of** the modelling phase begins in Chapter Five with a detailed review of the published literature related to indoor humidity modelling.

Amendments to Chapter Five:

Added to 5.1 introduction, justification and content

This chapter sets out to provide a chronological history of indoor humidity modelling and related research in sub-models and mechanisms. **The papers summarised here have been learnt or borrowed from in reaching the goals of the author's own modelling and it is intended that this chapter will provide a summarised reference source for future work in this area.**

The papers cover the period from 1976 to the latest relevant work in 1995 and approach the problem using various mathematical tools from pure analytical to simple numerical and more complex finite element methods. Early works focussed on individual mechanisms - particularly infiltration – but later models were combined, coinciding with the reducing cost of computational power.

Glen: I suggest "studied" rather than "learnt" in the above

also chapter summary, although not specified:

5.4 Chapter Summary

~~The~~ **Previous** research leading to the formulation of the model developed in this thesis has been summarised and referenced. The modelling practice used in the author's work was of the simple numerical following the foundation work of Tsuchiya, Kusuda and TenWolde.

Chapter Six **following ~~s to~~** define**s** the theoretical detail behind the author's model.

Amendments to Chapter Six:

typo's corrected
Amended to the end of the chapter:

6.11 Chapter Summary

The individual model elements; infiltration, sorption, condensation/evaporation and occupancy, have been discussed in terms of practical representation, theoretical approach, and the formulation and flow of computer code. The assumptions made in each model have been highlighted and justified in terms of the required outcome. Psychrometric calculation routines used in determining states from the basic data have also been described. The vapour diffusion model was neglected as being insignificant.

Chapter Seven proves the accuracy of the model and presents the results of the analysis that was carried out on a variety of different scenarios.

Amendments to Chapter Seven:

Additional detail in intro.

be created within Scott's hut. **These scenarios include:**

- **Examining individual component contributions**
- **Removing underfloor ice**
- **Altering the visitor group size, with open and closed doors**
- **Increasing the ventilation**
- **Determining the active layer depth in the timber of the walls**
- **Calculating the moisture load for a potential hygroscopic damping scheme**
- **Calculating the total summer condensate**

2nd M: I have a real problem with this one! The key in figures 7.2/4/6/8 IS in identical format as odd numbered graphs! I can understand that the 's'-prefix might put him off, but it was a unfortunate oversight when I wrote the code. All I would do would be to remove the 's' from the front anyway. Maybe I could paste a text-box over each key? ***You may recall I raised the same concern so its probably significant that both of us had the same reaction. A paste job (or Twink on the final copy!) would be fine.***

With regard to the x-axis (I assume this was what he meant) numbering, does he mean to renumber in hours of the year or do you think he missed the x-axis in the plot area (not in the white like the others)? The start-from-1 hourly step is used as a reference in the code, and would require rewriting the software to change away from the fixed reference. The references to the charts have been made in terms of the system depicted, (which he has highlighted as not corresponding) so I think he may have not seen this axis. ***I'm inclined to agree with you – once you spot where the axis scale is I don't think there's a particular problem.***

Either change would force me to rerun the model for each scenario in order to regenerate the original chart, of which I only have a metafile copy now. What do you think about this? I am firmly in the camp that an 's'-prefix is not a significant impedance to the reading of the thesis, as you can well imagine! ***No, don't re-run your model****.*

3rd M: Identified and labelled on chart: See §7.4.1 (d) with an arrow.

4th M: comment of effect of overdriving rh added to part (e)

This over-driving of the room relative humidity is caused by the heavy influence of the infiltration model during the very windy conditions present at the time. The model has calculated a higher infiltration rate than **was** actually present at the time. This is an unfortunate result of the lack of adaptability in the model that prevents it from predicting infiltration rates under all conditions. In addition, ~~catering~~ **specifying** shielding coefficients for every wind angle was not possible and in this particular circumstance the ~~wind~~ **hut** may have been more sheltered **from the wind** than actually modelled.

5th M: Definitions in context

attributable to the fact that the model is only replicative **(where the model can only reproduce a given scenario from full input data)**, not predictive **(where the external data and hut parameters are all that are required to determine the indoor conditions)**, so that the…

…assessed by running 'What if?' scenarios**, where changes can be made to the input data, such as increasing the ventilation of the hut, then running through the model again to see the relative effect of the changes.**

6th M: Labels added directly to charts with arrows pointing to individual lines.

Glen: I notice that you haven't added a wrap-up to Chapter 7, which makes it now the only one without.

Amendments to Chapter Eight:

1st M:

8.1 Introduction

This final chapter serves to ~~finish~~ **complete** the thesis by collating all the main findings from throughout the previous chapters and presenting the conclusions drawn from them. The main objectives of the thesis are answered in terms of the determined outcome**s**.

Several recommendations are made as a result of these conclusions, including ideas for future research or development of ideas that have stemmed from this work.

2nd M:

The **continuity** of the **logger** data was found to be sufficient for **the needs of this project**, but large…

I didn't feel the need to go into the optional area here ***Fair enough – your call***

3rd M: Relating to objectives more closely: Note: with addition of intro, the header numbers have changed, but are shown here the same as the original document.

8.1.2 Groundwater and Ice Heave

The observation-based work showed that the beach location had a propensity to attract…

8.1.3 Visitor Impact

One of the main objectives of the study was to examine the effects of the visitors on the hut micro-climate and then be able to extrapolate the numbers to obtain an indication of the effects that any variation in the policy might cause.

*Mod to **8.1.7 The Experimental Programme***

The field work generally went to plan, **achieving most of the objectives** with the **[add "principal"** exception…

*Added to end of **8.1.8 The Model***

Overall, the model performed well in accordance with the original objectives of the thesis in that it was adaptable and covered all the major mass transfer mechanisms.

*Mod to **8.3.2 Ice Removal***

The early objective to study the underfloor ice was not fully resolved in that the complete study would involve more structural and soil study than the author was qualified for. Investigation by a geotechnical…

CHAPTER TWO

ANECDOTAL RECORDS AND OBSERVATIONS

2.1 Introduction

Much of the necessary general background information related to the huts has been derived from historical records, conversations with Antarctic Heritage Trust conservationists and historians who have maintained the buildings and the artefacts over the last decade or more. Other information has been obtained from documental histories written by members of the expeditions that erected the buildings, published papers and my own observation. This chapter sets out to collate and present the wide scope of general information relevant to the project. An overview of the construction of the hut is presented initially (§2.2), followed by detailed discussion on groundwater and visitor moisture sources (§2.3 – 2.6). The later sections (§2.7 – 2.9) look at the effects of such moisture in the hut, specifically with the metallic and textile artefacts.

All of the observations made by the author were during the nine day period of field work carried out at Cape Evans from 20 to 29 January 1999. More detail on this field work will be presented in later chapters.

2.2 The Construction of the *Terra Nova* Hut

2.2.1 General

The hut is a prefabricated, rectangular wooden building of 14.6m by 7.4m. It has a 2.4m stud height with a skillion, or cathedral roof rising to a peak height of 4.3m. The building was extended the summer following it's construction with a stables for the ponies down the north-west side, and a stores annex enclosing the front entranceway, made with scrap materials. Inside, the darkroom provides the only fully enclosed space, located centrally at the far end of the building. The hut is cluttered with furnishings such as partitions, stores of food boxes and rows of bunk beds. See Appendix A for drawings.

Figure 2.1: Scott's Terra Nova hut at Cape Evans. *Photo by Author.*

2.2.2 Walls

The walls are of a much sturdier construction and better insulated than those of Shackleton's hut and Scott's earlier hut, an indication that Scott must have learnt from the lesson of his own and Shackleton's experience in such reputedly cold huts. The construction is of a double layer of tongue and groove

Baltic Pine[1] boards nailed vertically to the inside of timber framing with an insulation layer of seagrass[2] sewn into Jute (hessian-like) quilts sandwiched between. The outer skin was of a similar layering but the outermost layer was horizontally overlapped weather-board, as seen in Figure 2.2a. Overall, the walls appear in good order. The corners were not boxed in, but are fairly close fitting. Infiltration passages through the gaps are likely. An 800mm square section of the external weather boarding had been removed from the end wall in order to allow access to equipment located outside along this wall. On the inside there was a noticeable draught felt around this corner.

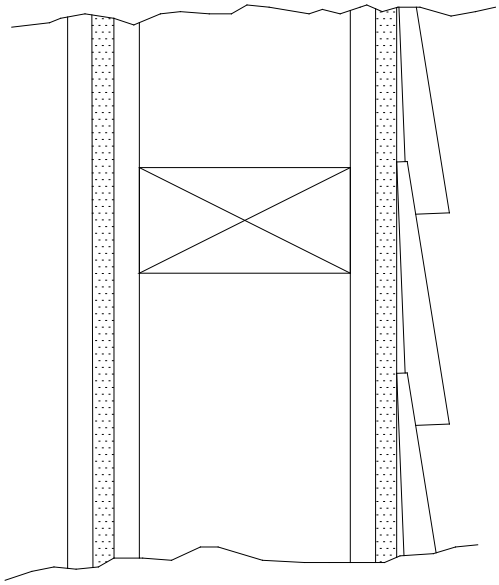

Figure 2.2a: *Terra Nova* hut wall section

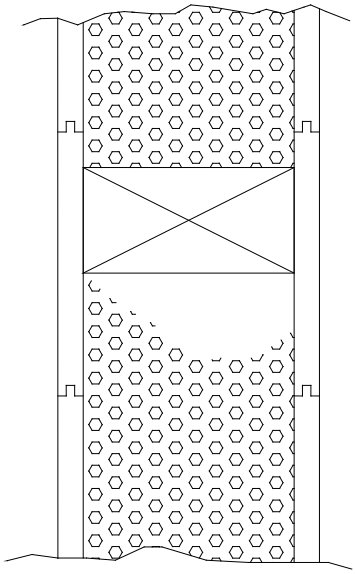

Figure 2.2b: Shackleton's hut wall section

For comparison, Shackleton's hut had a single layer 125mm tongue and groove match-boarding as a shell and lining; Fig. 2.2b. The boards were vertically arranged on the outer shell and horizontal in the lining. The walls remain in generally good condition considering the environment, suffering a few gaps from timber drying, erosion, missing timbers, and construction methods.

[1] *Pinus sylvestris*. Also known as Baltic Red, Scot's Pine, Red Deal. Similar in hygroscopic and thermodynamic properties to *Pinus Radiata.*

[2] Specifically 'Eel-grass', likely of the species *Zostera* as identified by Botanist, Dr. Paul Broady, University of Canterbury.

Insulation was provided with granulated cork, although some leakage has occurred leaving empty spaces.

2.3 Groundwater

2.3.1 Mechanism

Wood and other hygroscopic materials can lie in either of the two regions of moisture content, *pendular* (below saturation to saturation point) or *funicular* (above saturation point). In the pendular region, the moisture content of the hygroscopic material will swing, maintaining equilibrium with its surroundings by absorbing and desorbing water vapour. Water sources under the hut may allow for the wooden floor to wick the moisture up by capillary action and attain the higher state of funicular moisture content not normally found. This presents a buffer that will continually provide moisture to the air in most conditions, maintaining high humidity inside the building.

2.3.2 Investigation

The hut was built on a fairly low point of the beach, providing a geographical propensity for attracting ground water flow underneath the building when solar gain allowed melting. The flow rate of groundwater was observed to vary tremendously over the day and was weather dependant – cloud cover being the predominant obstruction to solar effects but also local shadowing as the sun's aspect changed relative to the building. Over the course of a week, flowing surface water was seen running down from the snow and ice drift above the hut (in which, during Scott's era were dug the ice caves for meat storage and scientific work) and ponding substantially in several locations. The surface water went underground closer to the hut. Lack of access beneath the hut inhibits any closer examination.

Quoting from Mason, 1999:

> *"Test pits were carefully dug on the west side of the hut to a depth of around 0.5m by Chris Jacomb. In places, the holes filled rapidly with water. The permafrost depth is the limit to which the water can flow (again, this depth is influenced by solar heating of the soil) keeping the liquid water close to the surface of the volcanic till. Jacomb also dug a trench leading from the SE corner of the hut towards the sea through which a decent amount of water drained away from the back of the hut, flowing intermittently. It is reasonable to assume that this is a significant source of water for the ice build-up under the hut, contributing to that which melts from the local snowdrifts due to radiant heat from the building. Here, snow drifts form against the lower walls of the building and melt away forming distinct channels between the wall and drift. As the wall absorbs high frequency solar energy, it emits low frequency energy which is absorbed by the snow causing a melt in the immediate vicinity of the hut. With no other obvious flow path alternative, the water is believed to flow under the hut."*

An effort to counter this action has been undertaken since the late 1980s, where a butylene skirt has been attached along the south-east wall and the snow and ice excavated on a nearly annual basis [AHT, 1997].

It is likely that liquid water may not be present for many seasons and then may only flow for a very short time. During this summer, it was remarked to have the greatest amount of free-running surface water since 1977 [Harrowfield, 1999].

Global warming may be a contributing factor to the increase in the melt water flowing under the hut. The distortion of the floor has only been noticed since the early 80s, and it may be that this flow has only been a significant factor in recent decades as the planet has warmed to a level enough to sustain water in the liquid phase. Increases in ultraviolet solar radiation as a result of the burgeoning zone of ozone depletion would probably not have a significant contribution to the problem. Although the flow of water at sub-zero

temperatures is possible due to direct solar radiation heating the ice crystals enough to melt them, the energy input comes more from the visible and infrared wavelengths, which are absorbed more readily into the snow [Hobbs, 1974: §3.1].

2.3.3 Possible Solutions

Potential methods to restrict the flow of water under the hut and remove the snow and ice from beneath the floor are:

- Channelling water around the hut to the sea by excavating trenches. It has been observed that the 'Jacomb trench' had the desired effect of allowing free running water to bypass the building in sufficient quantity. The main drawbacks of this quick and simple method are in the need for archaeological excavation and disturbance to the historic site and the on-going visual impropriety /physical disturbance of the trenches themselves.
- Channelling water by burying concrete training walls below the level of the till and set into the permafrost layer. Walls such as this have been used in more temperate climates to divert subterranean water flows from buildings, and it lacks the visual impact of the above method. Both these methods do not address the problem of removing the already present ice.
- Open ventilating the sub floor space, maybe requiring the raising of the building. Large crystals under Shackleton's hut were observed to sublimate quickly with the lifting of the butylene skirt. Ventilation may be the key to removing the ice from under the hut, as used in The Wilkes Hut Project with their passive venturi ventilation scheme [AICCM, 1998].

This is by no means a complete list of the possible solutions for this problem. The ice may present a much greater menace in the future, at which time all options would need to be considered and studied in more detail.

2.4 Other Moisture Sources

2.4.1 Snow Drifts

It is likely that drifting snow against the outside of the building allows moisture to wick through the wooden shell of the building as melt occurs in summer. In a similar manner the damp floor is thought to channel moisture from the underfloor sources. This idea is supported by measurements of moisture content of the timber taken at various points around the walls and the floor, the results of which are presented in Chapter Four.

Figure 2.3: The Terra Nova hut, showing location near beach and snow drifts, late summer 1999. *Photo by author*.

2.4.2 The Human Element

Visitor respiration is potentially a major factor in the moisture gain to the air space where up to 140 passengers from a tourist ship may pass through the hut over a period of a few hours. Limitations on the number of people allowed in the hut at any one time are in place, but this quota has been set without any real idea of the impact on the indoor humidity. Snow can also be inadvertently

brought in on clothing and footwear, but the brushes located in the entranceways to all the huts minimise this.

2.4.3 Seepage through Shell

With the butylclad covering the roof since the 1989/90 season, and the generally good condition of the exterior weather-boarding it seems unlikely that moisture could pervade the exterior shell in significant quantity. At Cape Royds, the situation may be quite different as the shell is not nearly as airtight as at Cape Evans.

2.5 Ice Heave

2.5.1 Mechanism

The general concept of ice heave relates to the cyclic thawing and re-freezing of water in the soil around the piles of a structure, loosening the pile and degrading the foundation of the structure. Basal, or uplifting forces result when the re-freeze cycle ends and the ice contracts (9% by volume) leaving a space below the foundation or grade beam that can be refilled by liquid melt water causing a ‘hydraulic jack’ effect when the freeze once again takes over. Influencing factors on the rate of this mechanism are many, but fall under the headings of soil type and condition, climate, foundation loading. [Johnston, 1981]

The occasional presence of liquid water under the hut is mandatory for ice to distort the floor. Ingress of snow, ice and water vapour will only pack available space, so cannot provide the distorting force. As an indication of the pressure provided by freezing (pure) water; to restrain water from expanding (freezing) at only –1ºC would exert a pressure of approximately 80 atmospheres (8 MPa, 1100psi) on the container [Hobbs, 1974: §3.1.2], in this case the hut. Thus the hut floor being lifted by water freezing into ice is clearly possible. A similar form of frost heave may also cause subsidence of the loose till that is characteristic of the area, and allow the building to settle into the ground. The floor may then

be damaged by the weight of the building bearing the floorboards directly on the ice below. At the time of construction, the quality of the foundation was thought to be good - *"The surface was like cinders, quite loose, but a few inches below it was frozen solid."*, as commented by Frank Davies RN, *Terra Nova* carpenter [Harrowfield, 1995].

2.5.2 Under-Floor Ice Formation

Understanding how the ice heave causes the distortion of the floor contributes little towards explaining how the ice came to fill the space under the building in the first place. The author expects the mechanism for ice formation under the hut would have proceeded as follows: Water flowing under the hut will freeze into layers that build up on each other, contributed to by the influx of windblown snow consolidating with a melt/re-freeze cycle. Air flow under the building would have had a greater effect in any ice removal at this early stage due to the larger flow rates possible in a more open space.

As the space was gradually filled, the airborne snow would have more difficulty packing in to the smaller available space, and so the contribution of the water flow would become more predominant. The time period in which this space would have become completely full is determined by weather conditions and the degree to which the space was open to windblown snow.

In the past the building had been surveyed accurately and the building was not shown to be moving within the ±1mm resolution of the equipment. A survey of the floor inside was also carried out to enable a full description of any movement. [Easdale, 1998].

2.5.3 Disclaimer

It became apparent during the course of this study that the author was not grounded in the appropriate theoretical areas to investigate the ice heave matter fully, and recommends any further work be completed by an

appropriately qualified and experienced person or organisation with skills in soil science, structural engineering and surveying.

2.6 Tourism

2.6.1 Overview

Antarctic tourism is increasing at a great rate. Data collected [Enzenbacher, 1992] over the 12 year period from 1980/81 through 1992/93 shows exponential growth from annual totals of about 1000 passengers to 7000 passengers. Recent figures indicate about 12,000 passengers annually.

Most tourists visit Antarctica on board cruise ships which are often leased ex-Russian government icebreakers and ice-strengthened ships complete with crews. While a majority of the annual tourism occurs in the Antarctic Peninsula area, several ships do ply the coast around the Ross Sea region.

2.6.2 Impact

The access method is resulting in ship-loads of people arriving at the huts at one time, causing a ‘step input’ of moisture to the hut microclimate. The effect of this latent load on the air state will be considered in more detail in Chapter Seven.

Additional impact from aerosol salt is likely with the breaking up of the sea ice directly outside the hut at Cape Evans caused by the icebreaker cutting passage to the closest shore access. While this sea ice would most likely break out to sea at some stage of the season anyway, it would not always directly coincide with the visitor movements in and out of the hut. The problem would be avoided if tourist vessels were required to stop further out in the sound.

2.6.3 Visitor Books

The tourism studies do not include the number of visits from Antarctic personnel and distinguished visitors, leaving the visitor book as the only record. Unfortunately it seems that Antarctic personnel stop signing the book after the first visit, and the record of people present in the hut is diminished. The visitor book provides an excellent way of matching the occupancy to the indoor air state, so it should be re-branded as more of an *occupant record* and people encouraging to note the party size (including helicopter pilots and the like entering the building), date and NZ time, on all visits. A note explaining the use of the data on each page and a note to key recipients should suffice.

2.7 Corrosion

2.7.1 Mechanism

Surface corrosion of metals unfortunately is a common sight in the *Terra Nova* hut. Corrosion is defined as the deterioration of a material resulting from chemical attack by its environment. Different metals react in different ways to the atmosphere and appear in the form of reddish-brown scaled rust on the cast iron and ferrous alloys, and a brown, later turning to blue-green patina (verdigris) on the copper-based alloys [Smith, 1993: Chap.12].

Rather than from direct chemical attack from solutions, the general atmospheric corrosion of these metals has been caused by uniform electrochemical attack, where small electric cells form with the presence of a surface electrolyte, and deplete the metal by conversion into metal oxides. Electrochemical reactions have a rate that is determined by temperature and concentrations of reactants and products [Fontana et al, 1978: Chap. 2]. In this case of non-submerged metal, the formation of the electrolyte is a key to triggering the start of corrosion.

2.7.2 Air State Contribution

Outside the hut, weather patterns are likely that will wet the surface but also clean the surface of contaminants. This is more so in temperate climates than in Antarctica where rain is less likely, although wind and snow would cause wetting and cleansing at a slower rate. Within the shelter of the hut, rain is not possible for surface wetting and reducing condensation becomes very important. Condensation occurs when the temperature of the surface falls below the dew point temperature of the air. In Antarctica, the constant 24hr summer days and 24hr winter nights tend to restrict any substantial diurnal, or daily temperature variation to the spring and autumn seasons, meaning condensation is more likely to occur then.

A surface dew is a more active (than direct wetting) cause of atmospheric corrosion and its high corrosivity lies in the high concentration of the electrolyte that forms. During the dry periods an aerosol dry deposition of contaminants (salt, sulphur dioxide) can occur on the surface of the metal which is wetted into an electrolyte by the relatively small amounts of water derived from condensation from the atmosphere [Schweitzer, 1987: Chap.5]. This makes for a much more concentrated electrolyte, and a better electron path for electrochemical corrosion. The high levels of pollutants[3] available from the sea are somewhat offset by the very low quantities of moisture available from the cold air of Antarctica, but potential for the formation of strong electrolytes, particularly on metals, exists when the relative humidity of the air state is high within the building.

A cycling relative humidity in the room space of the hut tends to concentrate the electrolyte by way of evaporating moisture droplets, so that the salt in solution migrates to the centre of a size-reducing droplet as the room relative humidity falls. Diffusion effects cause the contaminants to migrate to the surface of the drops, bringing a greater rate of corrosion surrounding the drop compared to that within the surface boundary [Haberecht, 1998]. This is seen on the cast

[3] The terms ‘pollutants’ and ‘contaminants’ refer to the unwanted substances that invade the hut from the atmosphere or otherwise. Salt, SO_2, and dirt are the most notable examples.

iron stoves, where the scale tends to form in rings around the rusted pits. These pits, en masse, form the transitional stage from pitting to general, or uniform corrosion and harbour moisture when condensation once again forms on the surface, as the relative humidity rises.

2.7.3 Corrosivity of the Atmosphere

The low temperatures occurring at all times of the year in Antarctica cause a slow reaction rate which is likely the reason that the artefacts are in the good condition that they are. While corrosion is slowed, it does still occur at rates of 10.83μm/yr using the standard alloy coupons and CLIMAT wire on bolt tests, which is a low to moderate amount [Hughes et al, 1995]. Time of wetness is another factor but is defined by the number of hours in a year that the relative humidity is greater than 80% and the temperature is greater than 0ºC. This of course is rare in Antarctica and solar heating of surfaces means that the wetted condition would exist on many more occasions that the time of wetness indicates. The time of wetness as defined in the standard is too limited for sub-zero temperature climates. The ISO 9223 [1992] standard classifies the corrosivity of the atmosphere for various metals, which will be covered in more detail in Chapter Four.

2.7.4 Contaminants

Cape Evans is a severe marine environment. Salt can be seen on the ground surrounding the hut where lack of rain allows it to build up. Sodium Chloride ionises in solution forming a strong electrolyte and will become saturated by hygroscopic absorption of moisture from an atmosphere of relative humidity greater than 75%. Extended exposure of salt to a relative humidity atmosphere greater than 75% will cause the salt solution to dilute [Garrecht et al, 1990]. Aerosol salt was collected during a month long period described in Chapter Four.

The location of an active volcano crater within 30km of Cape Evans implies the potential presence of sulphur dioxide (SO_2) which converts to sulphuric acid in solution - a strong electrolyte.

2.7.5 Passivation

The formation of rust or other oxide coatings on the surface of the metal may protect it by slowing further oxidation. This is known as passivation and is commonly known of aluminium and titanium. Iron and ferrous metals also form oxide layers, but compressive stresses from excessive metal-oxides formed in the layer cause it to crack and flake off, thus reducing its effectiveness [Smith, 1993: 677-679, 694].

Figure 2.4: Rusted heater body is shown covered in scale. *Photo by author.*

2.7.6 Filiform Corrosion

Worth mentioning for the quantity of enamelled plates in the huts is filiform corrosion. At high levels of relative humidity (>65%) enamelled or otherwise protected metal can be affected by filiform corrosion. If the relative humidity exceeds 90%, blisters may form under the enamel coating. Filiform corrosion is a result of moisture permeating the coating on the metal, and is identified by

filament tracks, as the corrosion front moves across the surface. Preventative measures are in the form of low vapour permeability coatings, or coatings that are brittle and expose the tunnelling corrosion front, halting activity [Fontana and Greene, 1978: 44-48].

2.8 Non-Metallic Items

Timber, fur, paper and textiles are also damaged by high and cyclic humidity and represent a good proportion of the artefacts inside the huts. Mould can form at excess material moisture contents. High humidity means greater levels of degradation. Several projects are currently under way by the Antarctic Heritage Trust to study these materials and mould occurrences, but these are not within the scope of the present work.

Figure 2.5: Pristine example of textile artefact; wind-proof trousers. *Photo by author.*

2.9 Moisture Patches Under Artefacts

Patches of water have been reported [Easdale, 1998] under artefacts that rest on the floor. This was a consequence of the under-floor moisture source and will likely continue until the ice has been removed. The basic mechanism that caused the water to condense can be likened to localised sorption, which is covered in detail in later chapters. The warming of the artefact in the sun causes a small, humid microclimate to exist in the space between the object and the floor. Water is drawn from the damp, wooden floorboards into the space where it later condenses with the falling temperature associated with the normal diurnal variation. This condition has been depicted in Fig. 2.6.

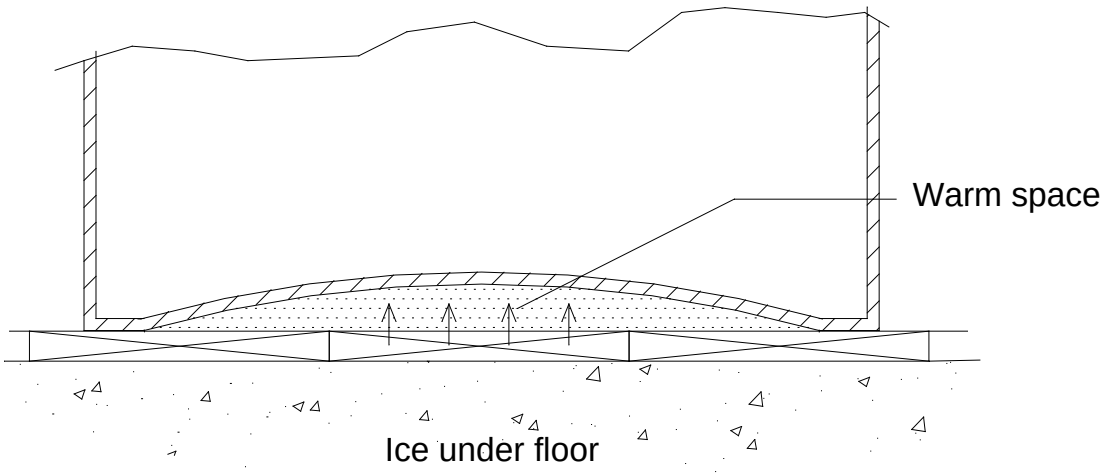

Figure 2.6: Sweating under artefacts resting on the floor

Metal artefacts resting on the floor may also act as a ‘cooling fin’ to the under-floor ice, causing an enhanced rate of condensation in some ambient conditions.

2.10 Chapter Summary

The shell of the hut has been examined in this chapter along with the major sources of moisture other than that from infiltrating air. Side issues such as ice heave under the floor have been discussed to the extent intended by the author. Effects of the high seasonal moisture on the artefacts have also been covered.

The next chapter sets out to examine the data provided by the loggers located in the huts. Analysis of this data provided information on the local and internal air states and moisture gained from infiltration, and various trends related information about the building shell.

CHAPTER THREE

DATA ANALYSIS

3.1 Introduction

Since early 1991, at least one battery powered data logger has been installed in Scott's hut at Cape Evans. More recently, three loggers have been used to measure the temperature and relative humidity at various locations and heights within the building. The loggers were positioned by non-technical conservation staff and have been moved at various stages, sometimes without documenting locations. There can never be too much data though and the loggers have served to provide a solid record of the annual variation in conditions within the last decade.

This chapter specifically targets the analysis of this data, initially presenting a critical assessment of the past use of the loggers covering the instruments, and extent and quality of the data (§3.1 – 3.4). A comparison of the difference in indoor and outdoor trends is provided (§3.5), highlighting notable exceptions to the general pattern. The existence of temperature stratification and the effects of occupancy are searched for (§3.6 – 3.7) before rounding out the chapter with a look at the wind patterns existing in the area (§3.8).

3.2 Apparatus

3.2.1 Data Loggers

The first loggers were *ACR Systems Inc. 'Stick-On' XT-102* models. *Smartreader* models were later used, also from ACR Systems with similar features. This is a combined temperature and relative humidity logger powered by a 10 year lithium battery, capable of storing a total of 32,768 eight bit readings with a maximum of 1/2hr interval. An external temperature probe was added to the loggers reducing the maximum storage period to a little over 5400 hours. This is short of a full calendar year (8760 hours) and the loggers were set to stop recording at the end of this period, rather than overwriting. As the data was really only needed in hourly time periods, the maximum half hour interval was the major drawback of these loggers.

3.2.2 Software

The loggers were used in conjunction with *Trendreader* software for calibration, downloading and data analysis. With this DOS version (1.56D), compressed data was converted into ASCII format files that could be imported into an Excel spreadsheet, but limitations on the file sizes meant a lot of cutting and pasting was necessary to bring the information together. For future work to be efficient, a more recent version of this software will be required.

3.3 Data Record

3.3.1 Locations

When the additional loggers were placed in the hut, temperature stratification was thought to be pertinent and the temperature probes spanned evenly between the floor and ceiling. The three loggers were labelled *A, B* and *C*, all of which had an external probe fitted to record two temperatures each. The suffixes 0 and 2 indicates an internal and external temperature probe respectively, in line with the default file format of the Trendreader software.

The probes and loggers, in order of the highest physical location down and as depicted in Figure 3.1 were as follows:

- Probe A2: Positioned outside, on the top of the chimney flue. Exposure to direct sunlight and wind precluded any meaningful results being obtained from this probe.
- Logger A0: Sitting on the top bunk belonging to Bowers, located fairly centrally in the main building.
- Probe B2: Attached to the Bowers/Cherry-Gerrard double bunk midway between the two bunks.
- Logger B0: Sitting on the lower bunk of Cherry/Gerrard.
- Logger C0: Resting on a shelf 50cm above the floor in the darkroom.
- Probe C2: Under-floor cavity, through a hole in the floor of the darkroom covered by an oilcloth.

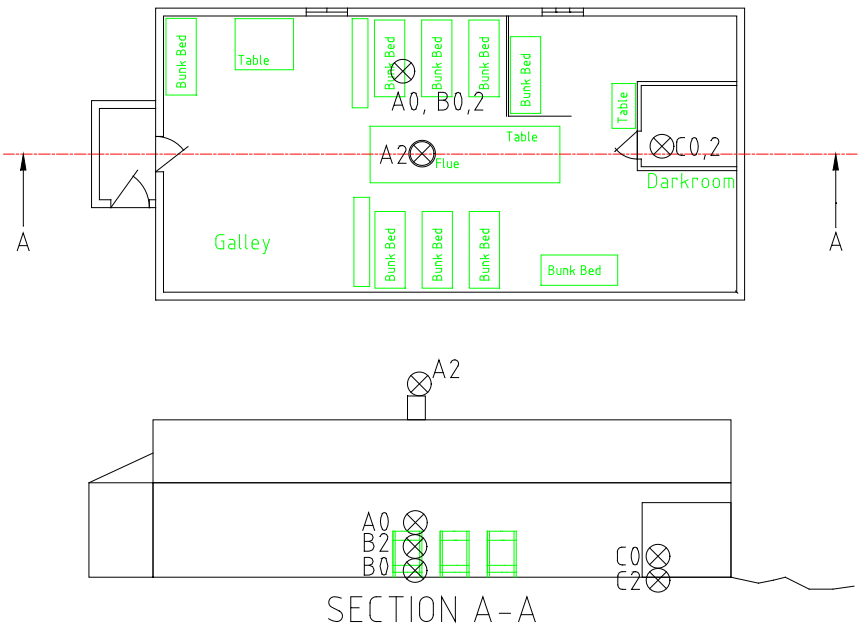

Figure 3.1: Location of loggers in Scott's hut

As the relative humidity sensors are built into the loggers, the physical locations of these readings were the same as for the in-built temperature probes. The identifying suffix for the relative humidity data files is '1'. ie. A1, B1 and C1 physically coincide with A0, B0 and C0.

There is little difference between the apparent height of loggers B0 and C0, as C0 was recorded as being 50 cm above the floor, which is about the same height as the bottom bunk of Cherry-Gerrard. Logger C0 however, is located on a low shelf within the darkroom which would provide substantial shielding to reflected sunlight.

The loggers were relocated during the field event associated with this work. The external temperature probe was brought in from the roof and repositioned in the apex of the cathedral ceiling. A logger was put in the latrine roof to record ambient conditions outside, providing backup to the NIWA data recorded at Scott Base. The two remaining loggers were shuffled to provide the best positioning for data gathering and were arranged to avoid dirty and dusty locations. The present locations have been described in detail in the K282 field report [Mason 1999].

3.3.2 Logger Data Record

The loggers provided a reasonably continuous picture of the room air state from the end of the Greenpeace camp in the beginning of 1991 right through to the present. The main disturbance to the record throughout this time was caused by the practice of removing the loggers back to base in order to download the information. This was carried out by the technical staff of Scott Base during the more accessible period of mid-summer, which unfortunately was when the room air was undergoing the most changeable and therefore interesting psychrometric conditions. Patches of interference have also surfaced in the logger files from time to time and are thought to occur due to moisture entering the circuitry of the device. Both the temperature and relative humidity data goes erratic for a period of perhaps weeks then sorts itself out and continues functioning normally again. A record describing the data history of the loggers is included in Appendix C.

Without the internal logged data this project would not have been possible, but to ascertain the driving forces across the building shell it was also necessary to

have a record of the external conditions. This was provided by the National Institute of Water and Atmospheric Research (NIWA) who have been continuously monitoring atmospheric conditions at Scott Base for several years. The Scott Base NIWA climatic log, which provided temperature, relative humidity, wind and solar data, was assumed to be reasonably consistent with the conditions at Cape Evans, only 25km away in a straight line.

3.3.3 Source Year for Modelling Work

The 1997 year was chosen as the data source for the model because of the quality and span of the logger data during this time and also the availability of NIWA data. The useful logger data spans from early February through to the end of 1997, with a five day gap (22/9/97 – 27/9/97) in which the devices were returned to Scott Base for downloading. Three loggers were in place at this time and the data files could be checked against each other if the need arose.

3.4 Logger Data Verification

3.4.1 Logger A Data

As expected from the location of the probe the data was found to vary excessively as compared to the shaded inside temperature measurements. Variations, as can be seen in Fig. 3.2, swing by up to 10°C from the nominal inside trend, however the basic trend is followed to a reasonable approximation. Direct sunlight has a heating effect on the probe which causes temperature readings to deviate from that of the ambient atmosphere. In a similar manner, if snow wets the probe, the wet bulb effect cools the probe to read below true ambient temperature in windy conditions. In placing the probe on the top of the flue, the data taken from this file becomes virtually useless.

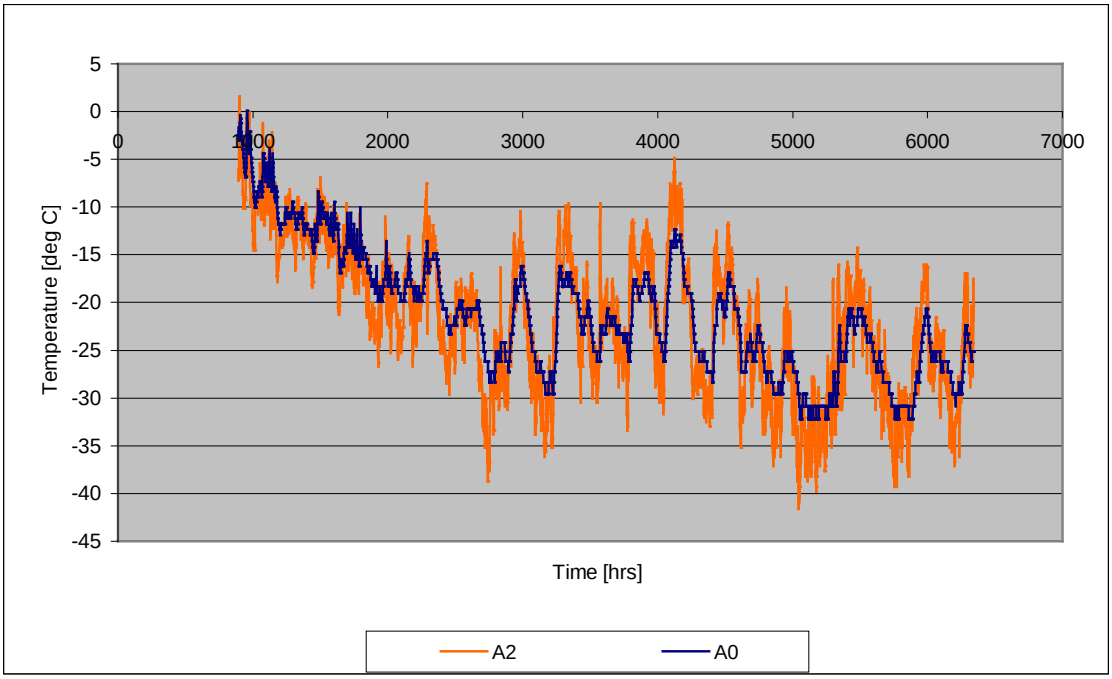

Figure 3.2: Outside temperature data variation due to solar effects clearly shows against the smoother inside trend.

3.4.2 Logger B Data

The plots for the temperatures of B0 and B2 showed a near constant difference of 5K with a nearly identical trend. This is demonstrated in Fig. 3.3. The existence of such a large difference in temperature over a height of perhaps 0.5m is very suspicious and highly unlikely. The near exact replication of the trend in conjunction with the error serves to strongly indicate that there exists a calibration error. A recalibration and/or reconfiguration of the in-built equation of at least this temperature logger would be prudent for continuing into the next season. To be of any use, all loggers should be recalibrated periodically.

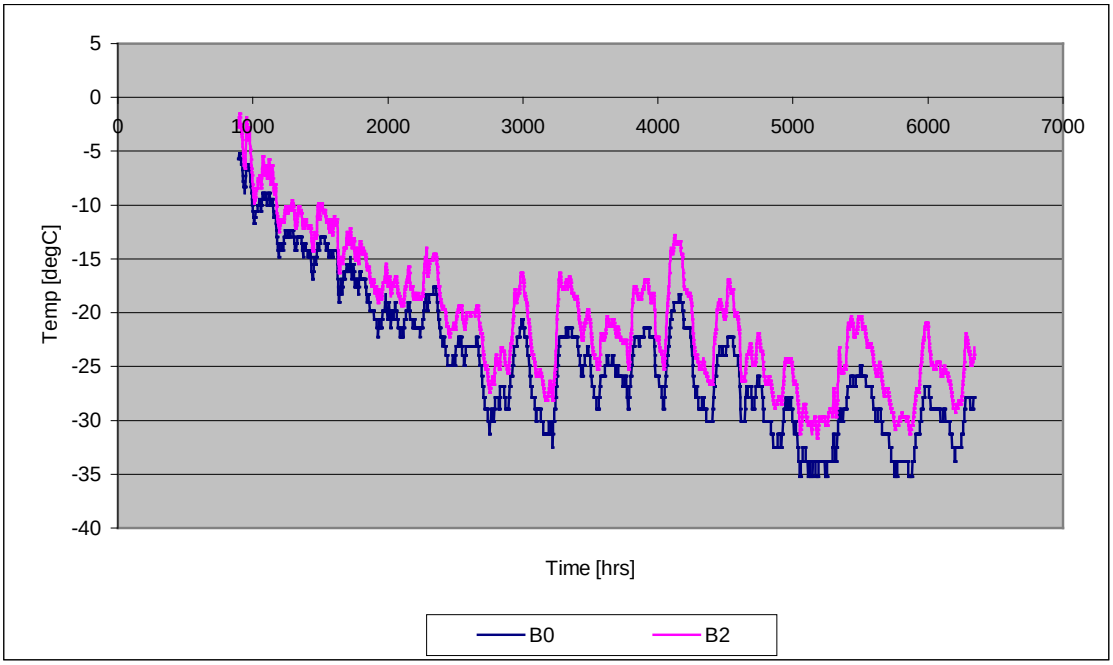

Figure 3.3: Comparison of logger B temperatures showing a clear differential between the data sets for the two probes on the same logger.

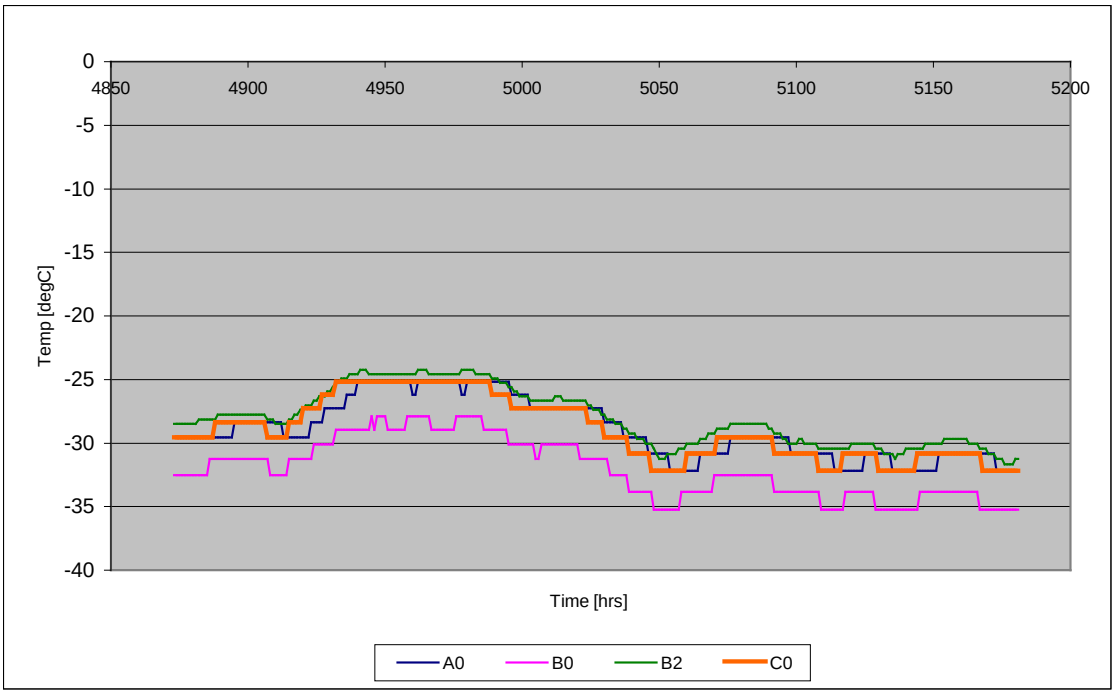

Figure 3.4: Close up on temperature data from various loggers. B0 stands out as being the lower trend in this comparison. While the individual trends are difficult to determine from this chart, it serves to show the similar trend for all but the B0 probe.

Comparison of the four interior temperature trends in Fig. 3.4 shows all but B0 to be fairly closely aligned.

3.4.3 Logger C Data

From the plot of the four temperature recordings, Fig. 3.4, we can see the good nature of the data for the internal probe which was positioned on the shelf in the darkroom. The external logger has quite a different trend, which is decidedly warmer than the rest of the temperature measurements throughout most of the recorded period, with a fairly smoothed rendition of the trend seen in the other files. This is shown separately in Fig. 3.5. The well boarded and insulated floor seems to be warmer than the inside of the hut. The temperature profile is much more smoothed than the corresponding hut temperature profile. This warmer, smoothed trend is due to the location of the probe near the thermal mass of the ground which responds slowly to external temperature change.

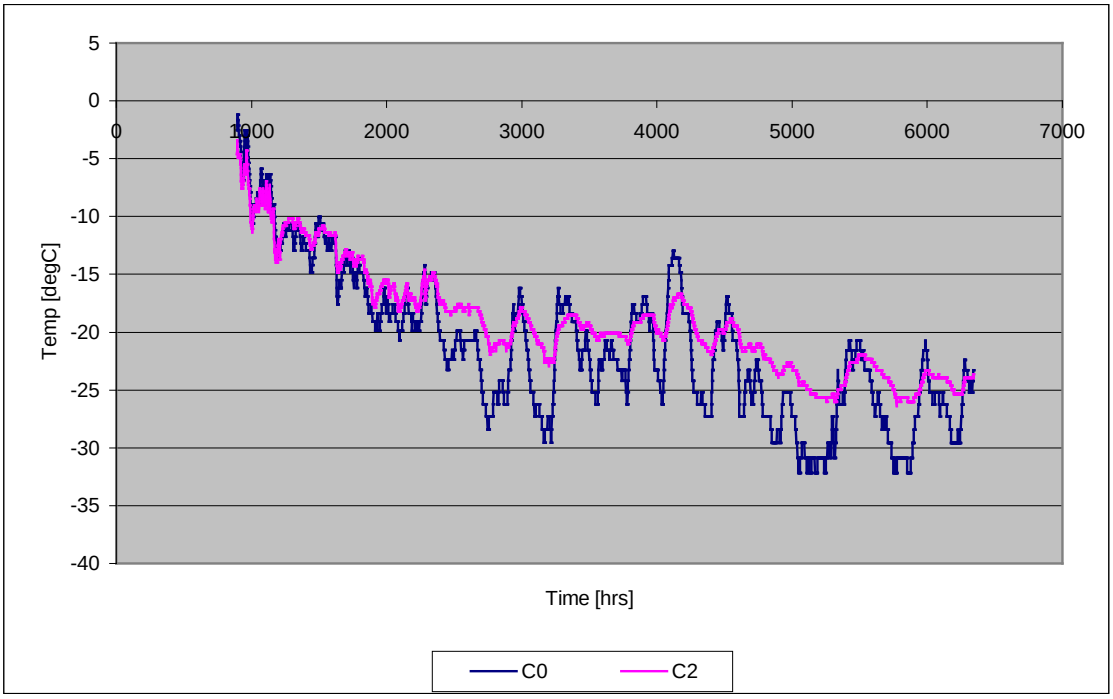

Figure 3.5: Plot of the logger C temperature probes, showing smoothed underfloor temperatures

3.5 Comparison of Indoor and Outdoor Climate

3.5.1 Temperature

As can be seen in Fig. 3.6, the temperature rarely rises above 0ºC at any time of the year at Cape Evans but inside the hut the conditions are influenced by solar radiation in the summer and may rise to 5ºC at times. At all times of the year, especially notable in winter when the sun is not present, the temperature follows external trend with the insulation of the hut dampening the magnitude of the variation.

It is not uncommon for the outdoor temperature to drop well below –40ºC in winter

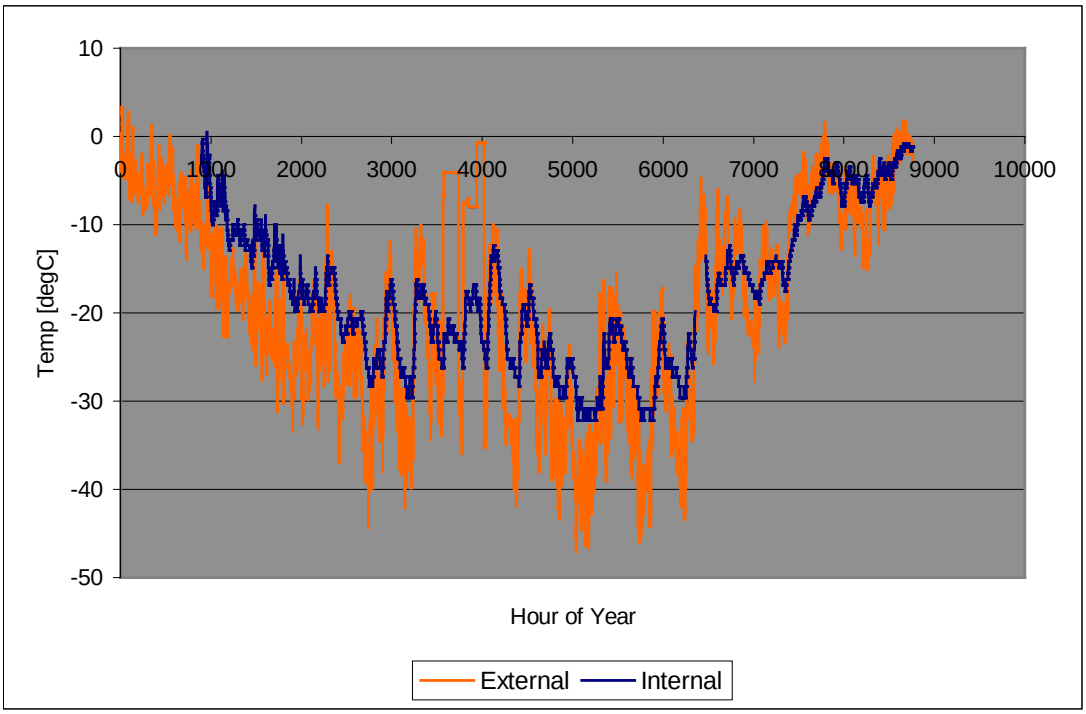

Figure 3.6: Raw temperature data for inside and outside the Terra Nova hut.

3.5.2 Relative Humidity

The external relative humidity over the whole year is shown in Fig. 3.7, with a moving average superimposed to clarify the trend. The relative humidity fluctuates between 60 and 80% with the occasional flutter to 50 and 90%. The period of the fluctuation is in the order of weeks.

When the smoothed trend of the external relative humidity is compared to the relative humidity inside the hut, Fig. 3.8, the reduction of the fluctuations in relative humidity becomes quite apparent. Inside the hut, the relative humidity of the inside air state is damped to a large extent due to the mass transfer processes that occur within the building.

The upward trend seen in Fig. 3.8 from the 6500 hour point onward demonstrates the natural rise of room relative humidity during spring, as the temperatures rise and the frequency of northerly weather patterns increases. This occurrence is discussed in more detail in the following Section 3.5.3.

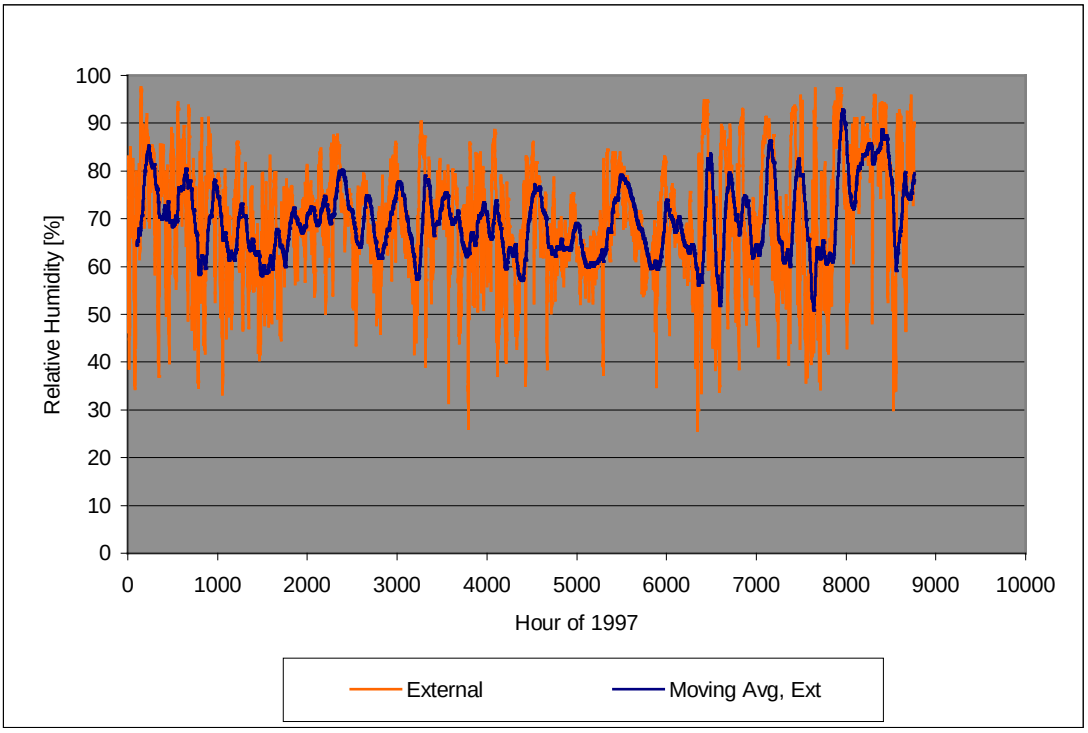

Figure 3.7: Plot of external relative humidity at Cape Evans during 1997

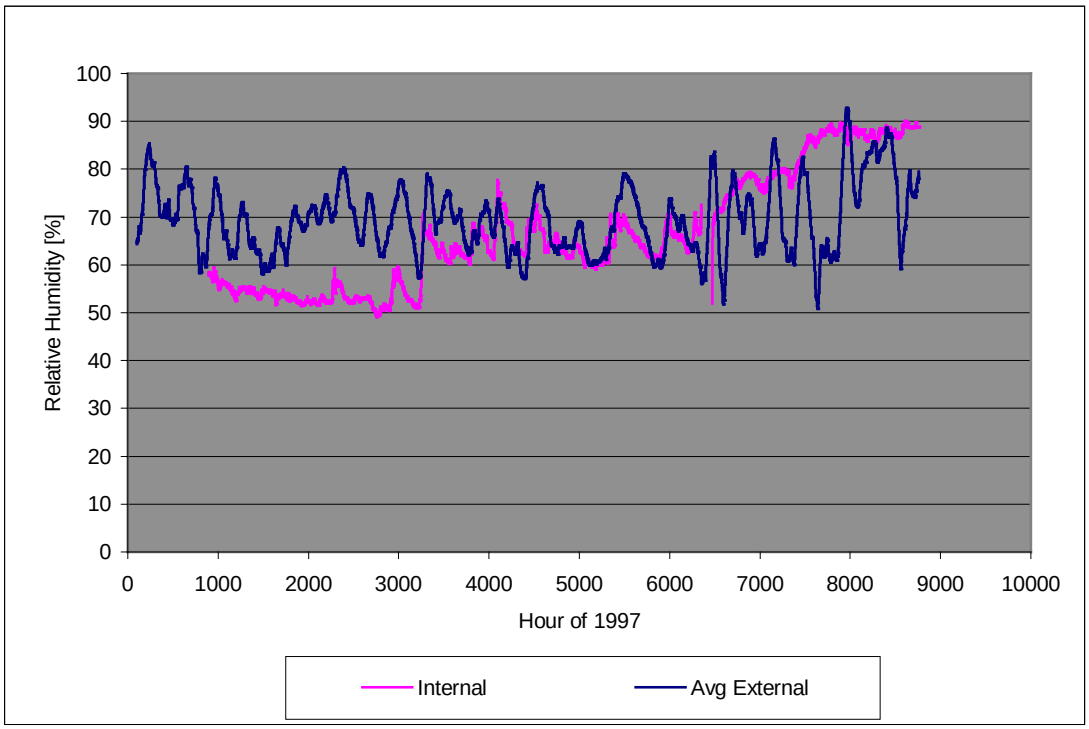

Figure 3.8: Relative humidity inside and outside at Cape Evans during 1997. Note the abrupt step in internal relative humidity which occurred during May (3300 hrs).

3.5.3 Observations from Data Trends

a) Sudden rise in relative humidity

Noticeable in Fig. 3.8 is the abrupt step in the indoor relative humidity at around the 3300 hour point, which corresponds to early May. The relative humidity rises by nearly 20% in under two days. Figure 3.9 provides a closer look at this period with the wind speed trend added. It seems a storm had closed in at Cape Evans from the Southern Ocean around this time. The external relative humidity had risen suddenly along with an increase in wind speed to around 30m/s coming from the north. This high wind speed has driven the infiltration above normal levels, and the replacement of dry air inside with the moist air outside was sustained for a long enough time to raise the equilibrium state of the building. When the storm died off, the high relative humidity level was maintained.

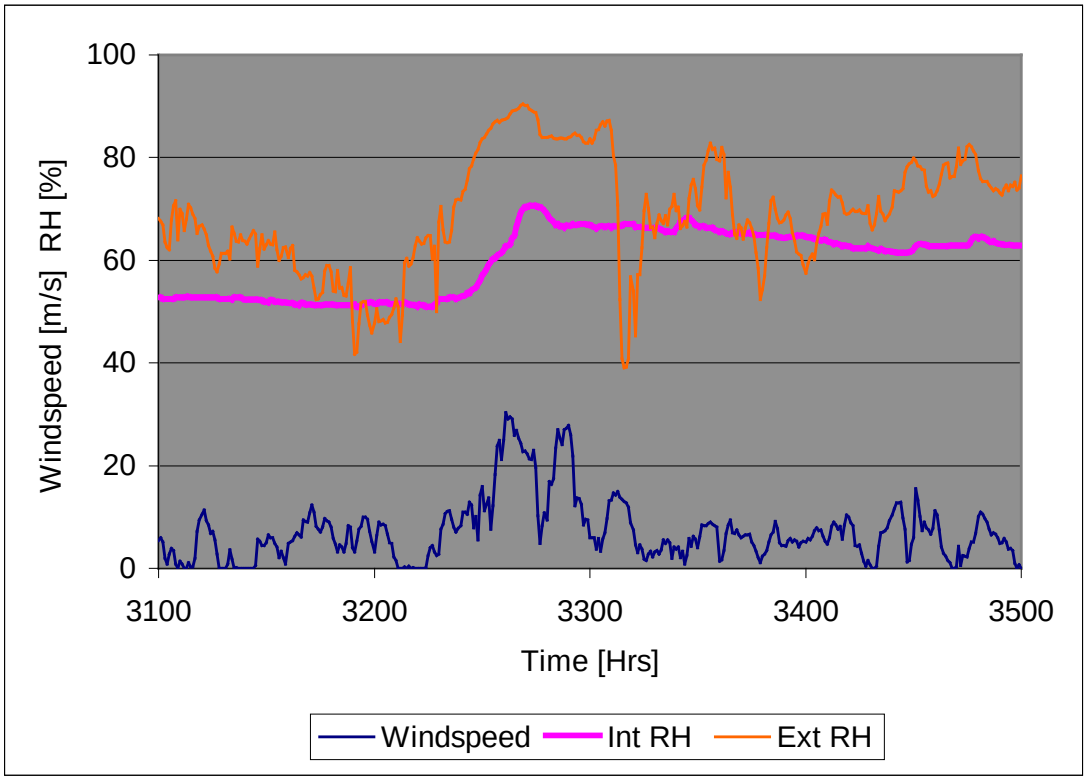

Figure 3.9: Local view of abrupt step in relative humidity inside the hut during May, 1997. The lower trend is windspeed in m/s.

This occurrence demonstrates the air-tight properties of the hut shell. If the building is considered as shelter for the inside air, the protective ability of the building is shown to be sufficient in all but stormy conditions. During normal weather, the smooth, damped nature of the room air state implies a reasonable level of protection.

b) Shell air-tightness

The air-tightness of the shell reflects in the data trends in that tight rooms are known to have low internal relative humidity fluctuations, independent of temperature and the temperature and vapour pressure trends track each other [Cunningham, 1994]. In loose rooms the temperature and relative humidity trends correlate inversely with each other and the internal and external vapour pressures are seen to follow each other not only in trend, but in magnitude

also. These relationships are explained by the hygroscopic damping from the materials in the room, which becomes less significant as the infiltration rate increases. The following Figures 3.10-3.12 serve to demonstrate that the data gives the impression of a air tight building.

A correlation of the data set was carried out in whole and in parts which allowed comparison of this result at different times of the year. An agreeable correlation was found only in data block two that had consistent conditions. The correlation coefficients do not allow for factors such as wind direction, which may have a distinct effect on how well the indoor and outdoor vapour pressures track.

The full correlation results have been included in Tables C.1 to 6, Appendix C.

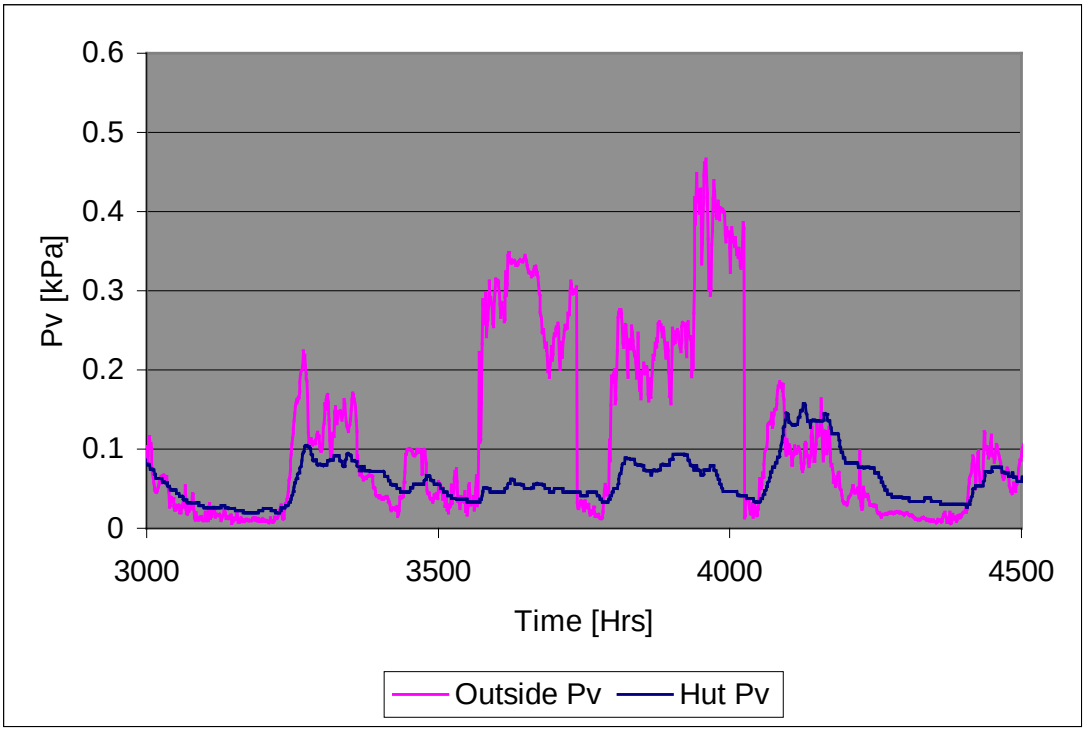

Figure 3.10: Internal vs. external vapour pressure. The internal P_v - whilst following the basic trend of the external P_v - does not approach the magnitude of the variation.

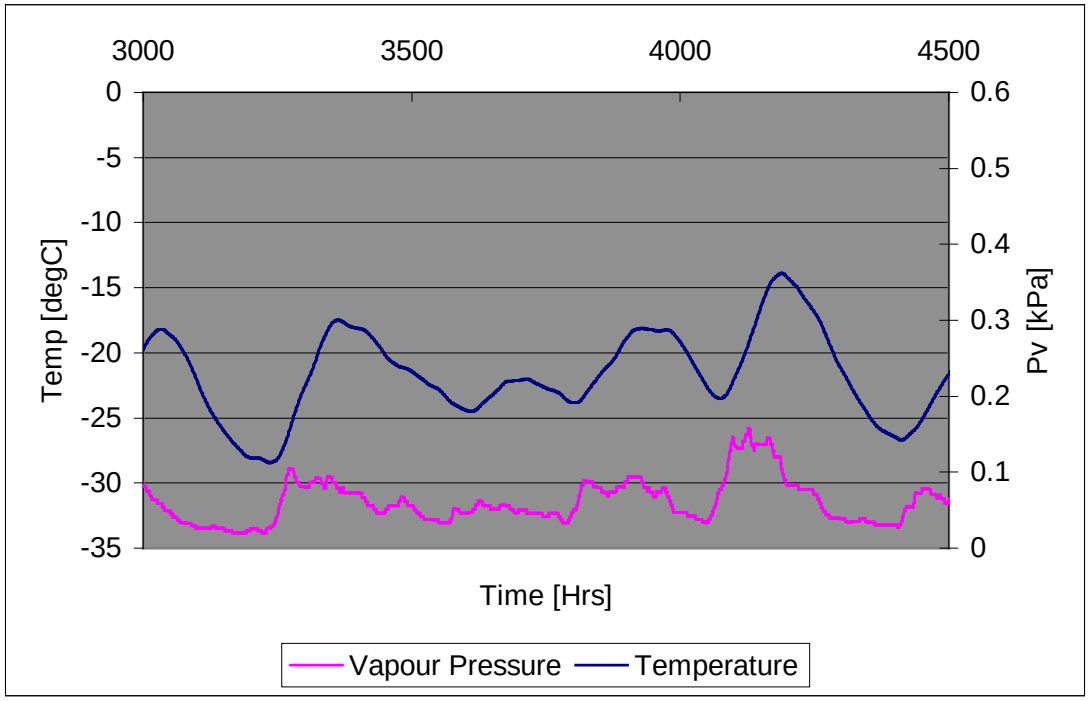

Figure 3.11: Internal temperature and relative humidity. The telltale sign of a tight enclosed space; independent relative humidity with minimal fluctuation.

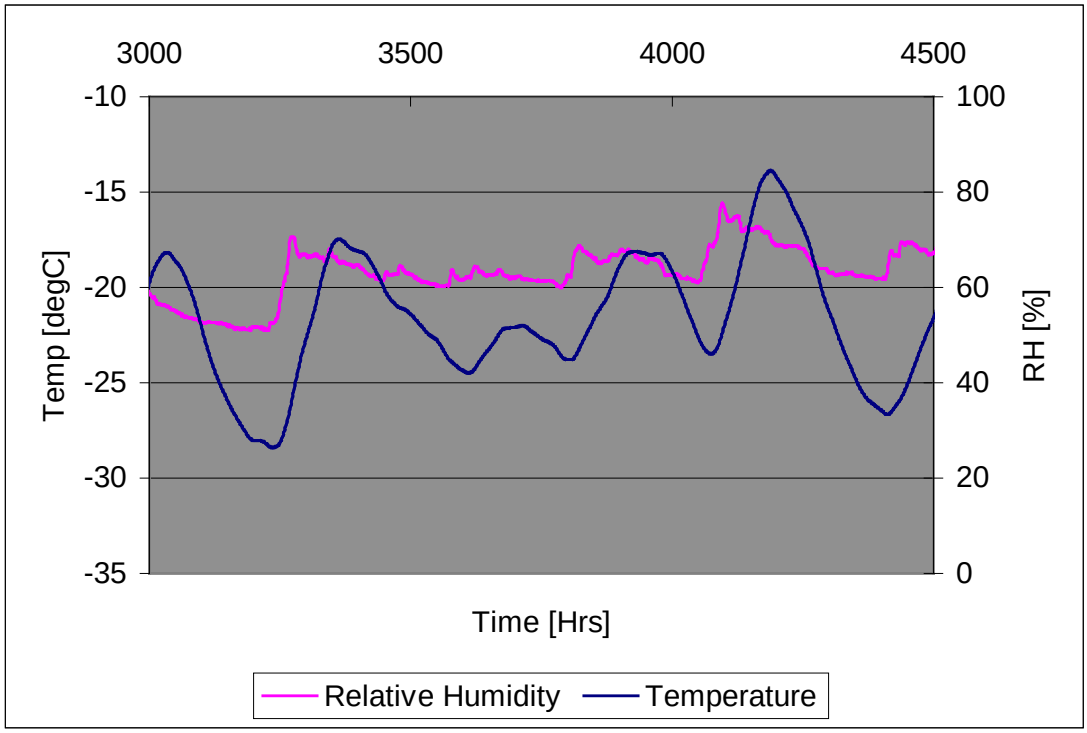

Figure 3.12: Good correlation between internal temperature and vapour pressure as a result of the small variation of relative humidity.

The sorption effect is demonstrated quite clearly in these data excerpts, so the room was known to be reasonably air-tight prior to the experimental phase.

3.6 Stratification

3.6.1 Introduction

Thermal stratification is related to the *stack effect*, where temperature differences exist between the inside and outside and the resulting pressure gradient promotes infiltration at low levels and an uprising convection current which can move contaminants around within the building.

3.6.2 Data Analysis

Figure 3.13 shows the trends of the temperature measurements taken within the hut at the different height levels all together, not giving any indication of thermal stratification in the measured zone.

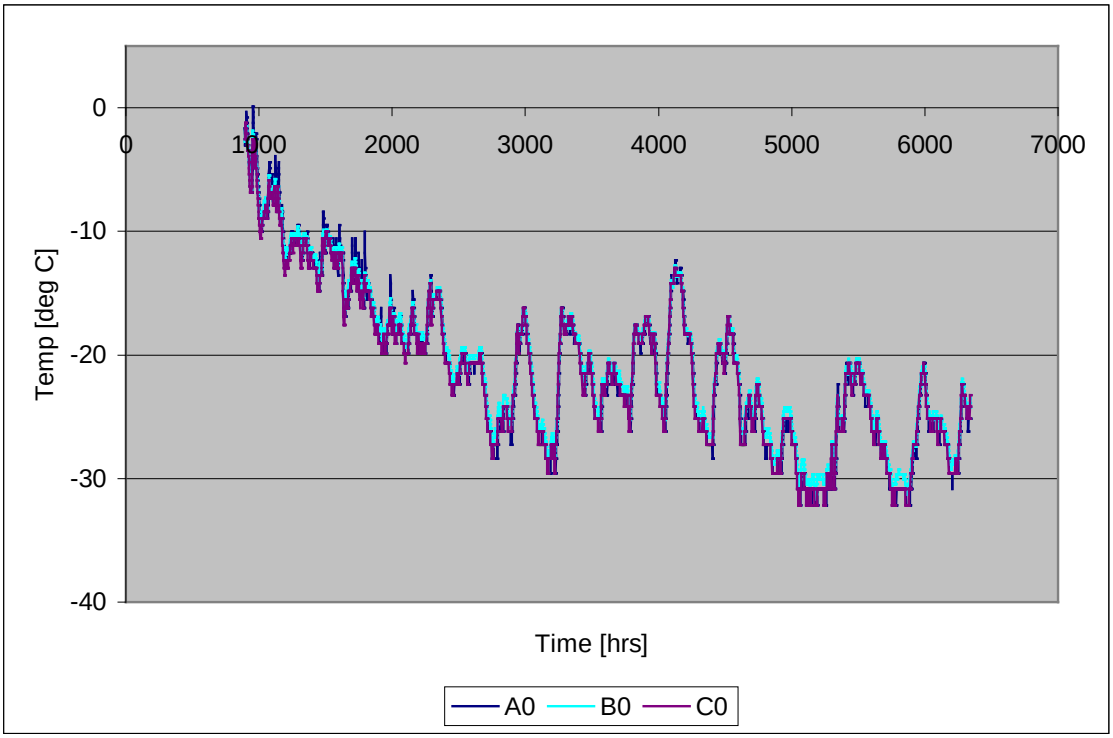

Figure 3.13: The trends of three room logger temperatures, exactly coincide, showing lack of significant thermal layering.

The combined trend of the inner temperatures, Fig. 3.13, shows that there is no noticeable thermal stratification occurring over the interval of the probes. The locations of the temperature probes were fairly closely spaced and the subsequent reshuffle of the probes may show up some better information, but this effect is not thought to be significant.

3.7 Occupancy Effects

3.7.1 Occupancy and the Room State

The visitor book signings for Cape Evans were meticulously counted for the 93/94, 94/95, 95/96 and 96/97 summer seasons. Later books were not available at the time of the study. The hut air state coinciding with several landing parties was examined for disturbance in the normal pattern.

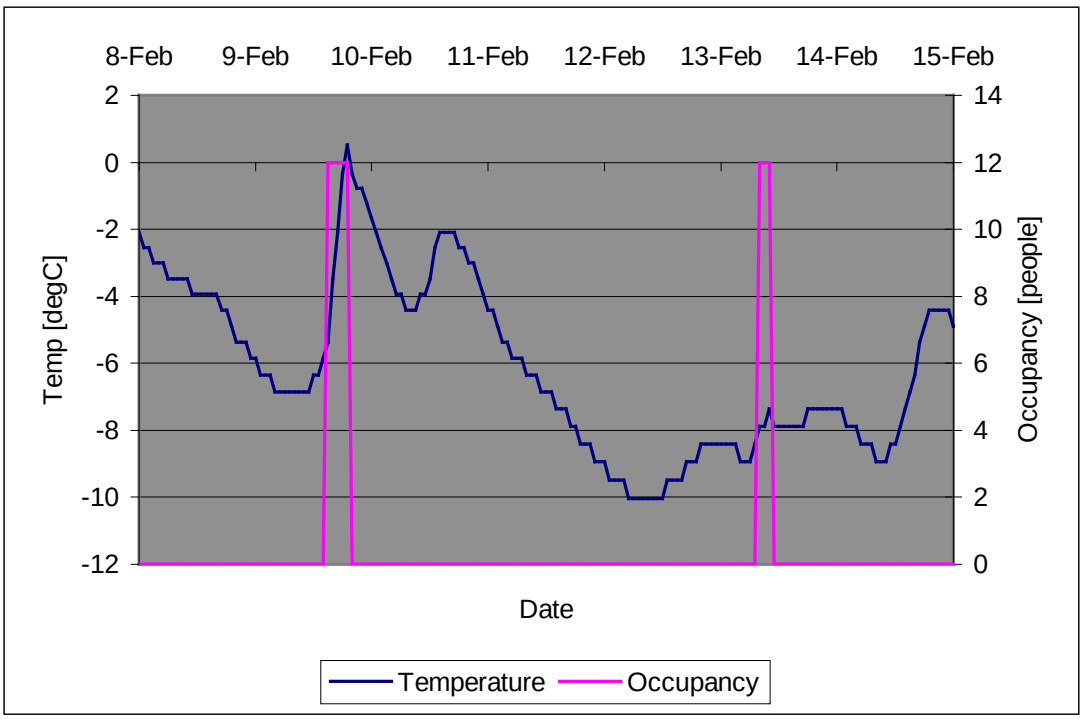

Figure 3.14: Visitor occupancy plotted against the indoor temperature of the *Terra Nova* hut. First visit by the *Bremen*, 124 passengers; Second visit by the *Kapitan Khlebnikov*, 97 passengers. Note double peak of Bremen visit.

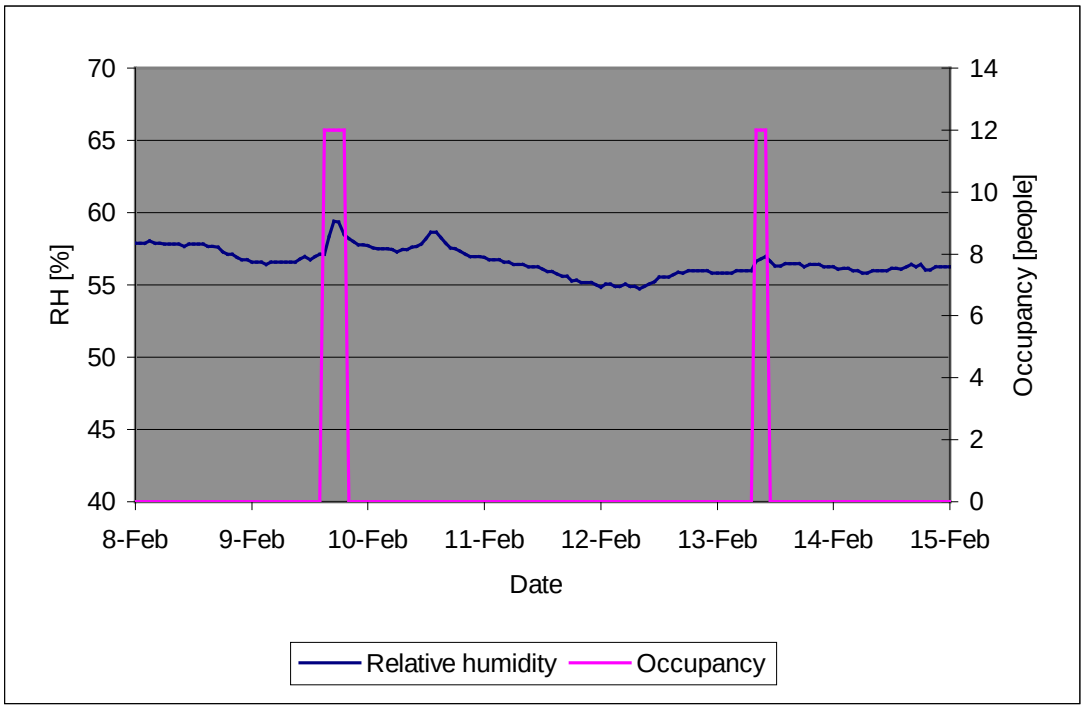

Figure 3.15: Visitor occupancy plotted against indoor relative humidity of *Terra Nova* hut.

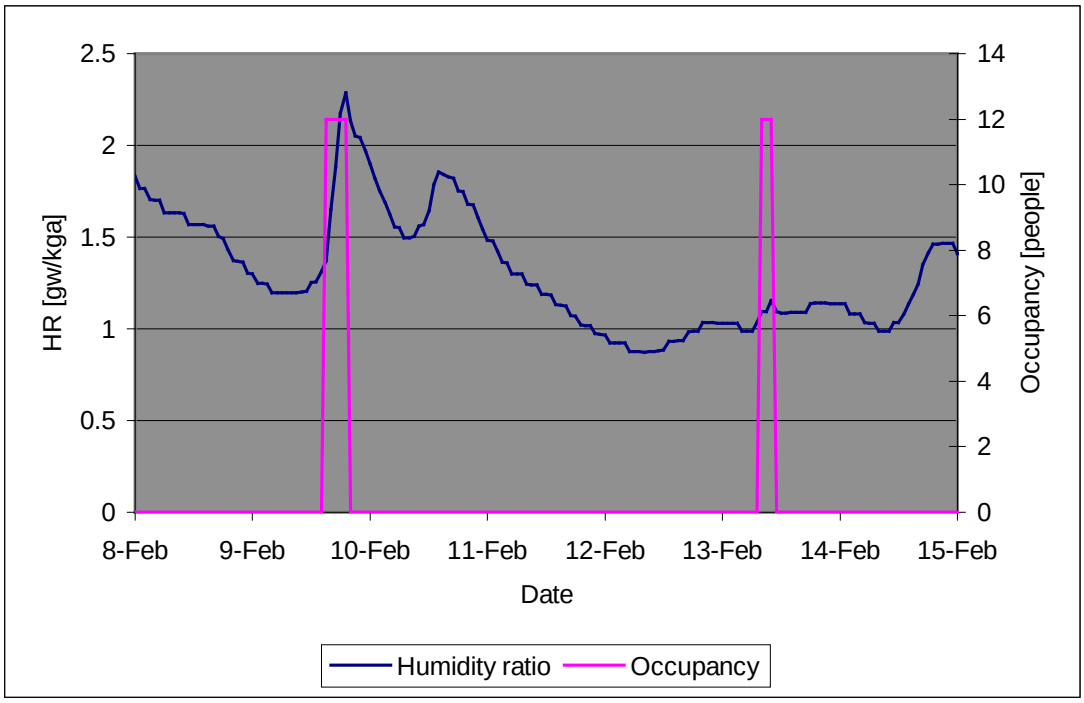

Figure 3.16: Visitor occupancy plotted against indoor humidity ratio, or absolute humidity of the *Terra Nova* hut.

A log including the details of the visitor book entries is included in Appendix C.

3.7.2 Discussion

Figures 3.14 - 3.16 are representative of the general influence the passengers of the visiting ships have on the room air state at Cape Evans. The trends describe a week in early February 1997, a typical late summer period with high visitor activity recorded in the hut book. During this week, two separate ships, the Bremen (9/2/97) and the Kapitan Khlebnikov (13/2/97) arrived at Cape Evans with 124 and 97 passengers respectively. Most ships arrive in the late summer when the sea ice has broken out from the shore and access is possible via inflatable rubber boats rather than expensive helicopter shuttles. While the visitor influence is covered in more detail in section two of this thesis, it is important to note the following observations from the data.

The visits marked in each of the Figures 3.14 – 3.16 with a spike of width equal to the recorded time of occupancy with 12 people present throughout this time. 12 people being the maximum occupancy allowed by AHT. The first visit showed a double peak in all three plots and it was assumed the Bremen stayed overnight and revisited the hut the next day.

The temperature inside the hut rose substantially during the passage of the tourists through the hut. Figure 3.14 shows a rise of 7ºC during the first Bremen visit, over a period of eight hours. The Kapitan Khlebnikov demonstrated a much smaller temperature rise with only 20% fewer passengers, which may be attributable to leaving the door open, as winds on the day were of similar magnitude and direction.

The relative humidity was not greatly disturbed by the influx of people to the hut as can be seen (noting the exaggerated scale of the plot) in Fig. 3.15. This is due to the combination of the moisture gain in the hut being largely offset by the rise in temperature. The absolute humidity rises during this time from 1.2 to $2.2 g_w/kg_a$ which equates to 0.5kg of water gained by the hut air. While it is

apparent that most of this gain would have come from respiration of the people in the hut, the rise in temperature would also have allowed the evaporation of any ice that was already contained in the building. The continual infiltration of dry, outside air means the net gain for 12 people over the 8 hour period is only 5g/person.hour, substantially less than the 40g/person.hour normal resting moisture rate [CIBSE 1986].

The peaks are noted in all figures to fall off as quickly as they rise, showing the effects of the mass transfer mechanisms in returning the air to the normal state. The magnitude of the disturbance from visitors is no greater than that from normal weather driven fluctuations seen throughout the collected data.

3.8 Wind Data

Wind data from NIWA was used in the modelling of the infiltration in the hut. The local wind pattern is most informatively and concisely presented in a wind rose [Blaisdell et al. 1998], which gives the wind speed, direction and frequency of each.

Being separated from the continent by the width of McMurdo Sound, Ross Island does not experience the full force of the katabatic winds that fade rapidly offshore, but exposure to the Southern Ocean means the likelihood of a good gale remains strong.

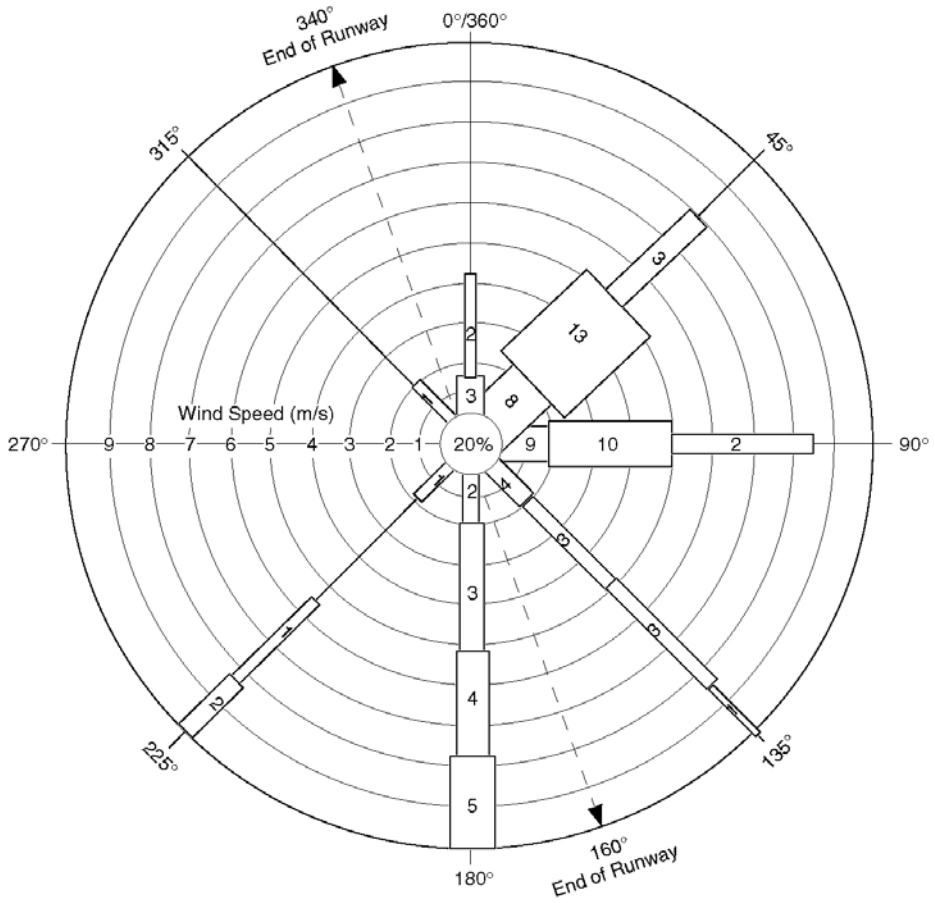

Figure 3.17: Wind rose from the Pegasus South automated weather station using monthly average data for the period 1 January 1993 to 31 December 1994. Note that this wind rose was not generated from the same data set as used in the project, but is from data recorded in the same locality. Source: CRREL monograph 98-1.

3.9 Chapter Summary

The data from the loggers that were installed in the hut was shown to be in good order, with the exceptions that have been noted. The influence of the building shell in damping the temperature and relative humidity variations has been shown to cause the internal micro-climate inside the building to differ substantially from the external climate; the sorption mechanism was seen to be effective in doing this. Northerly storms have been shown to influence the relative humidity inside the building to a great degree, especially heading into summer when the frequency of such storms appears to increase. The visitors

to the hut do not appear to make a huge impact on the temperature and relative humidity inside the hut, but a better documentation system would be necessary to track the effect of visitors more accurately.

Following naturally from the examination of existing data, Chapter Four sets out to describe the experimental phase, where the collection of information specific to the hut was carried out. This information was necessary to ensure that the model of the hut included appropriate values for key physical parameters.

CHAPTER FOUR

EXPERIMENTAL WORK

4.1 Introduction

The loggers, as described in Chapter Three, provided a good history of the psychrometric state of the interior. A base of knowledge about the shell of the building was also needed so that a prediction of the water mass passing in and out of the control volume[4] could be calculated with the indoor humidity model. The experiments included:

- Physical measurements; hygroscopic area, occupied volume (§4.2)
- Moisture content survey of the walls and floor (§4.3)
- Insulation resistance of the walls and roof (§4.4)
- CO_2 decay infiltration testing (§4.9)
- Blower door infiltration testing (§4.10)

The amount of salt deposition occurring in the huts was measured (§4.11), along with the analysis of the seagrass insulation (§4.5 – 4.7) to provide data of possible value in the corrosion prevention work. The general construction survey conducted during the time in the field, was not deemed to be particularly

[4] The control volume, where mass is conserved over a specified time period, was defined to contain room air only.

insightful in this thesis but is covered in the Antarctic Heritage Trust Field Report [Mason 1999].

4.2 Physical Measurements

4.2.1 Hygroscopic Area

The area of wooden material that participates in the sorptive exchange of moisture with the room state air was calculated. This process was simplified by approximating each type of timber board and post to be of a particular width. The number of boards of a particular length were counted and multiplied by the standard width to give the area, and then summed overall. Hygroscopic material other than the wooden hut lining and contents was neglected due to the vast area of the walls, floor and ceiling outweighing the minor surface area presented by the artefacts.

4.2.2 Occupied Volume

The room air volume was calculated on the basis of the total hut volume with the volume of the artefacts occupying the room subtracted from that. Approximations were carried out in a similar manner as in §4.2.1 above.

Table 4.1: Timber surface area inside Scott's hut

Item	Quantity/ Length	Surface area [m^2]	Notes
Boxes	80	48.56	*using a Vanesta box, 500Lx330Dx240H
Tables	3	17.67	Measured all tables
Boards	211m	29.56	Approx based on 120x20xL
Posts	66.4m	9.96	Approx based on 75x75xL
Trusses	4	4.85	Measured all trusses
Total Surface Area		**110.6**	

Table 4.2: Occupied volume inside Scott's hut

Item	Quantity/ Length	Volume [m^3]	Notes
Boxes	80	3.17	*using a Vanesta box, 500Lx330Dx240H
Tables	3	0.27	Measured all tables
Boards	211m	0.51	Approx based on 120x20xL
Posts	66.4m	0.37	Approx based on 75x75xL
Trusses	4	1.25	Measured all trusses
Total occupied volume		**5.57**	

4.3 Moisture Content Survey of Materials

4.3.1 Aim

Measuring the moisture content of the timber provides necessary information for refining the timber sorption model as well as giving a general indication of the areas that are exposed to external water sources.

4.3.2 EMC Readings

The equilibrium moisture content (EMC) is defined as the moisture percentage of the dry product. The relevance of the EMC is largely determined by the sorption properties of the material. For pine, the EMC is graded as follows, in terms of potential degradation:

0-14% Dry timber; varying from not possible to not likely to rot. This is the most likely range of MC corresponding with the atmosphere at typical values.

14-20% Medium MC; Mould is possible.

20-30% Danger zone; Mould is likely in a warm climate. In Antarctica, the cold prohibits mould growth except for high summer and very high MC's. MC is reaching the top of the sorption curve.

4.3.3 Apparatus

A *Protimeter digital mini*, hand held timber moisture content (MC) meter was used. This instrument provided quick and simple resistive moisture contents based on Douglas Fir which could be related to other timber species through the use of a set of tables. The instrument did not have driven pins like some types of wood MC meter, helping prevent damage to the timber. MC meters are not known for their high accuracy, but provide good indicative results using a non-destructive technique. A calibration standard was included with the device (an accurate, single-point resistance comparison) with which the meter was periodically checked during use and found to agree well with. The instrument was kindly lent by Mr. Murray Drake, of the Christchurch City Council, Building Inspectors Team.

4.3.4 Results and Discussion

a) Walls

The key to the wall locations is shown in Fig. 4.1.

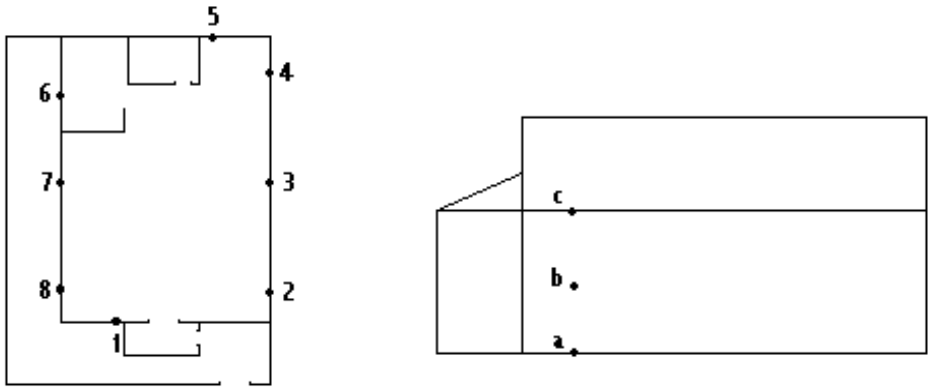

Figure 4.1: MC Measurement locations at Scott's Hut.

Table 4.3: Inside wall moisture contents

Location	a	b	c
1	16.4	14.6	15.4
2	19.9	12.7	11.7
3	25.6	16.2	11.8
4	29.2	16.3	16.1
5	17.9	13.5	13.5
6	17.7	14.6	12.6
7	23.2	14.4	11.6
8	27.4	17.8	13.5

The lower skirting (level a) of the building can suffer very high moisture contents in direct contact with the ground resting snow, ice and melt water. Points 3a and 4a had visible ice forming on the linoleum.

Areas of high MC were far more common at Cape Evans than at Cape Royds. The difference is likely to be attributable to the more abundant melt water at Cape Evans.

Table 4.4: Outside wall moisture contents

Location	a	b	c
1	20.0	14.2	22.5
2	27.5	16.4	13.2
3	30.0	12.4	8.8
4	29.4	13.0	10.0
5	8.9	9.0	10.2
6	23.3	12.5	n/a
7	27.5	14.9	n/a
8	21.5	20.5	n/a

The moisture contents found outside confirmed a mapping of the snow and ice build-up against the walls, which wicks through the timber with capillary action. High readings outside generally were found to coincide with high readings in the corresponding location inside.

b) Ceiling

A survey of the perimeter and midpoints of the ceiling found a good consistency of readings typically around the 12.5% mark. The ceiling and roof are not seen as a significant moisture source.

c) Floor

The floor is covered by a partially intact linoleum layer through which fragmented measurements were taken. Readings averaged around the 20% mark with a high of 27.8% in the entranceway, where walked-in dampness may have had a contribution.

4.4 Insulation Resistance

This test measures the heat flow through the wall (or roof) with a given temperature potential and is used to determine the one dimensional thermal resistance of the structure. This measurement helps to define the thermal properties of the building for thermal modelling or surface temperature calculations.

4.4.1 Apparatus

a) Hot Box

An enclosure was designed to allow local heating of 1m^2 wall area as the entire room space could not be heated for artefact conservation reasons. The enclosure was heated with a 1200W fan heater, modified for variable power input through an adjustable waveform-modifying circuit, similar to a light dimmer. The hot box was propped to hold it firmly against the wall, sealing with closed cell foam strips along the edges. The differential temperature of the wall was measured with a pair of Yokogawa digital thermometers.

b) Heat Flux Transducer

A International Thermal Instrument Company heat flux transducer (HFT) was sourced which indirectly measures the heat flow between its outer surfaces via a differential output generated across a wrapped thermopile. The heat flux is determined from Fourier's Law of one dimensional, steady state heat conduction.

$$\dot{q}_x = -kA\frac{\partial t}{\partial x} \qquad [4.1]$$

In a thermal series circuit, the heat flow through the HFT is assumed to be equal to that through the wall. Output was measured with a Fluke mV meter, the HFT conversion was a linear 23.5W/m^2.mV.

The calibration check of the heat flux transducer and assembled apparatus was carried out in the laboratory and is included in Appendix C. More information on the use and performance of heat flux transducer's can be found in ASME [1991], Trethowen [1986a], Trethowen [1986b], Isaacs [1986] and Trethowen [1990].

4.4.2 Method

The heat flux transducer was taped to the inner wall in the relatively open galley region after moving Lashly's bed frame. To the exposed side of the heat flux transducer and to the corresponding outer wall, thermocouples were connected. This section of the wall was assumed to be representative of the general construction. The hot box enclosure was mounted centrally over the area, and was heated to provide a minimum 20ºC differential with respect to the ambient outside temperature.

A settling time of about ¾hr appeared to be sufficient to heat through the elements of the compound wall. Thermocouple and HFT readings were taken from the start time, so that the approach of the heat flow to steady state conditions could be observed.

The somewhat excessive weight of the enclosure meant it was placed on the roof (for the ceiling measurement). Failure to give output revealed the pitfalls of using the HFT outside, in that it suffered from radiation heat transfer to the cold ambient air which counteracted the conduction heat flux and nulled the output. The HFT was then moved to the inside surface where it performed well. The lesson learnt was that the heat flux transducer must always be attached to the inside wall.

4.4.3 Results and Discussion

The R-value for the wall was taken as an average of the two test results;

$$R_{wall} = 0.282 \text{ m}^2\text{K/W}$$

$$R_{roof} = 1.17 \text{ m}^2\text{K/W}$$

The wall result seemed very low for this type of construction. The insulation resistance test results of the wall did not lie within the expected region (comparison is made to tabulated figures [ASHRAE, 1989a]), even though the test was repeated twice with a similar outcome. Saturated insulation alone is not enough to reduce the value to this extent. The wind was recorded as averaging 10m/s (35 km/hr) at the time of the wall test and may have influenced the results unduly. Assuming the heat flux measured was excessively high, the actual heat flux through the heat flux transducer would have had to have been greater than that through the wall. This indicates a lack of steady state condition at the time of the experiment, ie. the wall was not in thermal equilibrium with the hot box temperature.

Figure 4.2 shows the heat flux through the wall had not quite bottomed out and it may have continued dropping slowly for quite some time, meaning the test was called short. [In retrospect, the data from these tests should have been analysed during the tests themselves. This would have provided an immediate alert that steady state had not been achieved and the test duration could have been lengthened – although it is by no means certain that a sufficiently long test would have been achievable within the constraints that existed.]

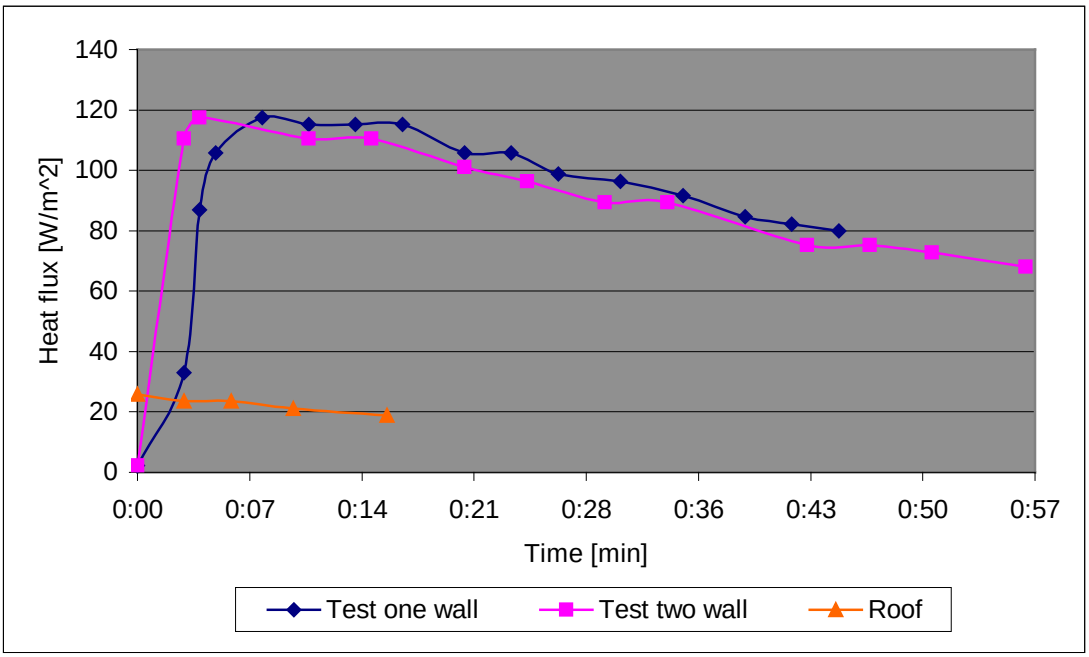

Figure 4.2: Heat flux measurements showing repeated high wall flux and more typical flux measurements through the roof.

The roof value is much more typical of what might have been expected and, given the similarity in construction of the roof and walls, typical of what was expected of the walls.

The full set of data for this experiment can be found in Appendix C.

4.5 Seagrass Identification

A small sample of the sea-grass used as insulation was collected by Ms. S. Easdale (in 1997) and brought back to be identified and analysed to determine the moisture and chloride content. Dr. Paul Broady from the Department of Plant and Microbial Science at the University of Canterbury quickly identified the sample as being a Sea-grass, or more specifically Eel-grass, likely of the species *Zostera* [Clayton and King, 1990].

4.6 Sea-Grass Moisture Composition

4.6.1 Introduction

The accurate modelling of the insulation as a moisture transfer layer of the wall depends on the known steady state moisture content. The number of years between when the sample was removed and when the testing was carried out could greatly influence the results in this test due to the potential for drying or moistening away from the removal state. The sample was stored in a sealed plastic bag during this time.

4.6.2 Method

The sample was weighed, then dried in an autoclave at 104ºC in steps of three hours, and reweighed until the sample showed less than 1% mass reduction.

4.6.3 Results and Discussion

Table 4.5: Mass reduction during drying of sea-grass sample.

Drying Mass and Water Composition			
	Initial	First Period	Second Period
Crucible only	59.3980g		
Crucible + sample	61.2905g	61.0283g	61.0157g
Sample weight	1.8925g	1.6303g	1.6177g
Mass reduction		0.2622g	0.0126g
Percent reduction		13.85%	**14.52%**

With less than 1% change in mass reduction, the final dry weight shows a 14.5% water composition. The moisture content of the insulation is at a similar level to what would be expected of timber in a similar environment. It therefore seems reasonable to assume that the seagrass would have a pendular limit similar to that of timber, ie. around 30%. The conclusions that could be drawn from this test were limited by the two year time period between when the sample was extracted and then tested.

4.7 Seagrass Chloride Content

4.7.1 Introduction

Salt concentration in the insulation acts as an indicator to the levels of salt in the air and may enhance the moisture transfer properties of the insulation. ASME C871-95 [1995] provides a standard method for obtaining specimen from bulk quantities of insulation but the small sample size available prohibited strict adherence. The standard provides for many sample testing methods, of which mercurimetric titration proved most convenient as it coincided with the ISO 9225 [1992] recommended method.

4.7.2 Method

In this standard method, the sample is dried completely, then boiled in distilled water for 30 minutes to leach the salt into solution. The solution is cooled and diluted to 100ml before being titrated against a standardised solution of Mercuric (II) Nitrate [Analar 1984: 451-2]. A full description of the mercurimetric method and equipment required can be found in Vogel [1989: 346-7].

Three samples were taken to ensure repeatability in the results. The results derived from this method assume that the chloride content is entirely due to association with the sodium chloride salt. In preparation of the mercuric nitrate solution, it was first titrated against a standard solution of sodium chloride, to determine the exact concentration. 12.2ml $Hg(NO_3)_2.H_2O$ solution was required to neutralise 10 ml of the salt solution, corresponding to the stoichiometry:

$$Hg^{2+} + 2Cl^{-} \Leftrightarrow HgCl_2 \qquad [4.2]$$

The molarity ratio provides for the following equivalency:

$$V_{NaCl}.c[NaCl] = 2.V_{Hg}.c[Hg(NO_3)_2] \qquad [4.3]$$

Thus, from equation 4.3 the concentration of the mercuric nitrate solution is found:

$$\frac{12.2}{10} = \frac{1}{2}\left(\frac{0.025}{c}\right)$$

$$c\ [Hg(NO_3)_2.H_2O] = \underline{0.01025\ M}$$

This known concentration of mercuric nitrate was then titrated against the unknown salt solution in three individual tests. The burette used had a resolution of 0.05ml.

4.7.3 Results and Discussion

Table 4.6: Results of mercurimetric titration.

Test	Vol. of Mercuric Nitrate solution
1	5.55
2	5.50
3	5.60
Average	**5.55 ml**

This can be directly related to the mass of sodium chloride in the sea-grass sample using the relationship between the mercuric nitrate solution equivalence volume and the mass of the salt in 100ml of standard solution.

$$\frac{12.2}{5.55} = \frac{0.1506}{m}$$

$$m = 0.0685\text{g}$$

$$\frac{0.0685}{1.6177} \times 100 = \underline{4.2\%\ m/m}$$

In proportion to the dry weight of the sea-grass sample, the sodium chloride salt constitutes 4.2% by mass.

It was also found by testing with both a single diphenylcarbazone indicator solution and a mixed diphenylcarbazone and bromophenol blue indicator solution that the mixed indicator presented a sharper appearing endpoint in the titration and was the preferred choice.

4.8 Infiltration

To model the indoor air state, the air exchange between the indoors and outdoors needs to be calculated. With no mechanical or otherwise ventilation by design existing in the building, the only mechanism left is infiltration.

Infiltration is the undesired exchange of air between the building and the outside environment, caused by wind and thermally driven pressure gradients between across the shell. Small gaps existing in any constructed composite surface will allow the passage of air with this driving force present. Infiltration is a strong function of the construction method used and is variable even within buildings of similar construction due to these adventitious openings, therefore site evaluation was necessary for an accurate model.

Infiltration is usually specified in terms of air changes per hour (ACH), or how many times in one hour the volume of air in the room (zone) is replaced with outside air. Infiltration theory is covered in more detail in Chapter Six.

4.9 CO_2 Tracer Decay Method

A common way of determining the air exchange in a single zone is through measuring the concentration of an introduced tracer gas over time. This type of test gives an infiltration value that is specific to the conditions present on the day of testing, rather than only to the building shell, ie. the greater the wind or temperature differential, the greater will be the infiltration rate indicated by the test.

4.9.1 Tracer Gas and Instrumentation

Carbon dioxide (CO_2) was chosen due to being the cheapest and most convenient tracer gas, complemented by the availability of good portable instrumentation for measurement. CO_2 is naturally occurring in the atmosphere but comprises only a very low percentage (around 0.033% or 330 ppm). It is non-toxic although the short term (any 15min/day) exposure limit for safe exposure (in terms of human metabolism) is 30,000ppm due to asphyxia complications [OSH 1999].

Carbon dioxide levels in the air up to 5000ppm were detected with the TSI Inc. *Q-Trak* Model 8551 Indoor Air Quality (IAQ) monitor [TSI 1999a]. This hand-held instrument utilises a non-dispersive infrared (NDIR) sensor which measures carbon dioxide concentration by relying on one of the natural properties of CO_2 molecules. CO_2 molecules absorb light at a specific wavelength of 4.26 μm. This wavelength is in the infrared range. High concentrations of CO_2 molecules absorb more light than low concentrations [TSI 1999b]. The IAQ monitor also comes with a comprehensive data analysis software package.

Figure 4.3: TSI handheld indoor air quality monitor, being downloaded at Scott's hut.

The wind speed was measured over the duration of the test using a cup anemometer, the calibration for which can be found in Appendix C.

4.9.2 Method

a) Options

There were several methods possible [Liddament and Thompson 1983, ASTM 1993] for the tracer gas measurement of infiltration in a single zone:

- Constant concentration
- Constant emission rate
- Concentration decay

The constant concentration method uses a feedback controller to maintain an elevated concentration of CO_2 in the zone air, meaning the infiltration rate is directly proportional to the tracer gas injection flowrate.

The constant emission rate is generally used to determine long term time averaged concentration where the released gas ideally forms an equilibrium condition, and then the flow rate of tracer gas becomes directly proportional to the infiltration rate as in the constant concentration method.

The most straightforward method is the concentration decay measurement, where a single point release is mixed into the room air and the concentration decay is measured over time. The infiltration rate is then given by the logarithmic gradient of the resulting decay curve, as in equation 4.4.

$$C_t = C_0 . e^{-\frac{Q}{V}t} \qquad [4.4]$$

The concentration decay method was subsequently chosen for simplicity and reliability with the testing programme being in such a difficult environment.

b) Procedure

The CO_2 was released into the building from regulated cylinders via a ring main and star configuration of PVC tubing. The ring main was intended to equalise the pressure in each line and make for more even distribution within the room. The air was fanned manually using a large sheet of plastic until the concentration built up to a sufficient level, and then the room was left closed for a period of several hours for the CO_2 concentration to decay uninhibited.

The data was downloaded from the *Q-Trak* into unformatted text files via a laptop computer and an RS-232 link cable. Back at base, the data was then imported into an Excel spreadsheet where it could be plotted and fitted to an exponential function using regression methods.

Four tests were successfully completed during the few days available at Cape Evans.

4.9.3 Results and Discussion

Table 4.7 lists the infiltration rates, in air changes per hour, calculated from the data along with the corresponding wind speed and regression constants according to Eqn 4.4, rearranged as

$$\ln C_t = -At + \ln C_0 \qquad [4.5]$$

Table 4.7: Infiltration measured at Cape Evans using CO_2 decay

	A [1/s}	ln C_0	Regression Coefficient	Windspeed [m/s]	Infiltration [1/hr]	ACH50 [1/hr]
1	0.000132	7.489	0.82	10.7	0.4756	9.51
2	0.000095	7.935	0.96	4.4	0.3406	6.81
3	0.000038	7.926	0.95	1.2	0.1364	2.73
4	0.000085	6.858	0.68	9.9	0.3053	6.11

The ACH50 values in Table 4.7 relates to the infiltration as measured by the 50Pa blower door test by a *rule of thumb* calculation [ASHRAE 1989a]. The blower door infiltration is generally equal to the natural infiltration multiplied by 20.

The decay of the CO_2 concentration did not follow an exact exponential path due to difficulties with mixing the gas evenly into the air, and uneven infiltration from different areas in the building. The results have been obtained from a best fit correlation and as can be seen in Fig. 4.4, the best fit of all the data sets (R^2 = 0.96 in test two) was a very close approximation to the actual decay. Test four had the most erratic decay and a correlation coefficient of, R^2 = 0.68 was obtained.

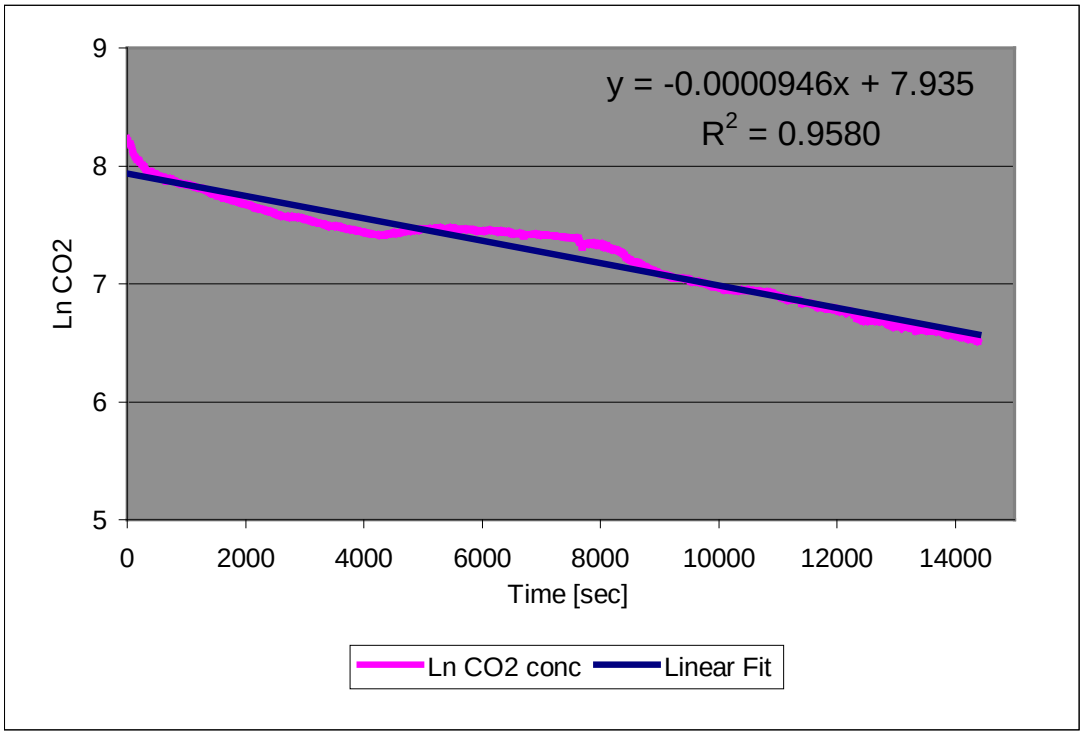

Figure 4.4: Chart showing exponential decay test two at Scott's hut. Inset shows the linear correlation equation relating to the natural logarithm of the CO_2 concentration and correlation coefficient.

A natural infiltration rate of 0.3 ACH indicates a reasonably airtight shell, as seemed apparent when visiting the building. ASHRAE Standard 62 [1989b]

characterises a building into a leakage class based on ventilation requirement if the building was occupied. As shown in Table 4.8, Scott's hut at Cape Evans would fall between leakage class B and E, depending on wind speed of the day.

Table 4.8: Characterisation by leakage class. *Source: ASHRAE Standard 62. [1989b]*

Leakage Class	Minimum NL	Maximum NL	Typical ACH50	Description*
A	0	0.10	1	Very Tight
B	0.10	0.14	2	Tight
C	0.14	0.20	3	Tight
D	0.20	0.28	5	Moderately Tight
E	0.28	0.40	7	Average
F	0.40	0.57	10	Moderately Loose
G	0.57	0.80	14	Loose
H	0.80	1.13	20	Loose
I	1.13	1.60	27	Too Loose
J	1.60			Excessively Loose

* Interpretation provided by author, not derived from source.

For comparison, a residential building would require a leakage class of A or B in the severe Antarctic climate, but this classification is more for energy loss reasons than moisture.

4.10 Blower Door De/Pressurisation Test

4.10.1 Introduction

As seen above in the results for the tracer gas infiltration test, the infiltration is dependent on the wind and thermal conditions of the day. The blower door pressurisation/depressurisation test [ASME 1987a] largely overcomes this downfall by measuring the infiltration with a fixed 50Pa pressure differential applied across the building envelope. In this way, the test provides a much more consistent picture of the air leakage properties of the shell. This test was intended for Cape Evans but failed due to technical difficulties at the time.

The information that this test would have provided was estimated instead from the four CO_2 decay infiltration tests that were carried out. The number of CO_2 tests in different conditions allowed the model to be adjusted to best reproduce the infiltration rates with similar input conditions. Put simply, rather than have a single well-defined parameter, the model was fitted to a set of lesser data. This was found to be quite sufficient given the poor nominal accuracy (±25%) of the model.

Much emphasis was placed on this test at the time and this thesis would be incomplete without a brief mention of the intention to carry out this experiment. The blower door apparatus was kindly loaned by the Building Research Association of New Zealand.

4.10.2 Apparatus and Method

The blower door itself consists of a large fan mounted in an adjustable, replacement door that fits into the existing frame. The fan motor is controlled by an AC variable drive from which the speed can be adjusted or ramped manually. To determine the air flow rate into the room and thus the infiltration, a venturi flow tube attaches to the fan and is calibrated in terms of differential pressure (DP) measured across the venturi. An additional DP transducer or inclined manometer was required to measure the inside/outside pressure difference.

The blower door is fitted and sealed against the door frame and run at discrete steps over a speed range. This causes the inside/outside pressure difference to span the 50Pa value, and the flow rate is recorded at each of these points. A still day is required in which to perform the test as the shell DP is prone to fluctuate uncontrollably when the wind blows.

4.10.3 Technical Difficulties

The blower door failed to operate when the equipment was initially set up. The blower door fan motor would start, but shut down before reaching full speed.

Testing of the generator mains output revealed a regulator problem, where the frequency of the supply fluctuated erroneously. A newer generator was brought in from Scott Base, utilising the many flights that were visiting Cape Evans during the course of our stay. The new generator was rated at 5kVA, alleviating all suspicions of the marginal capacity 2kVA generator. The problem remained, however.

Contact was made with BRANZ, the owners of the equipment, who had struck this problem running the equipment off generator supply before. The motor drive was particular susceptible to supply upsets, and an inductive load was suggested to smooth the supply. An isolating transformer was dispatched from Scott Base, but was too small to run the fan. The final solution was to run lighting from the isolating transformer, thus providing an inductive load on the generator. The blower door apparatus was then powered directly from the generator. This solved the problem and the fan started and ran normally. Unfortunately, strong winds began to buffet the building causing chaotic 30Pa variations in differential pressure between the inside and outside of the building. The equipment could not produce meaningful results under these conditions and the test was placed on standby but the winds did not subside before time ran out. The gear was carried back and packed up without producing a single shred of information.

4.10.4 Blower Door Leak Test

In addition to the blower door infiltration test, the same equipment can also be used to locate and quantify leakage paths [ASME 1987b] in the shell, by pressurising the building and blocking off expected gaps, noting the reduction in flow required to maintain the differential pressure.

The results of this test would have been more important had the building been found to be loose, and had there existed a need to tighten the shell against air infiltration.

4.11 Salt Deposition

4.11.1 Introduction

The major contaminant in the atmosphere, as discussed in Chapter Two, is salt blown in from the sea. The quantity of aerosol salt deposited on solid surfaces in and around the hut was to be determined with this experiment. No instrument was found in the literature which could provide a direct reading of suspended salt samples in air. This is likely to be due to the very low concentration of salt in the air and the long collection time required to obtain sufficient sample quantities.

4.11.2 Apparatus

Four sets of identical apparatus were constructed for the experiment.

a) Salt candle

Early literature [Duncan & Ballance 1988] describes an apparatus developed by Cawse [1974] which uses a flat 200 x 250mm sheet of filter paper mounted centrally under a $1m^2$ sheet of Perspex to stop rain from washing the salt from the sheet. This has largely been replaced by the ISO standard apparatus [ISO 9225 1992] which has the salt collected on a cylindrical 'candle' with $100cm^2$ surface area, covered in a fine, surgical grade, cotton gauze. The candle is fitted to a glycerol/water filled collector bottle and is wetted by capillary action of the fluid up through the tails of the gauze. Salt adheres to the wetted gauze and is transported down into the bottle by diffusion within the carrier liquid. The ISO standard provides for a general form of the device, and dimensions of the candle but only acts as a guide for the detail design.

The salt candle used was designed from scratch, and consisted of six parts:

- Bottle
- Lid
- Connector bung
- Candle stem
- Top bung
- Surgical gauze finger bandage

The bottle and lid were a standard wide neck proprietary unit with the lid machined to accept the connector bung and tighten against it as the lid was screwed to the bottle. The connector bung received the candle (with a press fit into the internal bore) over which the gauze was wrapped in a double layer. The top bung plugged into the top of the candle, clamping the gauze in place and sealing the excess away from the atmosphere. The connector bung had a chamfer for channelling wash water into the bottle without losing any of the salt sample. This apparatus received a substantial design investment which paid off in the field. Full engineering part drawings are included in Appendix A.

b) Stand

A stand was built to conform with the ISO standard requirements and also to survive the strong winds likely at the destination. A PVC pipe was held upright with a galvanised steel base that was staked to the ground. The pipe supported both the salt candle, via a bicycle water bottle cage, and the roof (a 500mm square opaque PVC sheet).

Figure 4.5: Salt candle collector and stand in position at Cape Evans.

4.11.3 Method

a) Setting up

The filling fluid used was the standard 20% (V/V) glycerol and water solution specified by the standard. The temperatures expected during the test period were not going to stretch below the –25ºC working limit of the fluid. The glycerol is included to prevent freezing or excessive evaporation.

The candles were set up a month prior to the K282[5] field event by field staff, and plastered with explanations and warnings for visitors to the huts not to interfere with the experiment. The visual imposition of the stands during the test was foreseen and these measures were taken to prevent interference from people wishing to take photographs.

The four candles were located outside, on either side of the hut and inside, by the door and further into the building. These locations were chosen to provide data for the more or less exposed external environment which could be compared to that entering the hut near the door and deep within the building. The exact locations and sample codes as shown in Fig. 4.6 were:

1. SH-O-1 Seaward side of Scott's hut, 10m away
2. SH-O-2 Behind Scott's hut, 10m away
3. SH-I-3 Beside the smaller mess deck table
4. SH-I-4 Stove end of the Afterguard table

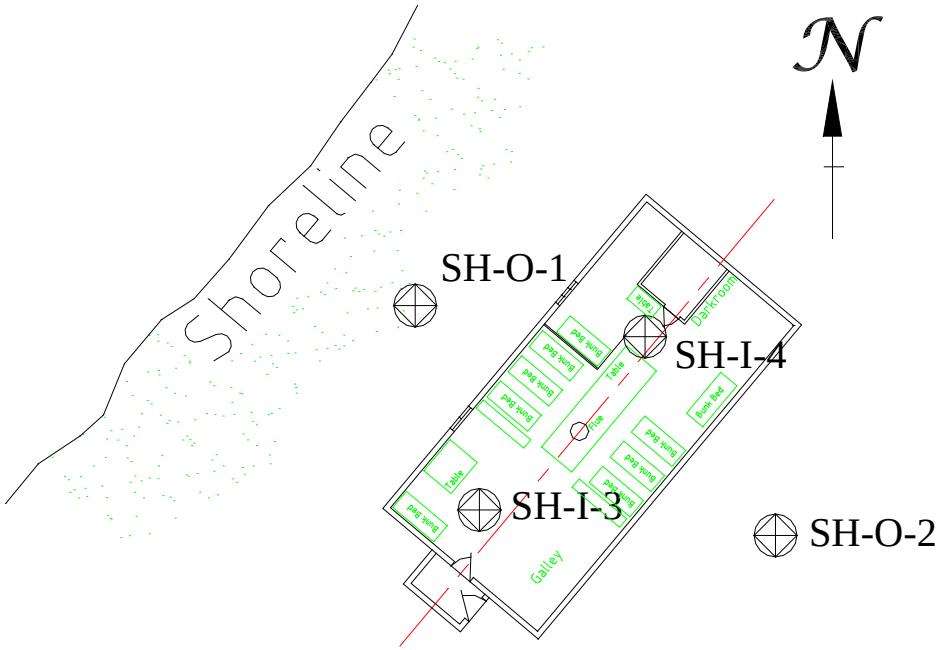

Figure 4.6: Locations of the salt collectors around the hut at Cape Evans.

[5] K282 was the Antarctic Heritage Trust field event designation code.

b) Collecting

The candles were to be exposed for 28 days, but event scheduling meant that the period was a little longer at 37 days. Results were interpolated from this longer period. The samples were collected by the author on his arrival at Cape Evans and the candles washed down with the reverse osmosis water (RO_2 water) supplied by Scott Base instead of the demineralised water intended.
At the close of this experiment, the sea ice was still firm in McMurdo Sound and the open water was approximately 4km away from the site. This means the effective shoreline was this distance away from the test site, which becomes important when comparison is made to other sites.

The bottles were capped and returned to Christchurch for analysis after the Antarctic field trip was concluded.

c) Analysis

The samples were analysed with a mercurimetric titration similar to that performed on the insulation sample in §4.7. Refer to ISO 9225 [1992], Analar [1984] and Vogel [1989] for detailed information on the titration method.

4.11.4 Results and Discussion

a) RO_2 water titration

Due to the use of reverse osmosis water instead of distilled water for washing down the salt candles, a sample was kept and analysed to ensure any salt content in the RO_2 water did not contaminate the results.

The RO_2 water was titrated three times and consistently found to contain a substantial amount of salt, 0.07mg/ml. As the initial wetting fluid volume was known to be 200ml, (a level was marked on each bottle) the proportion of RO_2 washing water to actual sample could be calculated, and the chloride contribution could then be accurately determined and subtracted from the total chloride in the bottled sample.

The RO_2 water chloride content is presented in Table 4.9 for the wash water volume in terms of effective accumulation rate, ie. the additional chloride content in the standard salt deposition units of $g/m^2.yr$. A sample calculation can be seen in §4.7 with details of the titration volumes included in Appendix C.

b) Collected sample titration

The results and error adjusted deposition rates are presented in Table 4.9.

Table 4.9: Salt deposition rates for Scott's hut at Cape Evans, Ross Is., Antarctica

Sample Code	Accumulation Rate		RO_2 Adjusted Accumulation Rate	
SH-O-1	60.1	21.9	45.4	16.6
SH-O-2	47.7	17.4	34.3	12.5
SH-I-3	19.2	7.0	15.1	5.5
SH-I-4	27.9	10.2	12.1	4.4
Units	**$mg/m^2.day$**	**$g/m^2.yr$**	**$mg/m^2.day$**	**$g/m^2.yr$**

The results show that the adjusted amounts represent a fair proportion of the deposited matter. The largest proportion was 56% in the lowest deposition rate sample, SH-I-4. The chemical analysis method can theoretically account for chloride ions in solution to such a great resolution (0.0002 $g/m^2.yr$) that the accuracy of the result with the correction can be justified.

The adjusted accumulation rates correspond to what was expected in terms of rate versus location trends. The seaward (outside) sample had the highest deposition, followed by the sheltered (outside) sample. Of the two inside samples, the sample closest to the door had the greater deposition but significantly less than either of the two outside samples.

The classification of airborne salinity based on the wet candle method (ranging S_0 to S_3) places all of these results into category S_1 which is one category above insignificant background levels [ISO 9223, 1992]. The distance of the

sea ice edge from the hut at the time of the test may be a significant factor in the low classification.

Classification of corrosivity takes into account a factor called time of wetness which by definition loses all credibility in Antarctica. The time of wetness is defined as a sum of the hours in a year when the relative humidity is greater than 80% and the air temperature is greater than zero degrees Celsius. There are very few times of the year when the air temperature rises above 0ºC (if at all) but condensation does occur due to solar loads pushing local temperatures above this point.

It is difficult to draw conclusions from only one set of data, so a repeat test at some time when the sea ice has broken out would be advisable.

4.12 Sulphur Dioxide Levels

Several Dräger SO_2 gas detection tubes were exposed for a period of 8 hours inside and outside both Scott's and Shackleton's huts and did not return any readings within the 5ppm/hr resolution of the tubes.

The ambient SO_2 level may be inhibited by the favourable location of Mt. Erebus in relation to the direction of the prevailing wind.

4.13 Airflow Direction Field

4.13.1 Introduction

The pattern of air flow within the building was intended for evaluation so that locations within the room that were susceptible to pollutant deposition could be established and artefacts removed from these areas.

4.13.2 Apparatus and Method

Two methods were considered for the measurement of the air flow field:

- Air field velocity measurement [Liddament 1991]
- Point release CO_2 dispersion field

a) Air field velocity

The first method involved the use of a hot wire anemometer that could be taken to grid marked locations within the room to measure the local air speed. A Cole-Parmer device was used with a 0.1m/s resolution but it was found that with the actual air velocity being much less than 1 m/s, the instrument did not provide the resolution nor the response time to accurately determine the field. This result of no measurable velocities shows that the air flow field in the room is sufficiently small to be randomly affected by any disturbance. Special hot wire anemometers are available for this testing method, but costs were not within the budget of the project.

b) CO_2 dispersion field

For the same reason as above this test would not have been possible, but delivery delays of the diffusion tubes meant they did not arrive in time for the flight anyway. The idea behind this test was that a continuous release of CO_2 could be injected near a source of infiltrating air (most likely the door) and the contaminant level recorded in several positions throughout the room. At an appropriate time, gauged by the indicated level on the most affected tube, the gas would be shut off and the levels on each tube recorded to give a relative level of site susceptibility.

4.14 Chapter Summary

Information regarding the physical construction of the hut was gathered, along with tests completed to establish the air-exchange between the inside and outside air states. This allowed essential parameters to be determined for the models. Side experiments of salt infiltration and seagrass insulation analysis were carried out as well during the time in Antarctica. The intended blower door and airfield direction tests were not carried out for technical reasons.

With the data and information gathering phases completed in the previous two chapters, a description of the modelling phase begins in Chapter Five with a detailed review of the published literature related to indoor humidity modelling.

CHAPTER FIVE

LITERATURE REVIEW OF INDOOR HUMIDITY MODELLING

5.1 Introduction

The 1970's energy crisis provided the motivation for government bodies to fund research into the thermal efficiencies of buildings which translated directly into energy savings and reduction of fossil fuel usage on a national scale in many developed countries. The development of thermal models was carried out to describe in detail the heat transfer occurring through the ceiling, wall and floor area in residential homes and help achieve these aims. Although for several years these thermal models received the most attention, it became apparent that great savings could be made in warmer climate regions by reducing the latent load on cooling and air conditioning equipment.

As residential buildings were made increasingly air-tight to reduce energy loss to the outdoors, problems were experienced with inadequate ventilation and moisture being trapped within the timber framing. Condensation and saturation of the wall materials promoted fungal rots and authorities recognised the need to find a balance between the cost of energy and the cost of degradation. Infiltration and ventilation levels were studied in more detail and mass transfer models were developed accordingly. The indoor humidity model has evolved

with input from parties interested in either energy savings or building moisture levels, but irrespectively, head in the same direction.

This chapter sets out to provide a chronological history of indoor humidity modelling and related research in sub-models and mechanisms. The papers summarised here have been studied or borrowed from in reaching the goals of the author's own modelling and it is intended that this chapter will provide a summarised reference source for future work in this area.

The papers cover the period from 1976 to the latest relevant work in 1995 and approach the problem using various mathematical tools from pure analytical to simple numerical and more complex finite element methods. Early works focussed on individual mechanisms - particularly infiltration – but later models were combined, coinciding with the reducing cost of computational power.

5.2 Chronology of Research

Early works by Keiper et al [1976] looked at vapour diffusion with a numerical approach where the effect of infiltration was ignored. An infiltration model was later added to this work by Trethowen [1979].

Tsuchiya [1980] provided an early sorption model, claiming that one third of moisture may be absorbed into hygroscopic materials in the room. Tsuchiya's approach to sorption assumed a thin film of the material surface was involved that attained instantaneous moisture equilibrium with room air. A moisture mass balance was carried out in the control volume of the building, requiring the simultaneous solution of three linear differential equations. The Lewis relationship was used to find the mass transfer coefficient.

New Zealander, Malcolm Cunningham (Building Research Association of New Zealand) developed a benchmark analytical model [Cunningham 1983a] to determine the moisture concentrations within building cavities that included the effects of diffusion, infiltration and sorption into hygroscopic materials.

Cunningham used reasonable assumptions to linearise the non-linear differential equations that describe these mechanisms and defined two principal time constants in describing the dynamic response. He was an early proponent of the effect of sorption and covered this effect thoroughly. He simultaneously published an extension to the first paper [Cunningham 1983b] which included the effect of condensation occurring in the wall linings. A result of this work was a calculation method for drying of newly constructed buildings and response to wetting and drying seasons.

An often-cited paper was published by Kusuda [1983] which provided a comparative study between modelled and experimental relative humidity in a residential test house with and without the sorption effect, using Tsuchiya's model.

Cunningham [1984] extended his previous analytical model [Cunningham 1983a,b] to include evaporating surfaces and fluctuating external climatic conditions.

Aimed at calculating cooling loads, Miller [1984] developed an indoor humidity model in the form of a post-processor for an existing thermal model that calculated the sensible loads. Called MOBAL3 and later LATENT3 (with adapted input requirements), an hourly mass balance of occupant rates, sorption, infiltration, and various equipment loads were accounted for. He used the Crall [1983] model for infiltration, and regarded diffusion as insignificant. Time constants were used to describe the dynamic responses of the mechanisms.

Fairey and Keresteciogl u [1985] and Keresteciogl u et al. [1985] both describe a sophisticated, three dimensional, finite element model called MADAM developed by Keresteciogl u as his PhD thesis. The MADAM (Moisture Absorption and Desorption Analysis Method) model module was added to TARP (Thermal Analysis Research Program [Walton 1983]) to provide a simultaneous heat and mass transfer model. Condensation was disregarded as it was developed for hot humid climates. Combined to be called MADTARP

this model was Unix-based to run on mainframe computers. Later criticism [Barringer & McGugan 1989] of this model was that it took a large amount of time and effort to assemble the required input data.

As an offshoot of his previous work, Cunningham [1987] presented a simplification of moisture behaviour calculations where various mass transfer mechanisms were represented as analogous electrical circuits.

Walldry, a computer model that simulates moisture migration through wood frame walls was produced as a commercial venture by Schuyler et al. [1987]. The paper describing the model was published in 1987, with computer software released in 1989.

As a further extension of his early 80's analytical work, Cunningham [1988] added new features in the timber framing drying model. He expanded the model for two dimensions, added a fill material option in the cavity and an initial moisture content option for materials above fibre saturation and anisotropic materials was allowed. Cunningham's approach remained firmly entrenched in describing the processes analytically.

Barringer and McGugan [1989] set out to provide a simple model to calculate indoor temperature and relative humidity. Included in their model were equipment loads and diffusion through concrete foundations. They concentrated on time dependent simulation, adding moisture models to a commercially available thermal modelling program.

Looking to improve the earlier finite element model, MADTARP, Keresteciogl u and Gu [1990] went in-depth into condensation and evaporation theory and produced an enhanced model, also solved with the finite element method.

A detailed look was also provided by Keresteciogl u et al. [1990] into the treatment of lumped and distributed analysis methods in the adsorption and desorption model. Effective moisture penetration depth theory was developed where the convective coefficient, surface area and moisture isotherm are actual

values, and the effective thickness of the material that is involved in exchanging moisture with the atmosphere is determined, i.e. no ‘effective’ mass transfer coefficient is used. Prior to this work, Kusuda [1983] had determined the existence of a boundary layer 4mm thick that responded to diurnal changes. Cunningham [1983a,b; 1984; 1988] used adjusted mass transfer coefficients and the full thickness of the material.

Cunningham [1992] took a deep look into moisture diffusion with an analytical and also a numerical solution using the finite difference method.

Mass transfer processes were modelled by El Diasty et al. [1992] with a first order differential equation using the fourth order Runge-Kutta numerical solver, where non-linear processes were assumed linear within a discrete time step (typically one hour).

A transient, one dimensional, finite difference model for coupled heat and mass transfer in a multi-layered wall was researched and developed by Burch and Thomas [1992]. The paper was the background to MOIST, a software package released by the US Government, National Institute of Standards and Technology the following year. This package allowed the analysis of added layers on wall properties, in climates described by standard ASHRAE Weather Year for Energy Calculations data files. Model results were proven experimentally by Burch and TenWolde [1993].

TenWolde [1994] built on previous work of his with a paper pertaining to modelling indoor relative humidity in manufactured houses - the semi-permanent trailer park homes found in North America. An infiltration model specific for manufactured houses was used and moisture transfer determined by a mass balance. The sorption model utilised an exponential time weighted average to describe the response of the material to indoor relative humidity.

An enhanced MOIST v3.0 was released [Burch and Chi 1997] with a friendly graphical user interface and indoor relative humidity model experimentally proven by Tsongas et al. [1995].

5.3 Infiltration

A detailed development of the infiltration models used in the above mass transfer models has been deliberately avoided as the subject has been extensively covered by the Air Infiltration and Ventilation Centre (AIVC) formerly known as the Air Infiltration Centre (AIC). AIVC work under Annex V of the International Energy Agency (IEA) agreement on energy conservation in buildings and community systems. Liddament and Allen [1983] sets out to describe in detail, compare and validate mathematical models from building research institutions in several countries and is a good reference on the capability of each model.

Infiltration theory and the chosen LBL infiltration model in particular, have been covered in full in Chapter Six.

5.4 Chapter Summary

Previous research leading to the formulation of the model developed in this thesis has been summarised and referenced. The modelling practice used in the author's work was of the simple numerical following the foundation work of Tsuchiya, Kusuda and TenWolde.

Chapter Six, following, defines the theoretical detail behind the author's model.

CHAPTER ONE

INTRODUCTION

1.1 A Brief History of Antarctica and the Ross Sea Region

1.1.1 Balancing the Planet

The earliest recorded visits to the great southern continent were undertaken to find *Terra Australis Incognita*, the landmass proposed by early Greek geographers and thought to 'balance' the known northern continents. The name Antarctica is derived from *Anti-Arktikos*, or the opposite of the Arctic. Sailing voyages of Sir Frances Drake (1577-80) and Abel Tasman (1642-44) proved the continent did not extend from the southern reaches of South America and Australia, but the continent was still believed to cover the globe from south of 50º South. Captain James Cook was the first person to venture in search of land, and sailed three voyages in consecutive summers (1772-75) travelling as far as 71º10'S with a complete circumnavigation and did not see land before giving up. He did however report a wealth of marine life and spurred a century of sealing in the Southern Ocean. Sealers reached further and further south bringing about the discovery of the South Shetland Islands and islands off the Antarctic Peninsula before at last in 1820, American, John Davis, set foot on the Peninsula itself, the first landing on the continent.

1.1.2 Science and the Continent

Over the remainder of the century, several expeditions also departed in the name of science, led by a precedent set by Cook and the Russian, von Bellingshausen, who also completed a circumnavigation (1819-21). Leading scientific interest was the fixing of the position of the southern magnetic pole, inland from Cape Adare at the time, but now drifting out to sea off the Adélie coast. In searching for this, James Clark Ross inadvertently discovered the huge ice shelf of the Ross Sea, allowing the easiest access to the South Pole for later explorers. Other interest in the area was mainly in annexing the commercially important continent as a national claim by several nations. Difficulty in defining the land boundary under the sea ice led to a general fade in enthusiasm. Only one expedition sailed south of the Antarctic circle in the next 50 years, (George Nares, 1872) but made the important discovery of continental rock types in the sea bed, thus proving the land mass was a continent, not a collection of islands.

1.1.3 The Heroic Era

In 1895, an International Geographical Conference was held in London to revive interest in Antarctic science and exploration. This combined with the then recent invention of the portable Primus gas stove caused a flurry of expeditions which we know as the heroic era. The heroic era is defined as the period of exploration from 1895 to 1917 where the Antarctic continental interior was probed by mainly British expeditions but also the notable Norwegian polar expedition led by Roald Amundsen.

Carsten Borchgrevink, also Norwegian, led a British expedition on the *Southern Cross* (1898-1900) which built and wintered-over in a hut at Cape Adare, and managed to sledge 15km inland. This was the first base and the beginning of inland Antarctic exploration.

1.1.4 The Race for the Pole

The British were preoccupied with becoming the first nation to reach the Geographic South Pole and sponsored three expeditions. Captain Robert Falcon Scott (1868-1912) was selected to command the *Discovery* expedition (1901-04) in which a hut was erected at Hut Point on Ross Island where the American McMurdo Base now sprawls. Scott failed to reach the pole, mainly due to inexperience with the dog-teams, and running out of food, making it to 82º16'S. Scott sent home on the relief ship a man whom he had felt had failed him on the return journey; that man - Ernest Shackleton, never forgave Scott for the insult and mounted his own private campaign for the conquest of the pole in competition.

Shackleton (1874-1922) returned to the pole in the *Nimrod* (1907-09) and attempted to reach the pole using Siberian ponies after failing with the dogs with Scott. His plans to use the Bay of Whales and not intrude on Scott's territory were shelved due to pack ice in the Ross Sea and he turned back to Ross Island, building his base at Cape Royds, somewhat north of the Discovery Hut at Hut Point. The following spring two parties departed the hut, one party headed by Shackleton for the Pole, and the other party successfully headed by the Australian, Douglas Mawson, (who later returned leading three expeditions of his own) for the South Magnetic Pole. Shackleton was forced to make the decision to turn back at 88º23' (160km from the pole) due to lack of food.

Scott headed South to gain the Pole once again in the *Terra Nova* expedition (1910-13) utilising ponies and dogs over the ice shelf, then manhauling over the plateau This time he succeeded, but paid for the honour with his life and those of his four polar party companions on the return journey. Scott reached the Pole on 17 January 1912 to find the Norwegian flag of Roald Amundsen flying - beaten by just over a month. On this same expedition, a scientific venture left the cosy base at Cape Evans on Ross Island to make a mid-winter sledging trip to Cape Crozier collecting Emperor penguin eggs. This trip was described in the book "The Worst Journey in the World" and fits the title well.

Amundsen was a seasoned Arctic explorer who turned towards the South Pole when the concurrent goal of the North Pole was denied him. He set up base for his *Fram* expedition (1910-12) in the Ross Sea, at the Bay of Whales, which Shackleton had attempted to reach earlier. His great experience with skis and the 97 dogs he had, combined with the shorter distance to travel, helped him reach his goal despite pioneering a new route onto the plateau, and he reached the Pole on 14 December 1911.

The Ross Sea huts - particularly the *Terra Nova* hut – were used to survive by the stranded members of the *Aurora*, who were the Ross Sea contingent of Shackleton's Trans-Antarctic Expedition (1914-17). Both the *Endurance* in the Weddell Sea and the *Aurora* in the Ross Sea, were trapped in pack ice. The *Endurance* was crushed, starting the amazing saga of Shackleton's return to South Georgia and the rescue of the men, and the *Aurora* managed to drift out with the crew and return to New Zealand. Surviving on leftovers from previous expeditions, the Ross Sea landing party was rescued in December 1916 by, in possibly the most unexpected scenario, Shackleton on the returning *Aurora*. The rescue of the men on the *Aurora* signified the end of the heroic era.

1.1.5 Modern Exploration

In the years to follow, Antarctica was explored more by the air, with aerial photography used to map particular areas and then later the entire coast line in Operation Highjump, post World War II.

In 1955, New Zealand started its direct involvement with the Commonwealth Trans-Antarctic expedition of Sir Vivian Fuchs and Sir Edmund Hillary, who used motor vehicles to travel across the vast expanse of the plateau. The International Geophysical Year (1957-58) caused another surge in interest in Antarctica and became the biggest scientific programme ever, with twelve nations building 50 stations emphasising meteorology, oceanography and geomagnetism. New Zealand set up Scott Base and the Americans built McMurdo Base at Hut Point on Ross Island to support their operations in Antarctica. Any commercial interests in Antarctica are now protected by The

Antarctic Treaty 1960, further backed by The (Madrid) Protocol on Environmental Protection. This is an international treaty signed by 42 nations restricting the use of Antarctica to science and other peaceful purposes.

1.2 The Preservation of the Buildings

1.2.1 Antarctic Heritage Trust

With the loss of Amundsen's hut from its icy perch in the Bay of Whales, four of the Ross Sea huts remain today included in a total of 34 historic sites, for which New Zealand has assumed responsibility since 1955. The four huts being:

- Borchgrevink's *Southern Cross* hut (1899) at Cape Adare
- Scott's *Discovery* hut (1901) at Hut Point, Ross Island
- Shackleton's *Nimrod* hut (1907) at Cape Royds, Ross Island
- Scott's *Terra Nova* hut (1911) at Cape Evans, Ross Island

In 1969, the New Zealand Department of Scientific and Industrial Research's Antarctic Division introduced a caretaker programme, sending down Antarctic Society members to conduct maintenance on the huts. Long term preservation required a better organisational structure and an Action Committee was formed in 1979 to develop a Preservation Strategy. Other committees were formed to address issues arising in the care of the historic sites, but a major conservation programme was needed, and in 1987, the Antarctic Heritage Trust was established. With the advice of professional conservators, archaeologists, museologists, historians and other specialists, the work of the Antarctic Heritage Trust continues today, protecting the heritage sites, and conserving and restoring the buildings and artefacts.

1.2.2 Scott's Terra Nova *Hut at Cape Evans*

Scott's *Terra Nova* hut was chosen over the other Ross Island huts to be the focus of the study in that it provided the worst case scenario of moisture

problems. Conservators had a record of sustained, high humidity levels and apparent patches of water and ice appearing at times on the floor. The building was thought likely to have less infiltration than the other buildings because of the closer fitting construction of the walls, thus the resulting effect of sorption would make a more interesting and revealing problem to study than a highly infiltration dominated situation.

This hut was excavated of snow and ice starting in 1960-61, using picks and shovels to chip away the ice, and thawing items outside in the sun. A great deal of expedition and personal belongings were left in the huts, which makes them such a valuable record for today, preserved in the ice away from the corrosive marine environment. The tragedy of the history that surrounds the hut, along with the vast range of artefacts present in good order makes the building the jewel in the crown for Antarctic historical remnants.

Personally, flying over the hut en route to my field station, I felt a sense of excitement looking down upon the hut. Having studied the building intensely for a year and then seeing it with my own eyes created quite a moment for me. Walking into the hut, the pungent aroma of the seal blubber hits you first, followed by amazement at the clutter inside the building. The range and number of artefacts inside the hut is unbelievable. In comparison to Shackleton's hut, Scott's hut gives much more of an impression of having been recently lived in, with more personal items scattered about the place.

Exposure to the environment has started the gradual decay of the items in the building. Irons have begun to rust, all metals to galvanically corrode, textiles and papers succumbing to the decay of nearly a hundred seasons of cyclic variations in the climate. This whole process is slowed considerably of course by the extreme cold climate restricting the reaction rate and activity of fungal moulds, but the location also brings a lack of accessibility which interrupts the efforts of Antarctic Heritage Trust conservation experts.

1.2.3 The Local Environment

Antarctica is characterised by harsh excesses in weather, but most of the descriptive clichés, ie: highest, driest coldest and windiest , refer to the continental plateau not so much the coastal regions in which Ross Island lies. Cape Evans sits at virtually sea level, the hut positioned on the beach with a clear view to the North West and McMurdo Sound, high tide reaching only tens of metres away. A marine environment is the classic description of this kind of location, but the sea is frozen over for all but a few months of the year, restricting the windblown aerosol salt. The soil is a coarse, loose, volcanic till – Cape Evans being ice-free in summer.

Not facing quite the consistent punishment enforced by the gravity fed, katabatic winds howling off the plateau, Cape Evans does offer itself to the frequent gales emanating from the Southern Ocean. Temperatures fluctuate between zero degrees Celsius in the Austral summer, where the land is warmed by 24hr sunlight for a couple of months, and –40ºC in mid-winter, where the few people who inhabit the research bases count the days until they see the sun again in the spring.

1.2.4 Problems Facing the Hut and Artefacts

In general conservation circles, the environment with regard to temperature, relative humidity and contaminants is strictly controlled within a range that limits the equilibrium moisture content of hygroscopic materials, and stops the wet/dry cycle that concentrates contaminants, such as salt, slowing the corrosion of metals. The artefacts do not have the benefit of this controlled environment, so are at the mercy of the conditions provided by the shelter of the building. In the years since the excavation, moisture levels have been noted as being quite high. Liquid water forms (with the ongoing solar gain heating the hut) and ‘pools’ around the base of items. This has been thought to be on a slow decline with the problem becoming less noticeable over time.

Visitor influence on the interior climate of the hut is a concern, and the number of people admitted to the building is limited to twelve at a time. Latent release

occurs during human respiration contributing potentially damaging moisture to the hut air state with an unknown response.

Marine sourced salt has accumulated in areas inside the hut and shows in the form of a fine, white powder dusting. This is common in widespread patches on the soil all along this coast, where lack of rain allows salt to stay where it settles.

The floor shows signs of deformation, thought to be lifted by formation of ice underneath the building, where no ventilated crawlspace was provided.

1.3 The Scope of the Study

1.3.1 Objectives

Some deviation from the original research proposal was made in the course of the study, as more important areas were examined in greater detail and some areas were found to be insignificant or irrelevant. The main area of study was to examine the existing situation and produce a model for the mass transfer processes occurring within the building. Specifically, the main areas that were intended to be investigated were as follows:

Observation Based (Chapter Two)

- Subterranean water
- Underfloor ice
- Infiltrating air
- Visitor throughput effects

Data analysis – Logger and weather-station data (Chapter Three)

- Data verification
- Climate study
- Indoor/Outdoor climate comparison
- Temperature stratification indoors
- Occupancy effects

Experimental - Building shell investigation (Chapter Four)

- Construction
- Air infiltration
- Moisture contents
- Aerosol salt infiltration

Modelling (Chapters Five, Six and Seven)

- Develop a mass transfer model, including all major mass transfer mechanisms
- Relative contribution of each psychrometric mechanism at Cape Evans
- Effect of removing underfloor moisture source
- Investigation of visitor effects
- Ventilation requirements
- Investigate means of reducing moisture within building

Conclusions and recommendations based on the above items are discussed in the final chapter (Chapter Eight).

The original research proposal is appended as Appendix E.

1.3.2 Author's Involvement in the Project

The author had a long-standing interest in Antarctica, relating to the history of exploration by Scott and Shackleton and was delighted to undertake a project in this part of the world and which also coincided with his chosen engineering specialty of heat and mass transfer.

1.3.3 Fieldwork and Experimentation

It was the intention of this work to investigate the physical characteristics of the building shell itself and the local and internal environment through the application and design of experiments that conform to existing standard methods, the analysis of previously gathered psychrometric data, and

historically recorded information. Field observation was also intended for gathering speculative information, important in understanding the overall problem and decision making, through the eyes of an engineer.

1.3.4 Modelling

The development of a model and computer simulation based on logged data was emphasised in the research proposal to establish the contribution of individual psychrometric mechanisms to the microclimate inside the building. The model could also be used to obtain a quantitative understanding in a range of 'What If?' scenarios offered by the sponsors, Antarctic Heritage Trust. The model was intended to be adaptable for use in describing the other huts provided that the input data was available, but for the purposes of this project, the model was to be developed specifically for the *Terra Nova* hut.

1.4 The Structure of the Thesis

This thesis has been written to describe the approach to the project in a largely chronological fashion. The first two chapters deal with the background history and early discussion that took place in the initial phase of understanding the problem and the environment in which it existed. Observations made by the author during the field work are included in Chapter Two to relate to the comments made by AHT staff.

Chapter Three presents an analysis of the large amount of data that had been gathered prior to this project, continuing on into Chapter Four with the additional information gathered during the experimental programme in the field.

The thesis then steps into the modelling phase in Chapter Five with an overview of the literature relating to indoor humidity modelling. The theory behind the author's model is covered in detail within Chapter Six, with reference to the work of others covered in the previous chapter.

The developed model was then used to analyse various scenarios, the results of which are discussed in full in Chapter Seven. Chapter Eight summarises the conclusions made from all aspects of the project and makes suggestions as to future continuation of the work.

CHAPTER SIX

MODEL THEORY

6.1 Introduction

This chapter describes in detail, the theory behind the indoor humidity model used in the project. The format is a discrete, time stepped indoor humidity model, that calculates the net mass transfer into and out of the room air on a hourly basis. For clarity, the indoor humidity model has been divided up into its constituent parts of infiltration, sorption, condensation and evaporation, and occupancy. Diffusion was neglected in comparison to the other mechanisms, but is described in brief for completeness.

The coding structure of each model is defined including the infrastructure module which ties together the individual components of the model into a fully descriptive computer simulation.

6.2 Convention

The convention used in all calculations within the sub-models described in this chapter is that moisture gain to space air is positive. For example, a positive mass transfer during isothermal conditions will cause the relative humidity to increase in the room space.

6.3 Infiltration

6.3.1 The LBL Infiltration Model

Infiltration is the unintentional air exchange between the outside and inside air states. No other form of ventilation occurs with the historic Antarctic huts, except the door being open when visitors are present. Infiltration is not a mechanism that can be described by a fundamental formula, but rather an empirical relationship between the building and the climate. As described in the literature, many single-cell models are available that predict the infiltration in terms of air changes per hour, but perhaps the best known and most used model is that developed by the Lawrence Berkeley Laboratory (LBL) [Sherman and Grimsrud 1980]. This model was chosen for the purposes of this project on the basis of a good reputation (adopted by ASHRAE) and availability of the correct input data.

Infiltration is a very important process in the building because it is the only notable mechanism by which moisture can be completely removed from the building. Water vapour can be absorbed into the wall linings and so leave the defined control volume, but it remains readily available to the air space through the process of desorption.

6.3.2 Theory of the LBL Infiltration Model

a) Assumptions

The LBL model is a single-cell or single-zone model, which means it approximates the air exchange between a single room and the outside air state only. Multi-cell models are also available that can calculate the airflow between networks of interconnected rooms, but these are not appropriate to the hut at Cape Evans. Within the cell, the air state is assumed to be perfectly mixed. The model also assumes constant conditions during each hourly calculation interval.

b) Formulation

The model calculates the flow rate, Q, according to [ASHRAE 1989a: 23.17];

$$Q = (3.6)L\sqrt{a.\Delta t + b.v^2} \qquad [6.1]$$

The infiltration, A, (in air changes per hour, hr^{-1}) can be calculated simply by dividing by the volume of the building, V;

$$A = \frac{Q}{V} \qquad [6.2]$$

where:

L = effective leakage area, cm^2

a = stack coefficient, $(L/s)^2 cm^{-4} (^oC)^{-2}$

b = wind coefficient, $(L/s)^2 cm^{-4} (m/s)^{-2}$

Δt = inside/outside temperature differential, K

v = wind speed, m/s

and the multiplier of 3.6 was for unit conversion.

c) Running input data

The infiltration model required the internal and external temperatures, wind speed and wind direction, which were sourced from the NIWA and logger data files discussed in Chapter Three.

d) Stack and Wind Coefficients

The stack coefficient is a function of the height of the building and a value of, $a = 0.000145$, was read from ASHRAE [1989a: 23.18]. The wind coefficient is a function of both the height of the building and the degree of exposure the building presents to the wind source, the latter described by a given shielding class. In the case of Cape Evans, likely shielding would come from the surrounding hills to the south. Wind coefficients used in this project were sourced from ASHRAE [1989a: 23.18].

e) Effective leakage area

The effective leakage area would normally be obtained from the blower door test at 4Pa, but this result did not eventuate, as discussed in Chapter Four. The CO_2 decay infiltration data was used instead and the *Solver* function of MS Excel was used to iterate the leakage area required to fit to Eqn. 6.1, the wind, temperature and infiltration conditions present at the time.

6.3.3 Infiltration Model Attributes

a) Wind direction compensation

To account for the hills in the south, the wind direction data was accounted for in the model along with the wind speed. The shielding class was greater from the south than from the north (the two most often experienced wind directions) and this translated to a lower wind coefficient. The model splits the wind direction as being from either hemisphere and adjusts the coefficient accordingly. Figure 6.1 is a flowchart of the infiltration model and demonstrates the logical progression of the code.

b) Visitor compensation

The model had the facility to use occupancy data to adjust the effective leakage area. In this manner, it was possible to consider the presence of visitors in the hut as being coincident with the door being open and the ventilation would increase proportionally.

6.3.4 Sources of Error

The infiltration model assumes even conditions throughout the hour for the wind speed data, but in reality this may vary tremendously around the mean on a typical gusty day. The wind direction is assumed to be evenly applied in either a northerly or southerly direction with no regard to the angle of the building. Pressure distributions that cause the infiltration of air would be affected by this assumption.

During warm periods, the building can be expected to expand and open structural gaps and the opposite during cold, dry periods, thus adding an unaccounted dynamic effect to the effective leakage area.

These factors influence the ability of the model to provide an accurate prediction of the infiltration flow rate through the building. Lack of blower door test data restricted the author's full evaluation of the model, but in controlled tests by Liddament and Allen [1983] over a variety of test houses, the LBL model was found to predict within ±25% of the measured infiltration rate.

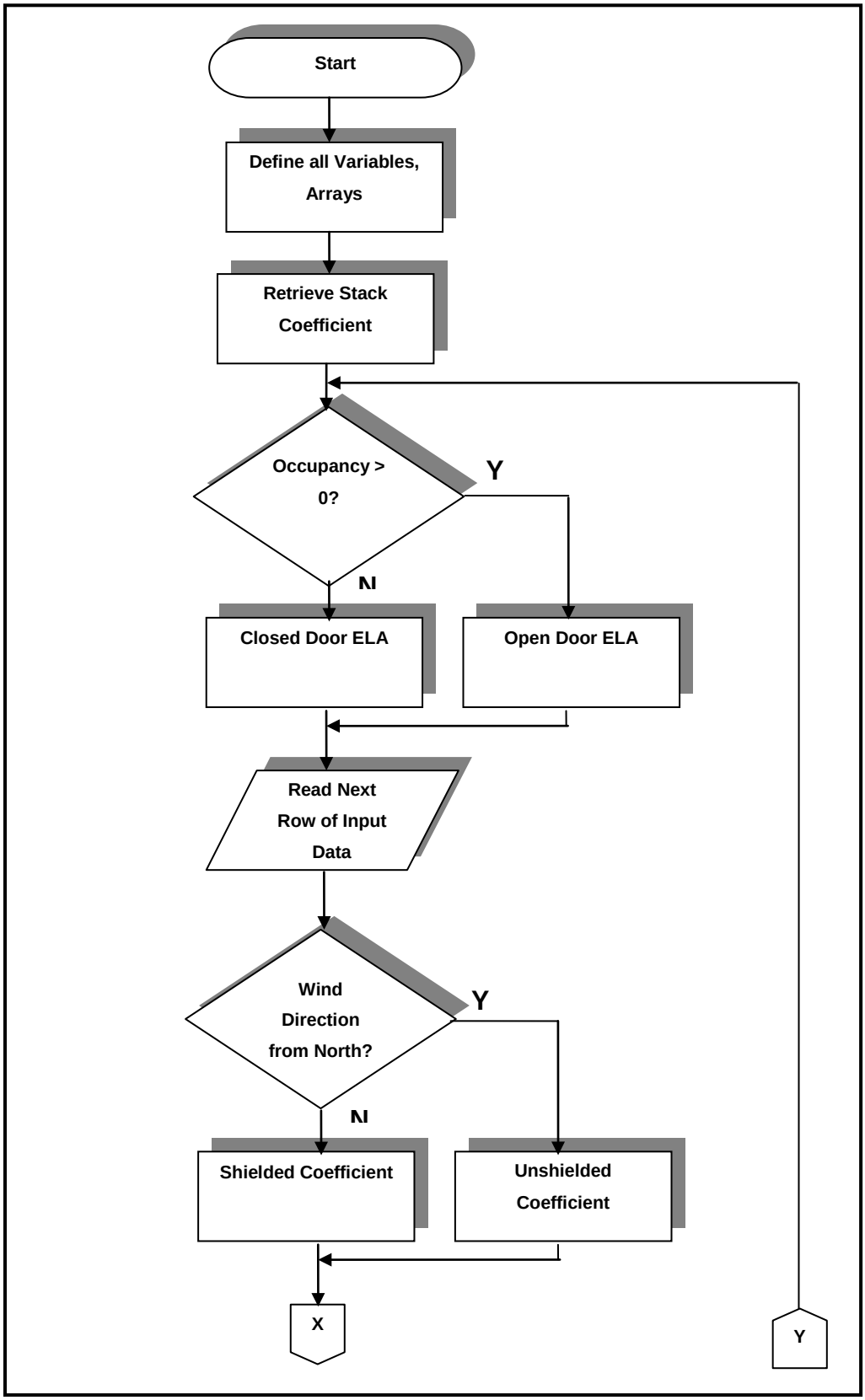

Figure 6.1a: Flowchart for infiltration model (continues…)

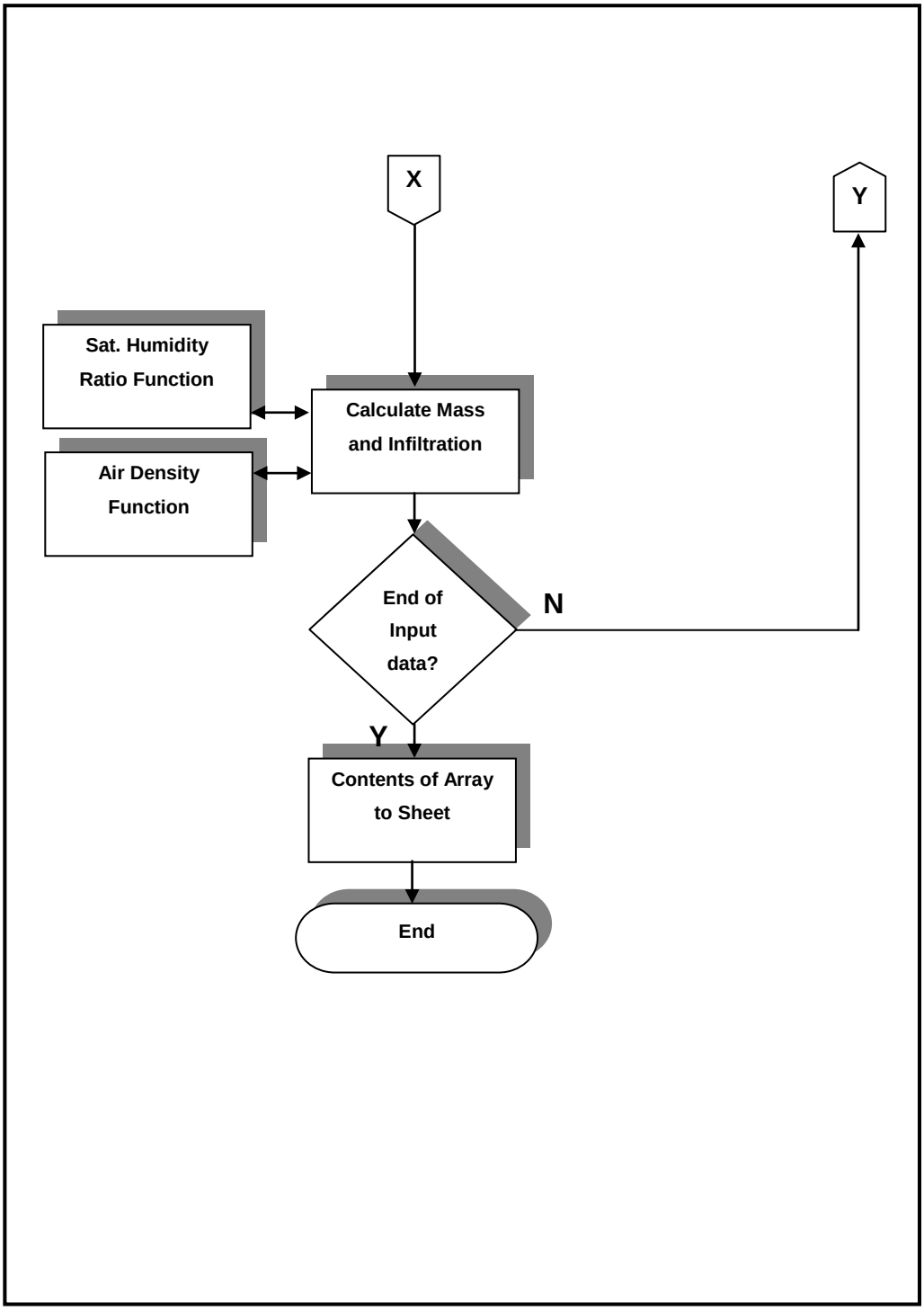

Figure 6.1b: Flowchart for infiltration model (continued)

6.4 Sorption Model

6.4.1 Background of the Model

The techniques implemented in modelling the sorption mechanism have been derived from a combination of past research methods. The procedure draws from simple, time stepped models from the research of Tsuchiya [1980], Kusuda [1983] and TenWolde [1994], but also includes ideas of the more sophisticated finite element models of Keresteciogl u [1990b], namely the inclusion of the sorption curve rather than a coarse exponential approximation.

6.4.2 Absorption and Desorption Processes

a) Physical mechanism

The term sorption refers to the dynamic interaction of water vapour in the air and the hygroscopic lining material of the walls, floor and ceiling. This covers both absorption[6] into and desorption from a surface layer of a given thickness considered to be participating in this process. Water vapour is absorbed into the surface of the material when the room relative humidity is greater than the relative humidity that would support the moisture content of the material at equilibrium. Likewise, desorption takes place when the room relative humidity drops below this level. The sorption curve serves to convert the material surface relative humidity into a material moisture content, allowing the effect of mass transfer on the material moisture content to be calculated. The active layer of material can be determined from this method.

b) Sorption curve

[6] Absorption means to soak or suck up fluids, not to be confused with adsorption where the fluid accumulates on the surface in a thin film. Adsorption, used by some authors in this field, implies a saturated surface condition that is independent of the moisture content of the material and insinuates a condition not present in this model.

The relationship between relative humidity, ϕ, and the equilibrium moisture content, U, is shown by the sorption isotherm. This must be determined experimentally for each material.

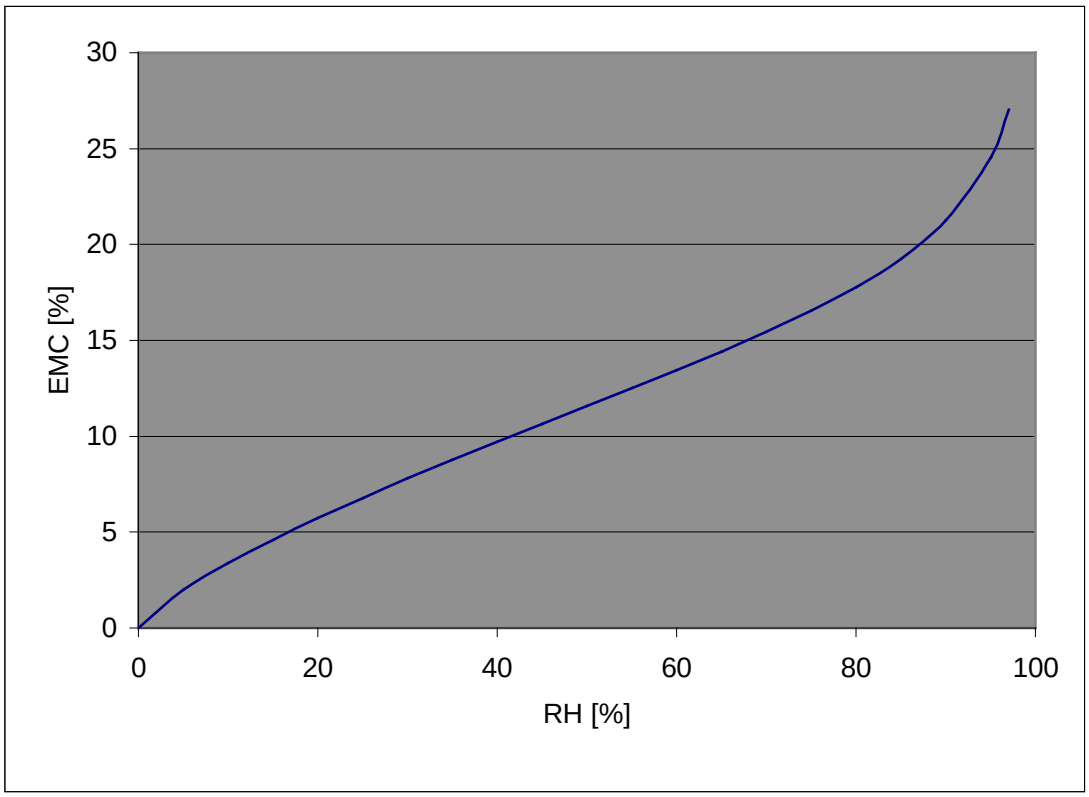

Figure 6.2: Sorption isotherm for untreated pinus radiata at 15ºC (similar in properties to the baltic pine hut lining at Cape Evans).

The experimental data for *pinus radiata* was determined and fitted to Eqn. 6.3 by Cunningham and Sprott [1984] and used in the model to represent baltic pine because data was not available. This was thought to be a reasonable assumption because the thermodynamic and mass properties of the two materials were very similar.

$$\ln U = a + b.\ln\left[\phi^{-c} - 1\right] \qquad [6.3]$$

where: a = 2.97, b = -0.17 and c = 4.48

c) Active layer

The response time of the wooden lining to variations in the indoor relative humidity is dependent on the thickness of the material. The greater the depth beneath the surface of the material, the slower the response time to changes in the relative humidity. Close to the surface, rapid or diurnal changes in relative humidity will affect the moisture content of the timber, but a centimetre below the surface may only respond to seasonal changes. This is analogous to soil temperature response to solar and seasonal variations.

A form of *lumped* analysis was used in this model. An active layer of material was considered to be involved and this layer was assumed to be of even moisture content that dynamically responded to the room relative humidity, evenly throughout its thickness. Beneath this layer, there was considered to be no interaction with the room, as if an impermeable layer was present.

In the calculation of mass transfer, the moisture content of this layer doesn't enter the equation explicitly, but rather is modelled by the time weighted average of the indoor relative humidity. The moisture content is used to establish the active layer, and the effect on the moisture content of the wood.

d) Mass transfer theory

Mass concentration provides the driving force for the flow of moisture through a medium. *Fick's Law of Diffusion*, the mass transfer counterpart of Fourier's Law of Heat Transfer [Tucker 1997a: 75] is

$$\frac{\dot{m}}{A} = -D.\frac{\partial C}{\partial x} \qquad [6.4]$$

where:

A = material surface area, m^2

D = diffusion coefficient, m^2/s

C = water vapour concentration, kg/m^3

The form of Eqn. 6.4 refers to the one-dimensional case of the diffusion of a single-component. The *mass transfer coefficient,* h_m*,* can be implemented into Eqn. 6.4 and rearranged in the form

$$\frac{dm}{d\tau} = h_m A(C_1 - C_2) \qquad [6.5]$$

The model used humidity ratio, W, as the driving force, so the mass transfer coefficient, h_{mc}, was modified by the air density, ρ_a:

$$h_{mc} = h_m . \rho_a \qquad [6.6]$$

leading to the final form of the mass transfer rate equation:

$$\frac{dm}{d\tau} = h_{mc} A_m \left(W_{twa} - W_{room}\right) \qquad [6.7]$$

Absorption occurs when the humidity ratio of the room is greater than that of the material and vice versa for desorption.

e) Mass transfer coefficient

The mass transfer coefficient used in Equation 6.5 can be derived from the heat transfer coefficient, h_c, using the *Lewis relation*:

$$h_m = \frac{h_c}{(\rho . c_p)} \qquad [6.8]$$

This relationship is appropriate for water vapour in air, and assumes that the Lewis number[7] is approximately equal to one.

[7] The Lewis number is the dimensionless ratio of the Schmidt number by the Prandtl number which relates the thermal diffusivity to the mass diffusivity.

f) Timber moisture mass

The mass of moisture in the timber is calculated using:

$$m_w = \frac{m_{wood,dry}.U_{wood}}{(1-U_{wood})} \quad [6.9]$$

the derivation of which is included in Appendix D.

where:

m_w = mass of water contained, kg

$m_{wood,dry}$ = dry mass of timber, kg

U_{wood} = moisture content of timber, 0 to 1

6.4.3 Sorption Model Attributes

a) Time weighted average

The time dependant relationship between the room relative humidity and the moisture content of the timber [TenWolde 1994] was modelled with an exponential time weighted average room humidity;

$$\phi_{i,\tau} = \frac{\sum_{n=N-4\tau}^{N-1} W(n).\phi_i(n)}{\sum_{n=N-4\tau}^{N-1} W(n)} \quad [6.10]$$

In this equation, the exponential weighting factor; $W(n) = e^{-\frac{(N-n)}{\tau}}$ attenuated the contribution of values, with an exponentially decreasing factor, away from the current discrete time step, N, so that the current relative humidity had the most influence.

The wooden surfaces in the room were calculated to be in equilibrium with this value of relative humidity through the sorption function, Eqn. 6.3.. The length of

the time constant was determined from the literature and trial and error tests to be about 24 hours. Beyond four time constants there is assumed to be negligible effect.

b) Rolling stack

In coding the above function, it was necessary to define a fixed length rolling stack of relative humidity values. This was a non-referenced chronological listing of the prior relative humidity values, where the most significant value was added to the end of the stack, knocking off the least significant. The stack contained enough data to satisfy Eqn. 6.10 over four time constants. The stack was preloaded with data immediately prior to the model input period.

c) Surface condition for mass transfer

The temperature of the surface was defined as a fixed ratio (approximately 98%, very close to the indoor temperature) of the internal and external temperature difference which is effectively the same as applying Fourier's Law to the wall, but without confusing the issue with additional parameters. A sample calculation in determining the ratio has been included in Appendix D.

The saturated surface humidity ratio, $W_{s,sat}$, is a function of surface temperature, t_s, only.

$$W_{s,sat} = f(t_s)$$

With the surface relative humidity, W_s, determined from the time weighted average, the surface humidity ratio was found via the saturated surface humidity ratio using;

$$W_s = W_{s,sat}.\phi_s \qquad [6.11]$$

Equation 6.11 assumes that the relative humidity is equivalent to the degree of saturation, μ, as in Eqn. 6.12, and this approximation is very good at low temperatures.

$$\phi \approx \mu = \frac{W}{W_{sat}} \qquad \text{for } t < 0^{o}C \qquad [6.12]$$

A proof of this approximation is included in Appendix D. Figure 6.3 is a flowchart of the sorption model and demonstrates the logical progression of the code.

6.4.4 Sources of Error

The sorption model assumed equal affinity for the water vapour to absorb into the material as that required to desorb. Surface tension forces may exist that would require additional energy to allow the moisture to move into the room air.

The assumption of the time weighted average (TWA) function in establishing the surface relative humidity was not tuned for the conditions at Scott's hut. A medium term experiment could have been devised to measure the moisture content response of a wooden sample over a given period of time. This data could have been matched with the output of the TWA function.

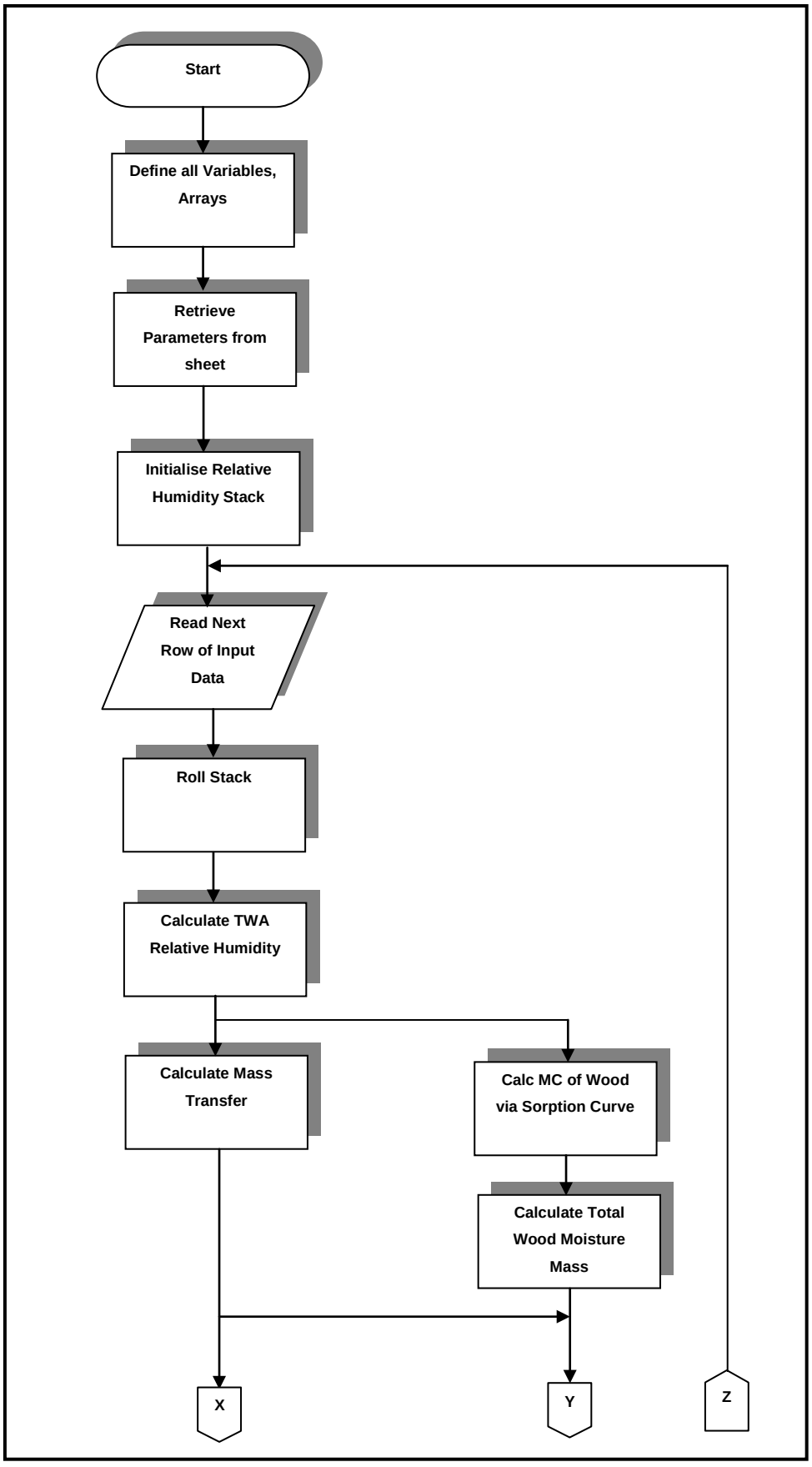

Figure 6.3a: Flowchart of sorption model (continues…)

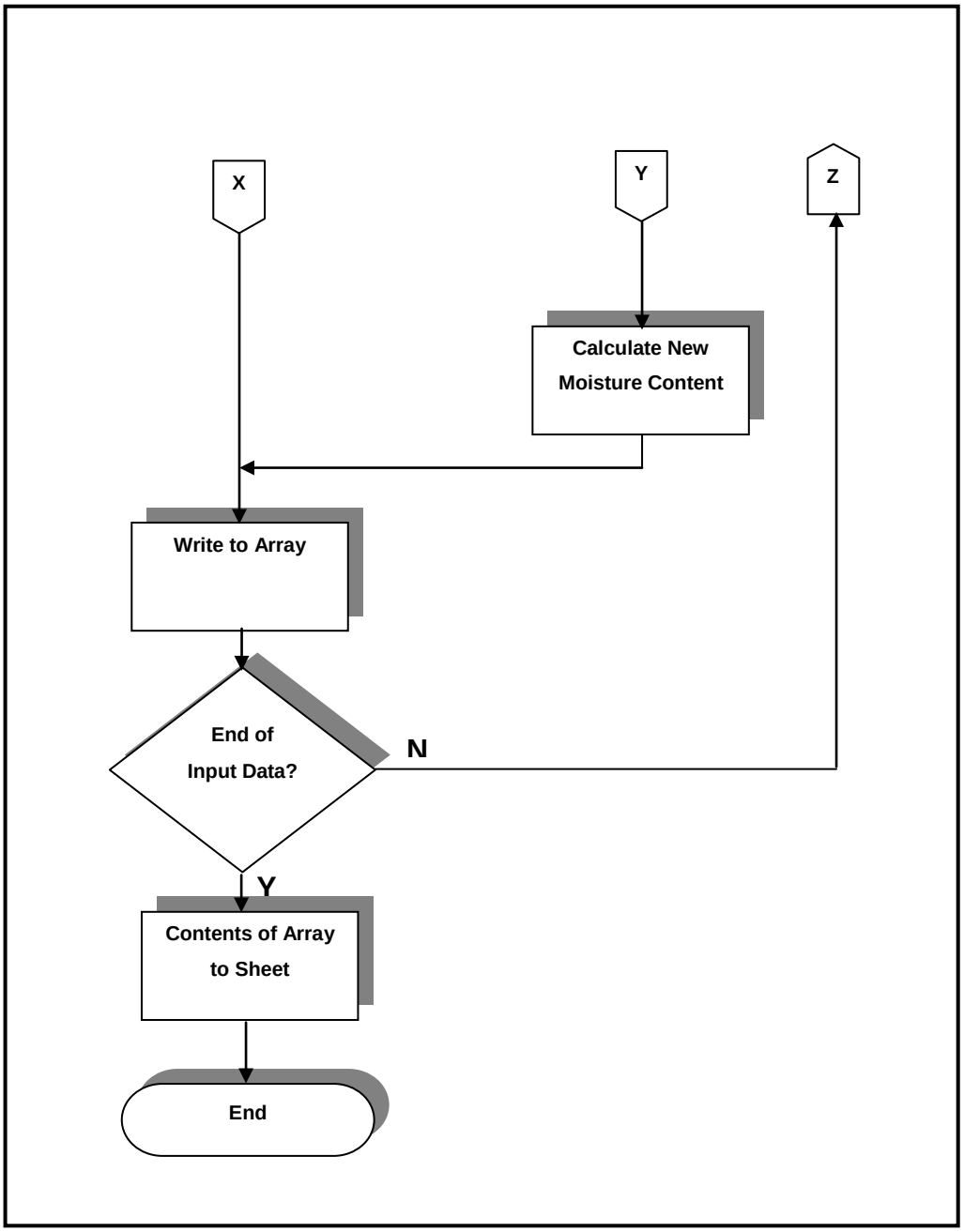

Figure 6.3b: Flowchart of sorption model (continued)

6.5 Condensation and Evaporation Model

6.5.1 Background of the Model

The condensation and evaporation model followed much the same mass transfer algorithm as the sorption model with different treatment of the surface condition. This method stems from the work of Tsuchiya [1980], Kusuda [1983], Barringer and McGugan [1989] and TenWolde [1994].

6.5.2 Condensation and Evaporation Processes

a) Definitions

Condensation occurs when moist air comes into contact with a surface that has a temperature less than the dewpoint[8] temperature of the moist air state. When moisture has condensed onto a surface, it is then available for evaporation back into the air state and will proceed to do so when the air state humidity ratio descends below that of the surface humidity ratio. Condensation occurs on cold surfaces such as the windows and the thermally bridged areas of the floor where ice often appears. Both of these surfaces have been modelled independently with identical code and varying parameters.

b) Mass transfer theory

The mass transfer process was driven by the concentration gradient, as in the sorption model, but the surface on which the moisture condensed was assumed to be covered by a uniform layer of moisture, meaning the surface humidity ratio was equal to the saturation humidity ratio at the given surface temperature. This process is represented by;

$$\frac{dm}{d\tau} = h_{mc} A_m \left(W_{s,sat} - W_{room} \right) \qquad [6.13]$$

6.5.3 Condensation/

[8] Dewpoint temperature is the temperature at which the given moist air humidity ratio would just saturate the air, in isobaric conditions.

Evaporation Model Attributes

a) Dewpoint check

The surface temperature was calculated in a similar manner to the sorption model surface temperature, but the temperature was much closer to the outdoor state. This reflected the cold nature of the windows and floor area examined. The dewpoint was calculated and compared to the surface temperature. If the surface temperature was not less than the dewpoint temperature then condensation could not proceed.

b) Condensate check

A running total of the mass of condensate collected on the given surface area was kept, from which evaporation could occur. If there had been no condensation or the total had completely evaporated then no further evaporation could occur. Figure 6.4 is a flowchart showing the working algorithm of the condensation and evaporation model.

6.5.4 Sources of Error

The main source of error in the condensation side of the model is related to the lack of a detailed thermal model. When moisture condenses onto a sub-dewpoint temperature surface, the latent heat of condensation is transferred from the moisture mass to the surface of the glass. This raises the temperature of the glass (this can be neglected for the floor materials due to a much greater mass), so that at some point in time the temperature of the glass may rise above the dewpoint temperature of the air and thus cease to condense water vapour from the air. The model calculates the surface temperature of the glass with consideration of the internal and external temperatures only.

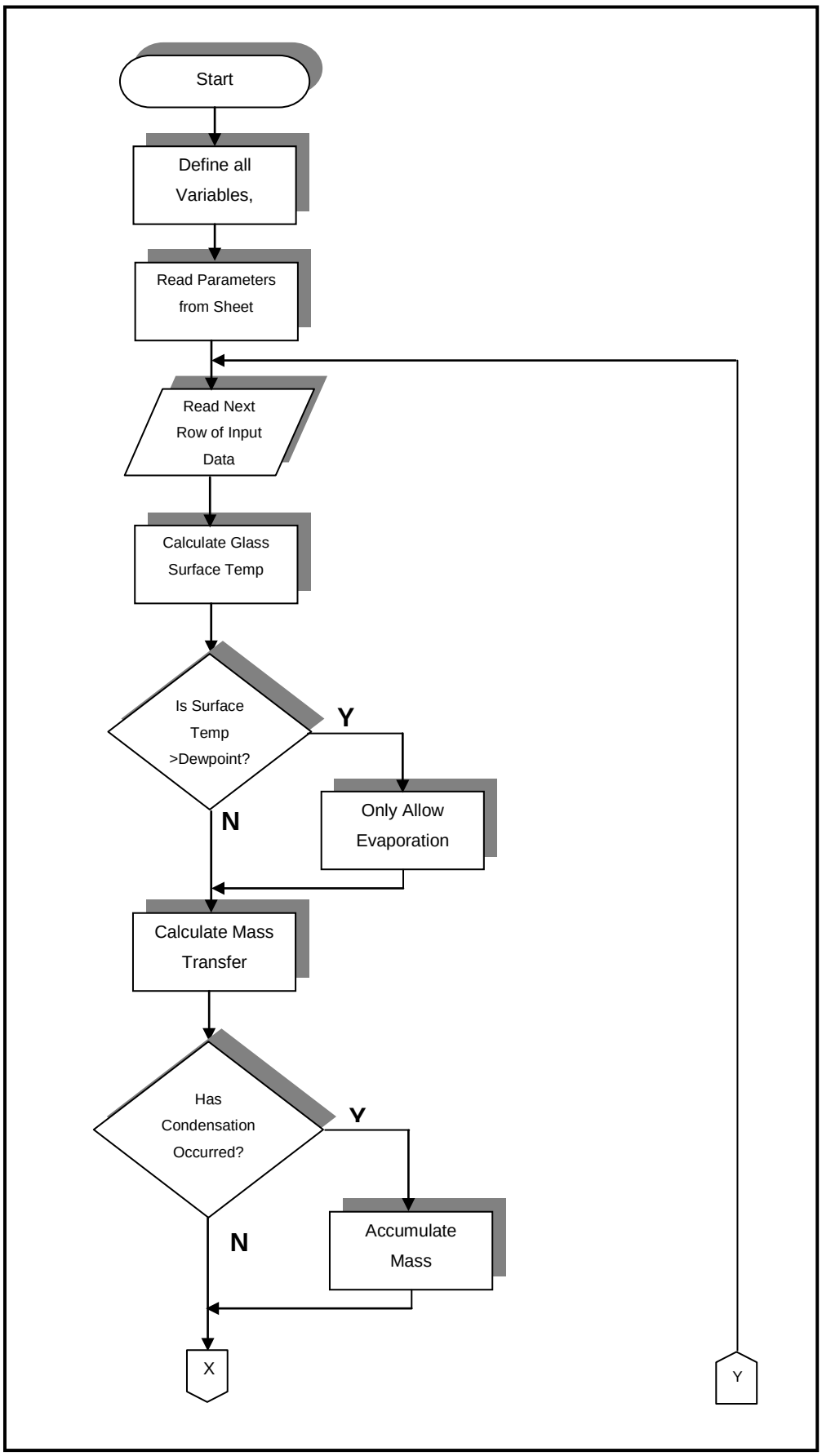

Figure 6.4a: Flowchart for glass condensation model (continues…)

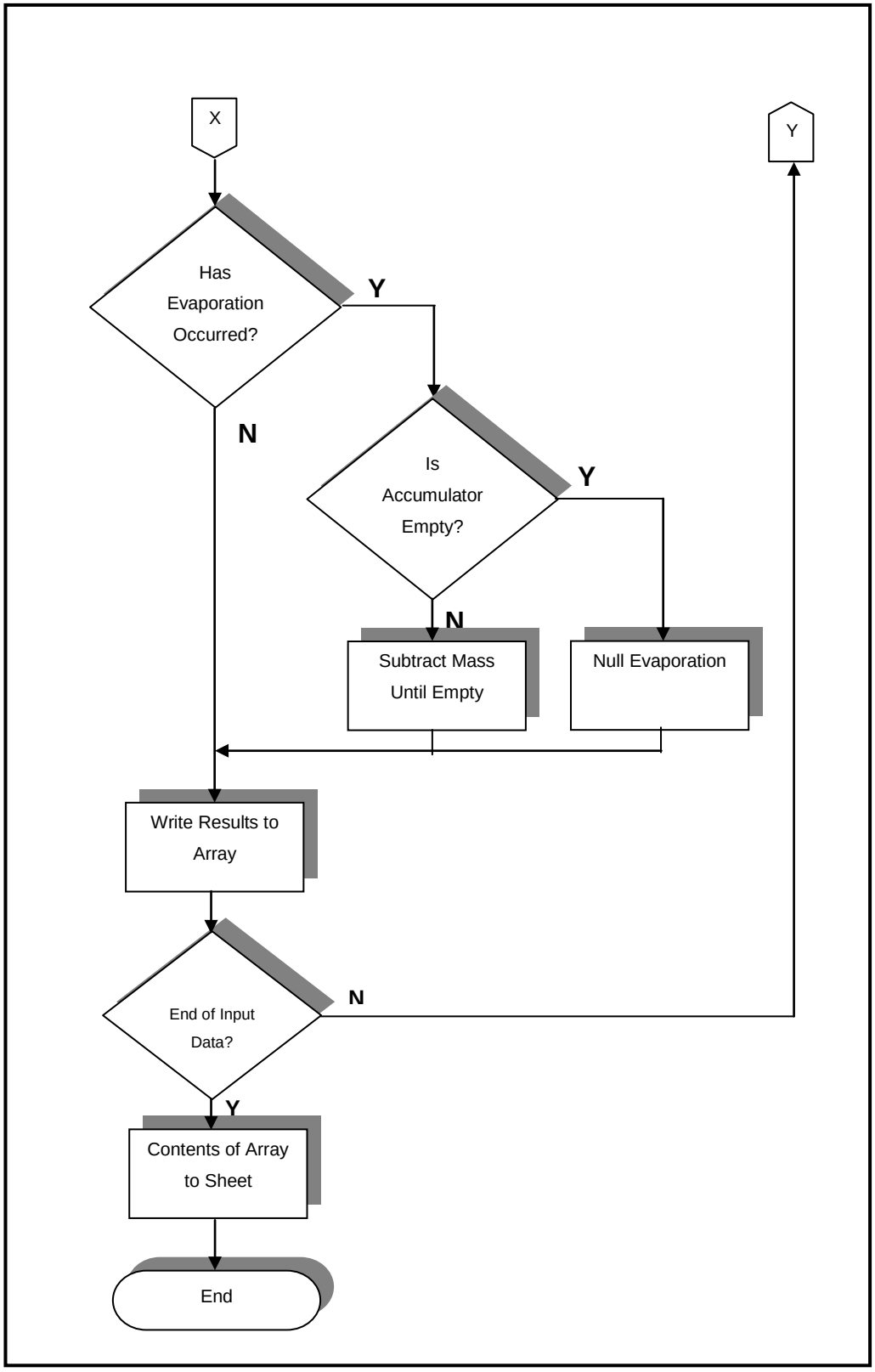

Figure 6.4b: Flowchart for glass condensation model (continued)

6.6 Visitor Occupancy Model

6.6.1 Human Respiration

As people breathe, they humidify the air before exhalation and so add moisture to the air state of their surroundings. The amount of moisture added to the air state depends on the level of activity that the person is undertaking, but varies from 0.04 to 0.1kg/hr, for respiration and perspiration. In the case of Antarctic visitors, the body was exceptionally well insulated and the temperatures cold enough to neglect the effect of perspiration, and values lower than this range were used to represent the gain to the space. These values were determined from known occupancy time periods.

6.6.2 Occupancy Model Attributes

The model assumed a direct gain to the room air state as a simple, step input with perfect, instantaneous mixing. This was not wholly unreasonable considering that the total gain is derived from 12 individuals all moving around the building independently.

This was linked to the infiltration model in that the effective leakage area could be boosted while people were present in the building.

6.6.3 Sources of Error

Errors associated with this model would be minimal as the assumptions were reasonably sound. There was a limited amount of precision time based data with known occupancy, door position and air state to match the model output, but this is offset by the simple nature of the model.

6.7 Vapour Diffusion Through Walls

6.7.1 The Diffusion Model

a) Definitions

Vapour diffusion through the walls, or other internal boundaries, is an important process when the building is both air tight and has lining materials with sufficient vapour permeability to allow the process to progress at a modest rate. This mechanism is driven by the presence of a vapour pressure differential across the wall.

b) Mass transfer theory

The rate of mass transfer [CIBSE 1986: A10-5] is given by;

$$\frac{dm}{d\tau} = \frac{\Delta p_v}{R.\Delta x} \qquad [6.14]$$

where;

Δp_v = differential vapour pressure across material, Pa

R = vapour resistivity of material, GNs/kgm

Δx = thickness of material, m

6.7.2 Neglecting Diffusion

Preliminary calculations substituting typical values into Eqn. 6.14, gave mass transfer rates of one to two orders of magnitude less than those of the other mechanisms. The vapour diffusion model contribution was then neglected in favour of faster computational time.

6.8 Indoor Relative Humidity Calculation

6.8.1 Representing Air Mixing

Once the mass transfer rates were evaluated over the hour for the individual models, the combined mass was added to a time weighted average function of identical form to Eqn. 6.10. This represented the mixing of the indoor air state and was found by trial and error to have a time constant of two or three hours.

6.8.2 Relative Humidity Trend

The time weighted average mass was evenly divided into the mass of air in the room then added to the internal absolute humidity found at the beginning of the hour, to obtain the new indoor absolute humidity. This was then used to calculate the indoor relative humidity.

6.9 Psychrometric Functions

6.9.1 Air Density

The change in air density as a function of temperature, Eqn. 6.15, was modelled by fitting the linear function to data derived from tabulated values [Tucker, 1997b];

$$\rho_a = -0.0049.t + 1.3061 \qquad [6.15]$$

accurate to ±2.5% within the range ±50ºC.

6.9.2 Vapour Pressure

The saturated vapour pressure over ice was found using the empirical formulation [Hyland and Wexler 1983];

$$\ln p_{v,sat} = \sum_{i=0}^{5} m_i T^{i-1} + m_6 \ln T \qquad [6.16]$$

where:

m_0 = -0.56745359 x 10^4 m_4 = 0.20747825 x 10^{-8}

m_1 = 0.63925247 x 10^1 m_5 = -0.94840240 x 10^{-12}

m_2 = -0.96778430 x 10^{-2} m_6 = 0.41635019 x 10^1

m_3 = 0.62215701 x 10^{-6}

which is appropriate for temperatures from 0 to –100ºC. As at no time did the ambient temperature rise above 0ºC, no formulation was included in the model for saturated vapour pressures above this value.

State vapour pressure is obtained by multiplying the above result by the relative humidity;

$$p_v = \phi . p_{v,sat} \qquad [6.17]$$

6.9.3 Humidity Ratio

The saturated humidity ratio was then calculated from the elementary relation [Tucker, 1997a];

$$W_{sat} = 0.622 \left(\frac{p_{v,sat}}{\left(p_v - p_{v,sat} \right)} \right) \qquad [6.18]$$

The state vapour pressure was calculated using Eqn. 6.12, and the same assumptions.

6.10 Programming the Model

6.10.1 Platform Selection

There were many ways to approach the coding structure, and indeed which platform to base the coding upon, but Microsoft Excel's Visual Basic for Applications (VBA) was chosen for its familiar user interface and mathematical aptitude. Matlab and Visual Basic 5 were also considered for the task. VBA allows the model parameters to be input from spreadsheets, which act as ready-made forms. The powerful mathematical routines of Matlab were not required on the simple time stepped models.

6.10.2 The Code Infrastructure

a) Heirarchy

The code was structured with each model being a separate subroutine branching from a main body, as depicted in Fig. 6.5. VBA is a completely separate object-oriented programming language application that resides in the background of Excel to allow the user to create and run macros. The model could be thought of as residing in two planes; the visual interface plane containing the input and output data and model parameters, and the invisible, functional plane where the calculations are carried out.

To start the code running, a small piece of code was attached to a command button on the main data spreadsheet that contained the whereabouts of the particular input data to be analysed. A separate command button was assigned to each block of data.

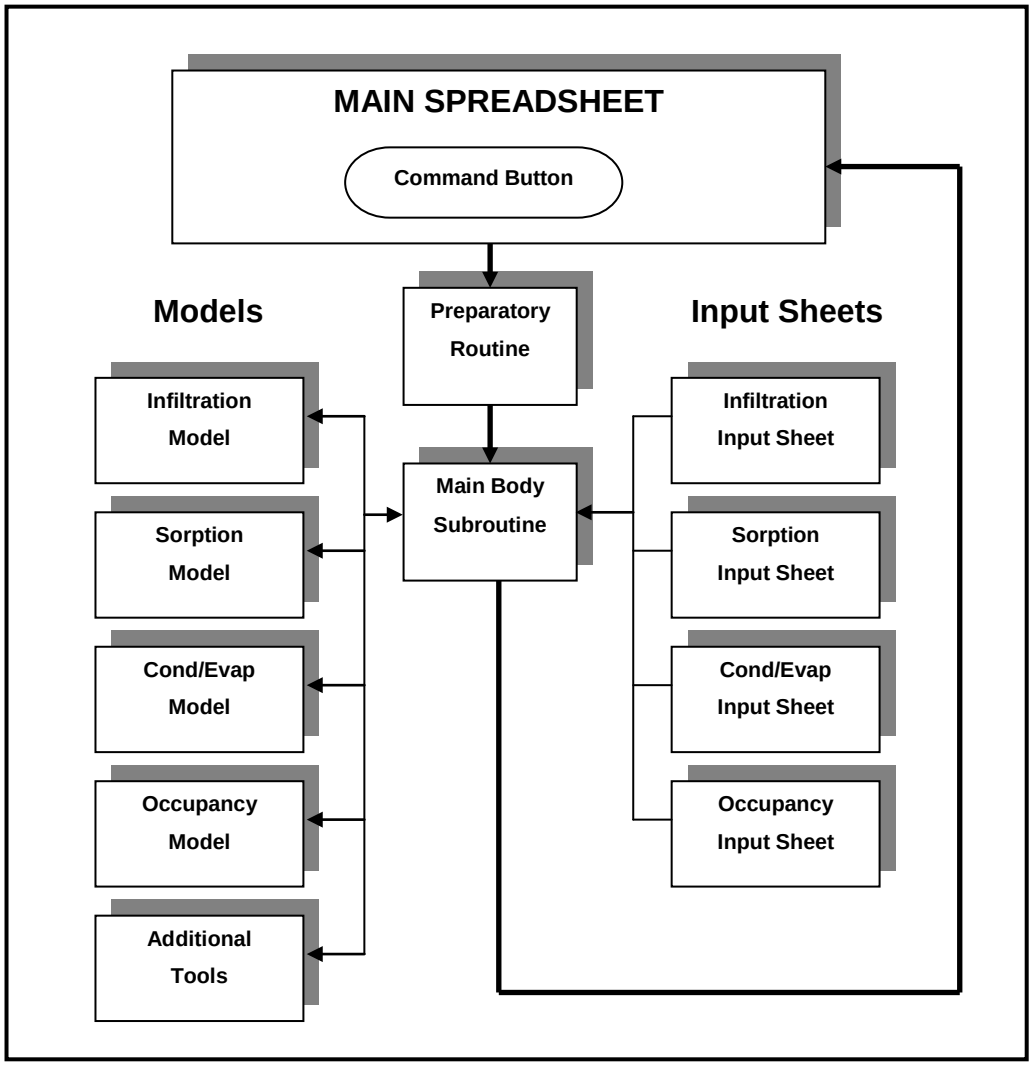

Figure 6.5: Flowchart of complete model

b) Main body

The main body subroutine had three purposes:

- Assign input data into two dimensional arrays
- Pre-condition the input data, if necessary
- Activate each of the models in turn

In addition, several automated analysis tools were built into the code (such as charting the results) which the main body also managed. These were installed in much the same way as the model subroutines.

c) Data sheet

A spreadsheet in the model workbook was dedicated to contain the input data and the command buttons to run the models. The output of the model is also returned back to this sheet.

d) Input sheets

Parameters used in the formulation of the mass transfer rates were also stored in spreadsheets attached to the model workbook. This allowed quick and simple tuning of the model without having to prepare Microsoft Windows-based input forms, and modification of the input data could be done outside the execution cycle of the code.

Printed hard-copies of the data and input sheets have been included in Appendix B.

6.10.3 Code Optimisation

a) Multidimensional Arrays

Reading the data directly from the worksheet is possible with VBA, but this was found to be much slower than using multidimensional arrays. The data was read into two dimensional arrays and could be accessed using subscripted variables. As a general rule for fast code, avoid using application based operations whenever possible.

b) Scope of variables

The risk of accidentally transferring a variable containing the data from one model to the next is avoided by keeping the scope of all variables as limited as possible. All data variables were kept local to the subroutine in which they were to be used.

c) Psychrometric calculation engines

In order to minimise the storage of unnecessary data, the additional state calculations were performed with functions in the code. Given temperature and relative humidity, the humidity ratio, air density and vapour pressure could be calculated as required, during code execution.

The psychrometric calculation functions are included in the program listings in Appendix B.

6.11 Chapter Summary

The individual model elements; infiltration, sorption, condensation/evaporation and occupancy, have been discussed in terms of practical representation, theoretical approach, and the formulation and flow of computer code. The assumptions made in each model have been highlighted and justified in terms of the required outcome. Psychrometric calculation routines used in determining states from the basic data have also been described. The vapour diffusion model was neglected as being insignificant.

Chapter Seven proves the accuracy of the model and presents the results of the analysis that was carried out on a variety of different scenarios.

CHAPTER SEVEN

MODEL ANALYSIS

7.1 Introduction

Having defined the theory and structure of the model in Chapter Six, this chapter sets out to provide an analysis of possible scenarios that exist or could be created within Scott's hut. These scenarios include:

- Examining individual component contributions
- Removing underfloor ice
- Altering the visitor group size, with open and closed doors
- Increasing the ventilation
- Determining the active layer depth in the timber of the walls
- Calculating the moisture load for a potential hygroscopic damping scheme
- Calculating the total summer condensate

The necessary running parameters required for the tuning of the model and selection of input data has also been covered in detail within this chapter. These factors are responsible for turning a general cold climate, indoor humidity model into a representative model of the micro-climate that exists specifically within the *Terra Nova* hut.

7.2 Parameter Selection

The following parameters represent baseline model input data, where no values have been adjusted to achieve any desired outcome. The values presented are typical and have been either sourced from handbooks or experimentally determined.

The heat transfer coefficient is given rather than the mass transfer coefficient, as the latter was derived from this value using the Lewis relation.

7.2.1 Infiltration Parameters

The input parameters used in the infiltration model are described in Table 7.1. The effective leakage areas used in the infiltration model were derived from a best fit to the experimental data, and refer to a 4Pa pressure differential.

Table 7.1: Infiltration model parameters

Parameter	Symbol	Nominal Value	Special Value	Unit
Effective leakage area	L	200	800*	cm^2
Stack coefficient	a	0.000145	-	$(L/s)^2 cm^{-4} (°C)^{-1}$
Wind coefficient	b	0.000174†	0.000104‡	$(L/s)^2 cm^{-4} (m/s)^{-1}$
Hut volume	V	358	-	m^3

* Effective leakage area modified during occupancy to allow for the door being open.

† Northerly wind direction under shielding class 3 [ASHRAE 1989a]

‡ Southerly wind direction under shielding class 4 [ASHRAE 1989a]

7.2.2 Sorption Parameters

The input parameters used in the sorption model are presented in Table 7.2.

Table 7.2: Sorption model parameters

Parameter	Symbol	Timber Wall	Unit
Heat transfer coefficient	h_c	3.0	W/m^2K
Surface area	A	110*	m^2
Surface temp. ratio	$t/\Delta t$	98	%
Oven dry density	ρ_m	440	kg/m^3

* See §4.2 for derivation of this value

The time-based function with which the sorption model estimated the material moisture content was based around a time constant which described the rate of change of moisture content. The model was found by trial and error to fit the data better with a time constant of 8 hours. The model was coded to respond fully within 4 time constants, or 32 hours.

7.2.3 Condensation and Evaporation Parameters

The condensation and evaporation model input parameters are described in Table 7.3. The floor and windows were treated as separate surfaces in the model and have different parameters.

Table 7.3: Condensation and evaporation model parameters

Parameter	Symbol	Windows	Floor	Unit
Heat transfer coefficient	h_c	6.0	3.0	W/m^2K
Surface area	A	1.8	1.47	m^2
Surface temp. ratio	$t/\Delta t$	50	10	%

7.2.4 Occupancy Parameters

The input parameters used in the occupancy model are similarly described in Table 7.4.

Table 7.4: Occupancy model parameters

Parameter	Symbol	Windows	Unit
Respiration Moisture	m_R	0.02	*kg/person.hr*
Maximum Occupancy	N_{max}	12	*people*

7.3 Transient Input Data

From the 1997 data year, five data blocks were chosen, each with a duration within the range of five days to two weeks (119 to 300 hours).

7.3.1 Block One: Early February

Block One spanned a period during summer from 7 February to 12 February inclusive. This was the earliest logger data for the 1997 test year and contained two logged visits and an unlogged visit[9] from tourist vessels. These visits have been well described in §3.6.

7.3.2 Block Two: Mid-April

Block Two covered a calm period during the year from 14 April to 21 April inclusive. This was used as a baseline to check the model.

7.3.3 Block Three: Mid-May

Block Three covered a fortnight from 14 May to 21 May inclusive. A substantial jump in the indoor relative humidity was noted which was discussed in §3.4.3.

7.3.4 Block Four: Late June

Block Four spanned from 18 June to 24 June inclusive. This block was chosen for having a step in indoor relative humidity that was similar to Block Three, but the lasting effect on the equilibrium state of the indoor microclimate was not quite as pronounced in Block Four, with the indoor state quickly returning to normal.

[9] Unlogged visit means that the hut visitor book was not signed on the day and the author does not wish to imply any illegal activity of the visiting vessel.

7.3.5 Block Five: Early November

The rise into a peak period of indoor relative humidity was covered by Block Five, from 2 November to 14 November. During this time, the sun was reappearing for a short time of the day and the temperature was rising from the mid-winter trough.

Figure 7.1 shows the indoor temperature and relative humidity trends for the 1997 calendar year with the five block boundaries marked.

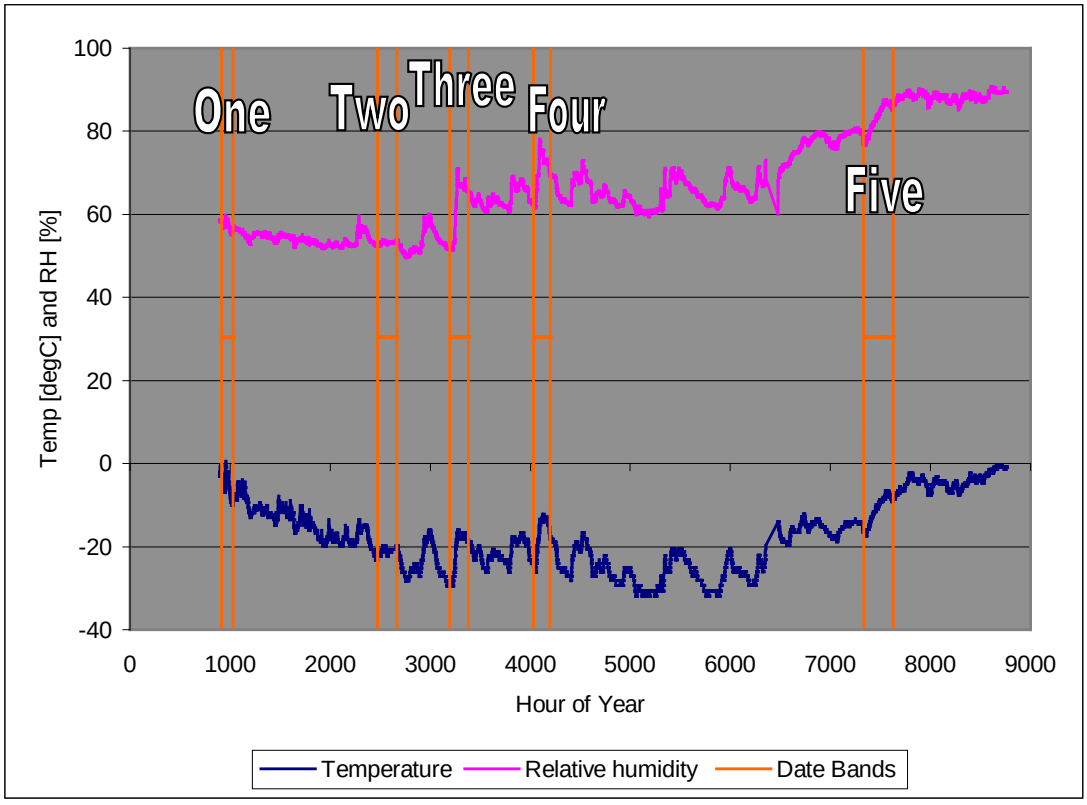

Figure 7.1: The four data blocks defined against the indoor temperature and relative humidity trends.

7.4 Representation of the System

To assess how well the model represented the microclimate inside the hut a simple mass balance, with which the modelled mass transfer could be compared was calculated over the input data period. The calculated air space gains and losses were also used to derive a modelled room relative humidity which provides a good comparison to the actual room relative humidity.

7.4.1 Study Period Comparisons

The mass transfer in any given hour was found to be very low due to the low humidity ratio of the air at the ambient temperature and the hourly variation of the input data was close to the measurement resolution of the 8-bit logger. These factors combined to produce a mass transfer trend that generally consisted of spikes projecting from the baseline into or out of the space air. The model, on the other hand, had the advantage of the computational resolution of a 32-bit variable type, so the trends are more 'analogue' in appearance. This makes the mass trends difficult to compare, but the magnitude of the variation can be established. The relative humidity trends provided the best comparison of the modelled versus the actual conditions that existed inside the hut and, in all cases, showed good reproduction.

It should be noted that some variation of the x and y-axis scaling exists in Figs. 7.2 – 7.11.

a) Block One data

The visitors to the hut provided a step disturbance to the air state which was modelled with good replication. The visitor effect is specifically covered in Section §7.7. Figure 7.2 show the stable mass transfer conditions except for the peaks where visitors entered the hut. The modelled relative humidity tracks indoor relative humidity around a stable 55% in Fig. 7.3, with a minor over-reaction to the times of occupancy. The lack of exact data on visitor movements contributes to this error.

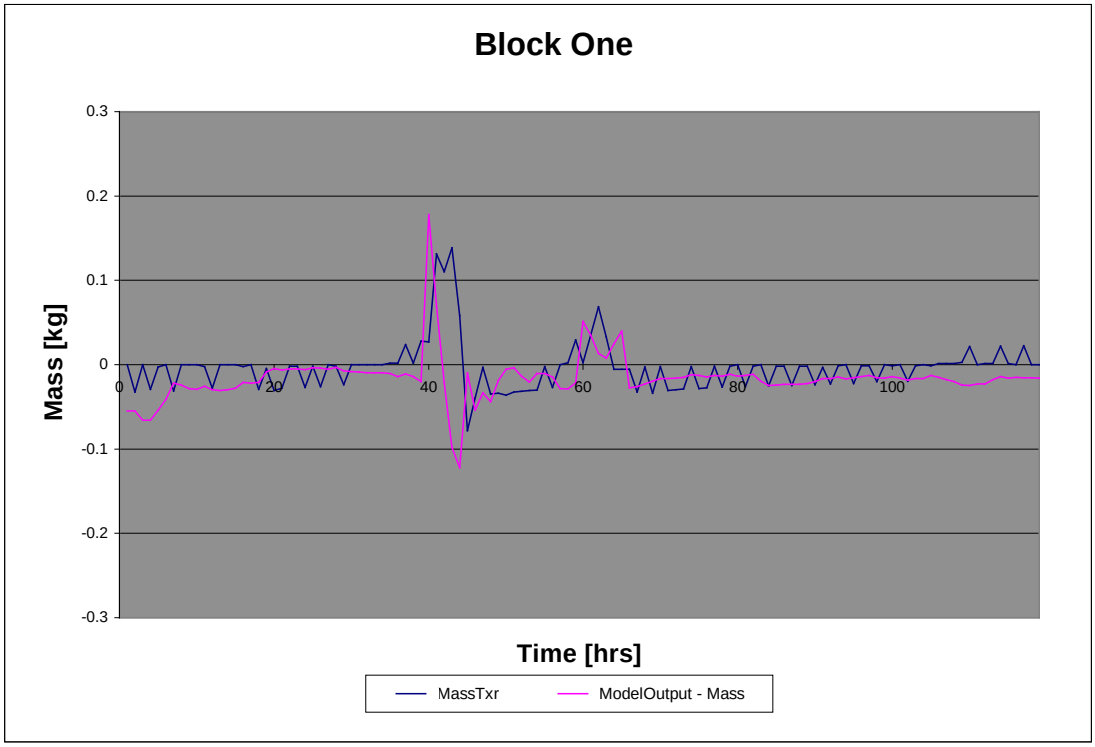

Figure 7.2: Modelled and actual mass balance of Scott's hut using data Block One.

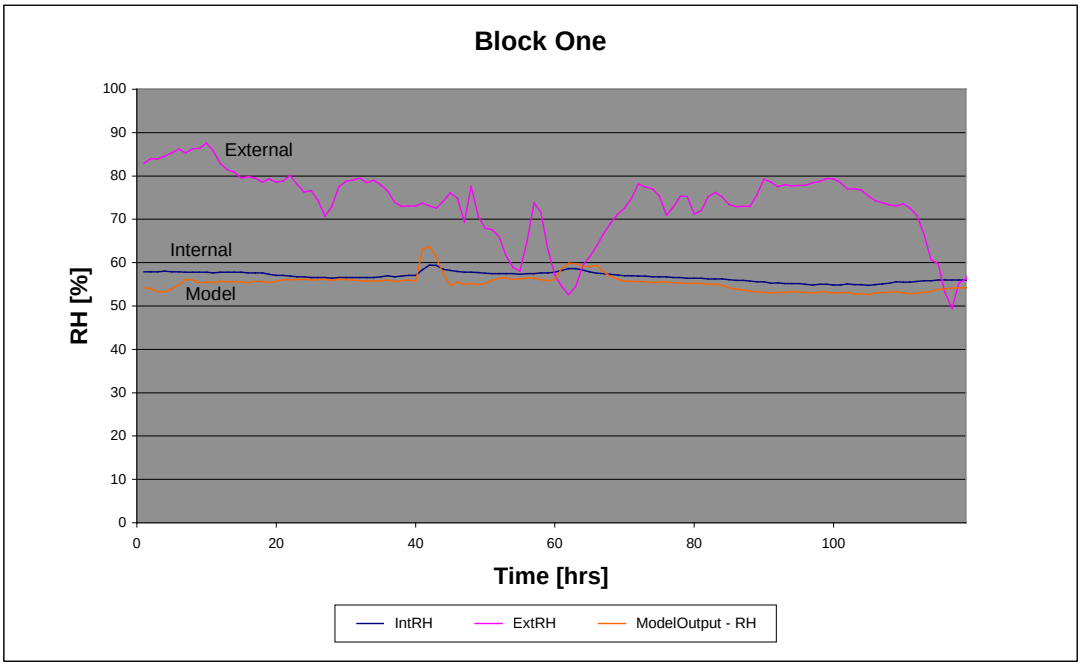

Figure 7.3: Modelled and actual indoor relative humidity also compared to external relative humidity, with Block One data.

b) Block Two data

Block Two demonstrates a period of very little atmospheric activity in and around the hut. The hourly mass transfer presented in Figure 7.4 is very low and the model replicates in magnitude only. Discrepancies in the model output are prone with model error being significant at these rates.

The relative humidity in Fig. 7.5 is likewise very stable, with little change overall and some minor influence of the external relative humidity in places.

c) Block Three data

A period of net gain to the space is shown in Fig. 7.6 as more of a peak in the model output, and a series of discrete gains in the data. Later in the sample, the model over-estimates the mass gain to space, but not significantly altering the relative humidity over this time, as shown in Fig. 7.7. The external relative humidity climb that spurred the change in equilibrium state can also be seen in Fig. 7.7.

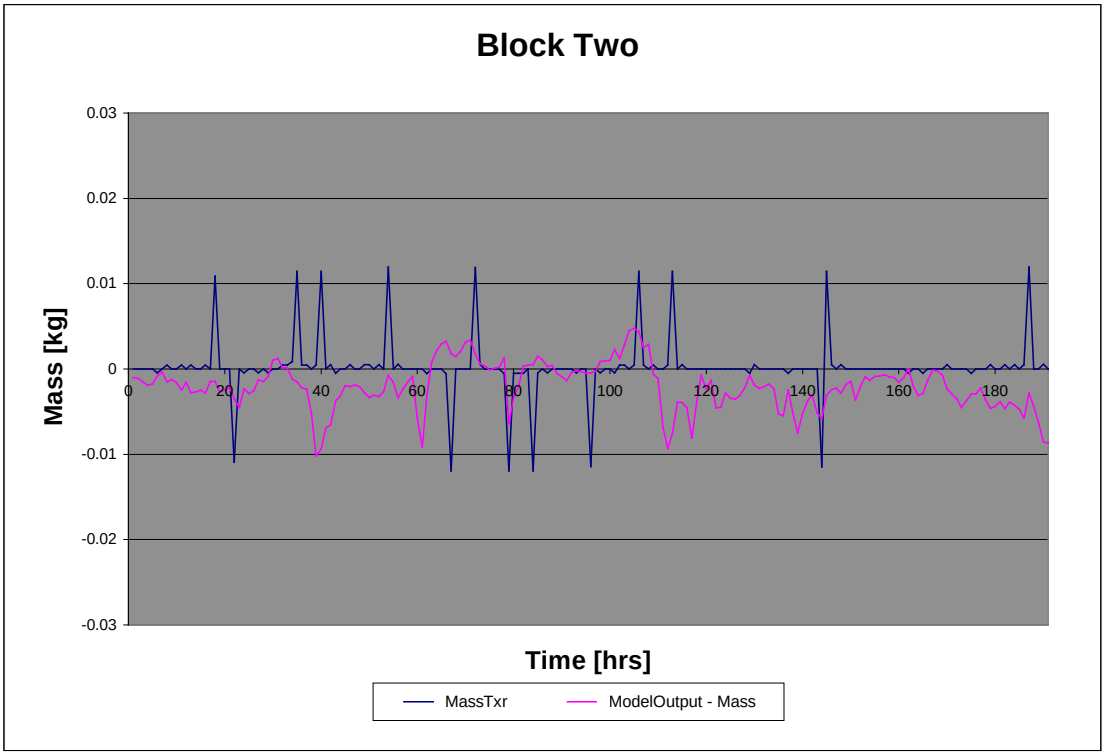

Figure 7.4: Modelled and actual mass balance of Scott's hut using data Block Two.

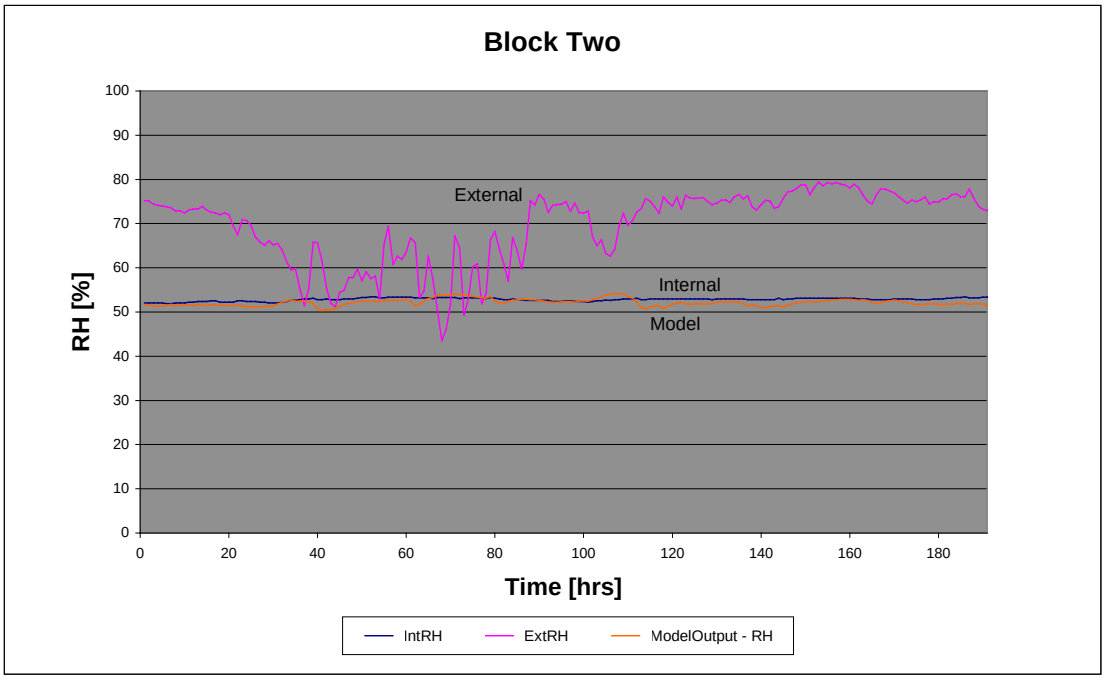

Figure 7.5: Modelled and actual indoor relative humidity also compared to external relative humidity, with Block Two data.

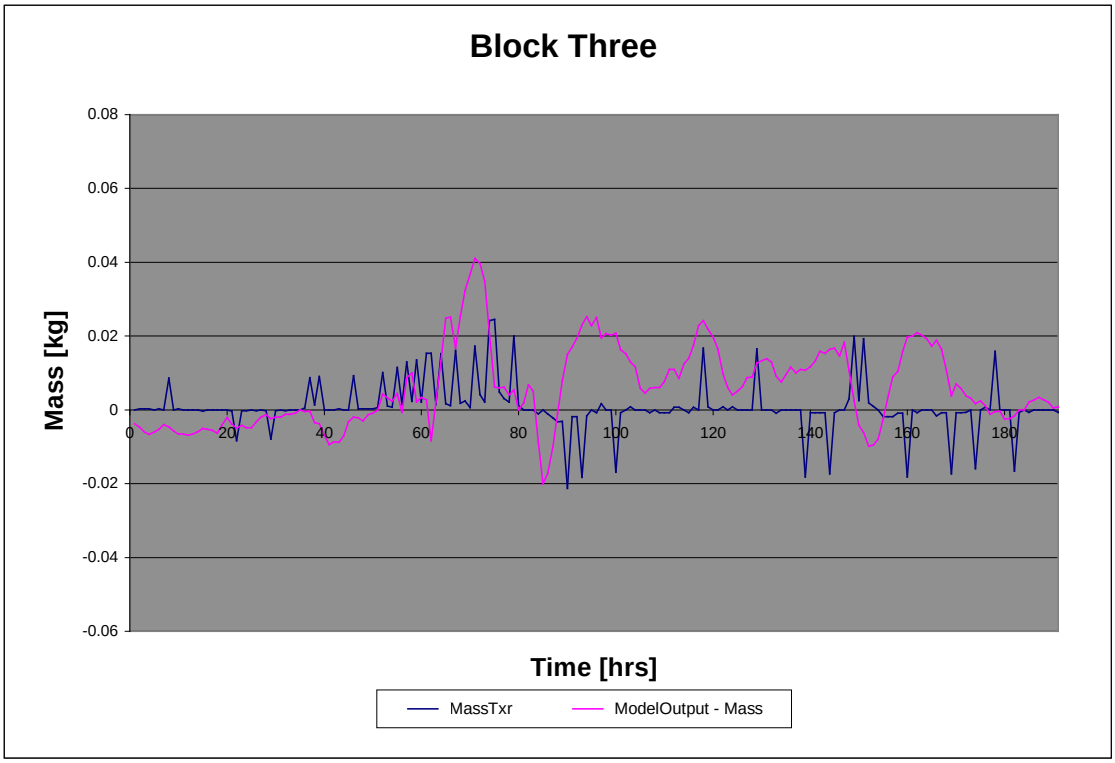

Figure 7.6: Modelled and actual mass balance of Scott's hut using data Block Three.

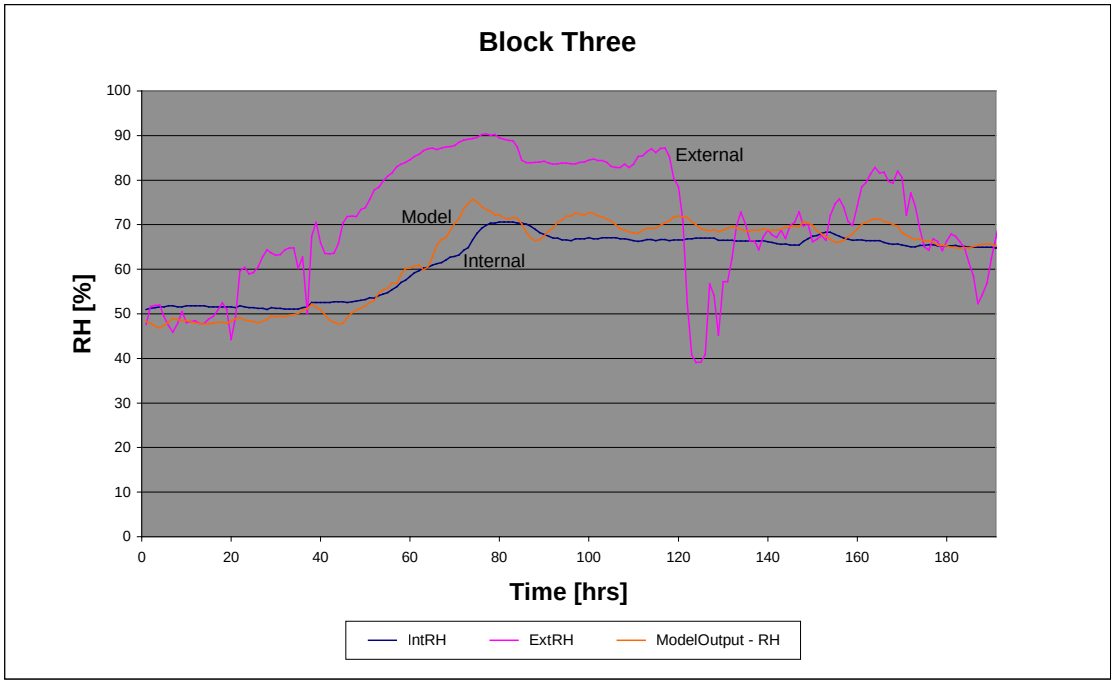

Figure 7.7: Modelled and actual indoor relative humidity also compared to external relative humidity, with Block Three data.

d) Block Four data

From about hour 50 to 65, Fig. 7.8 shows a large loss from the room air which is caused by the time-delayed sorption responding to the sudden increase in indoor relative humidity. This helps to settle the modelled relative humidity to the offset state shown in Fig. 7.9.

e) Block Five data

Figures 7.10 and 7.11 cover a longer period of 300 hours. The long term continual net gain to the space is apparent in Fig. 7.10, but the model tends to be over-driven by the high external relative humidity conditions occurring twice in the period. This also shows in the modelled relative humidity, Fig. 7.11, where a discrepancy occurs during these times.

This over-driving of the room relative humidity is caused by the heavy influence of the infiltration model during the very windy conditions present at the time. The model has calculated a higher infiltration rate than was actually present at the time. This is an unfortunate result of the lack of adaptability in the model that prevents it from predicting infiltration rates under all conditions. In addition, specifying shielding coefficients for every wind angle was not possible and in this particular circumstance the hut may have been more sheltered from the wind than actually modelled.

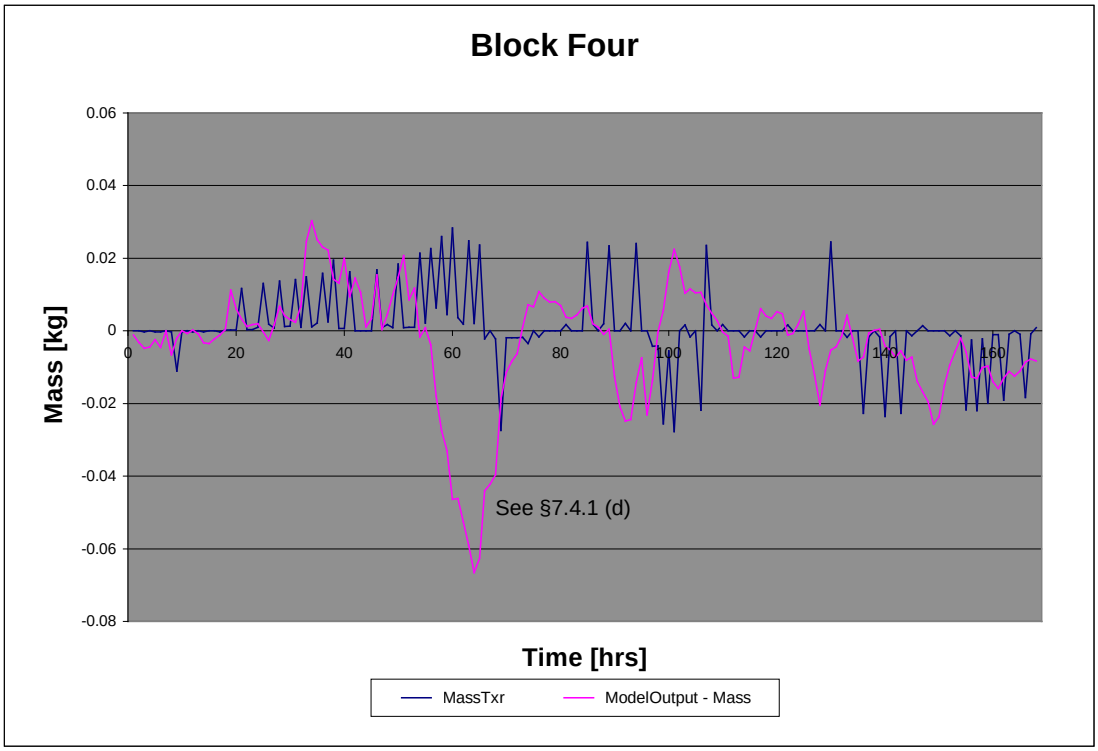

Figure 7.8: Modelled and actual mass balance of Scott's hut using data Block Four.

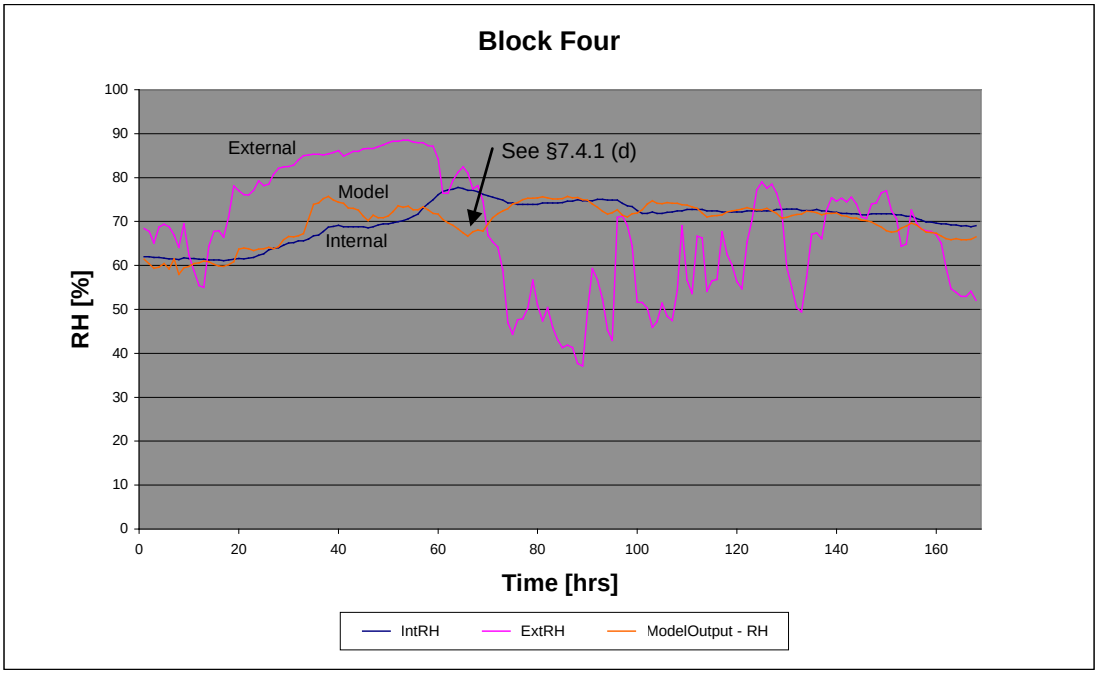

Figure 7.9: Modelled and actual indoor relative humidity also compared to external relative humidity, with Block Four data.

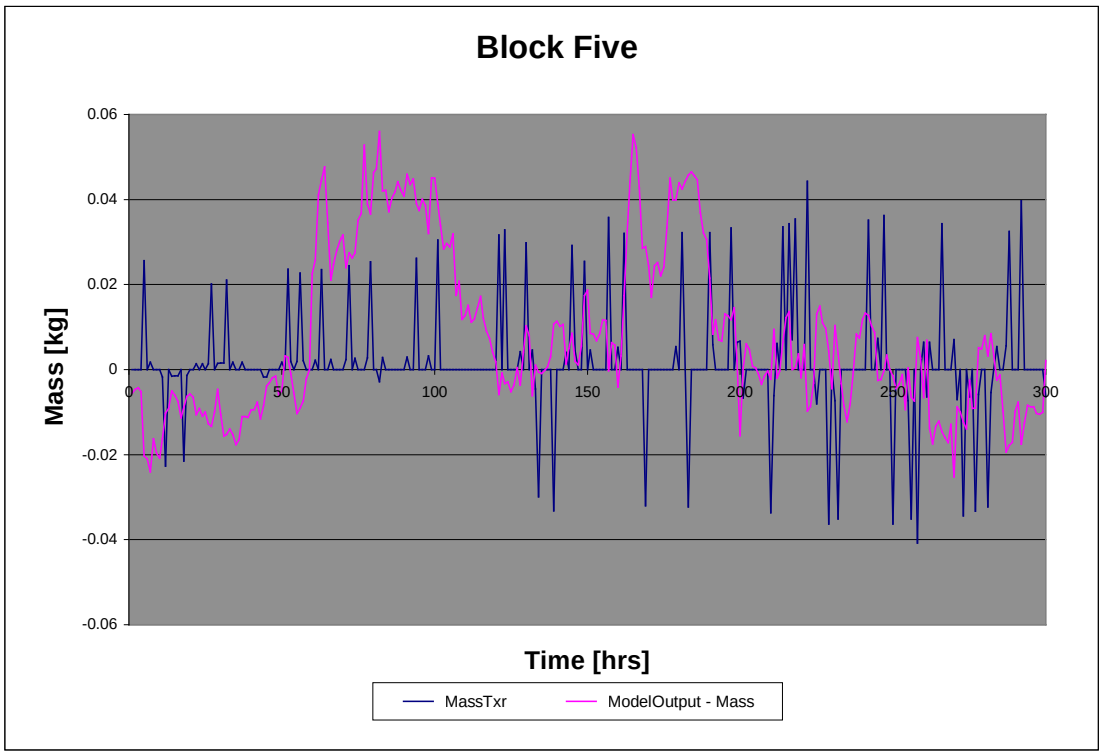

Figure 7.10: Modelled and actual mass balance of Scott's hut using data Block Five.

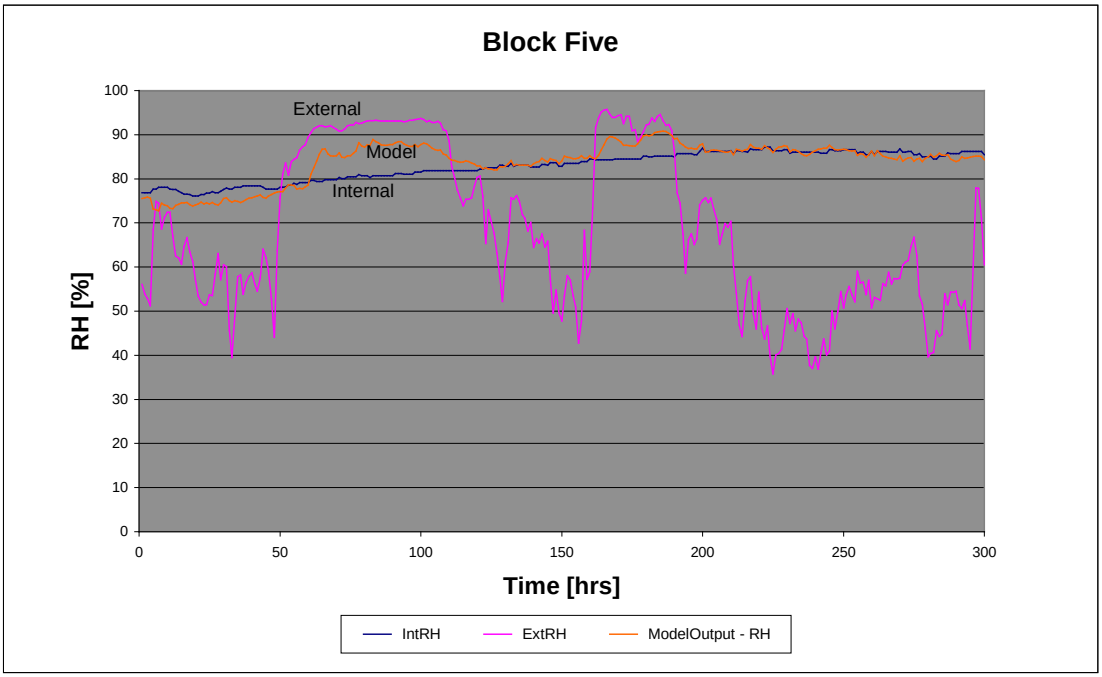

Figure 7.11: Modelled and actual indoor relative humidity also compared to external relative humidity, with Block Five data.

7.4.2 General Comments on Model Quality

The model achieves the goal of replicating the indoor humidity within reasonable error. The mean and population standard deviation of the error between the actual and modelled relative humidity in each data block is summarised in Table 7.5.

Table 7.5: Summary of relative humidity model error†

Block Number	Mean [%]	Pop. Standard Deviation [%]	Maximum [%]
One	1.78	0.90	4.74
Two	0.85	0.53	2.48
Three	2.75	1.85	9.93
Four	2.26	2.16	10.48
Five	2.25	2.15	8.15

† Error values expressed as a percentage of the range

The typical error was around 2 to 3% but errors above 10% were encountered at times. This close replication of the model to the actual relative humidity is mainly attributable to the fact that the model is only replicative (where the model can only reproduce a given scenario from full input data), not predictive (where the external data and hut parameters are all that are required to determine the indoor conditions), so that the actual indoor humidity is a key factor in determining the mass transfer. While this model does not allow prediction of the indoor conditions from knowledge of the outdoor state only, it does perform the useful task of comparing the contribution of the individual mechanisms and sensitivity analysis of parameters. The model also allows the effects of possible changes to the hut to be assessed by running 'What if?' scenarios, where changes can be made to the input data, such as increasing the ventilation of the hut, then running through the model again to see the relative effect of the changes.

7.5 Individual Component Contributions

7.5.1 Infiltration

Although the building was reasonably tight, infiltration of outside air into the hut proved to be the greatest source of moisture to the air state in most circumstances. This is normally the case and was expected from the outset. For most of the year, the external air state had a lesser humidity ratio than indoors, so any infiltration meant a moisture loss from the space. Unfortunately, in the frequently occurring storms, the humidity of the outside air was found to increase a great deal above that indoors, resulting in a short term, high moisture gain to the hut.

Figures 7.12 and 7.13 which follow show the individual modelled components of mass transfer and demonstrate a time with a mild infiltration rate and a period of high infiltration, respectively. Figure 7.13 clearly shows the infiltration gain to the space caused by a storm which has been discussed in Chapter Three.

7.5.2 Sorption

Sorption was generally seen to remove water from the air, at times removing large quantities of moisture at rates similar to that of the infiltration mechanism. The influence of sorption in the hut at Cape Evans is quite substantial and manages to buffer all but the large storms.

During low infiltration times as seen in Fig. 7.12, the sorption mechanism dominates the infiltration. In the steady state conditions shown, this resulted in a net loss from the space.

The sorption response in Figure 7.13 was to an increasing relative humidity inside the room due to high outside humidity and high infiltration rate. This particular period increased the indoor relative humidity substantially.

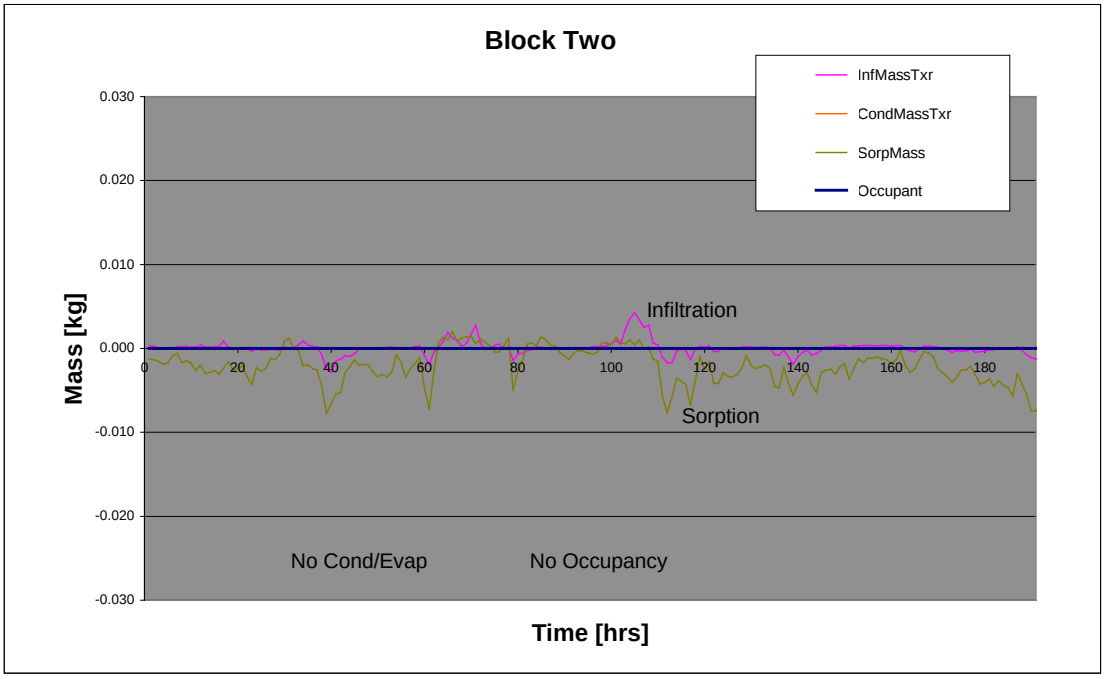

Figure 7.12: The Block Two data shows the mild infiltration rate being dominated by the absorption of water vapour into the hut linings.

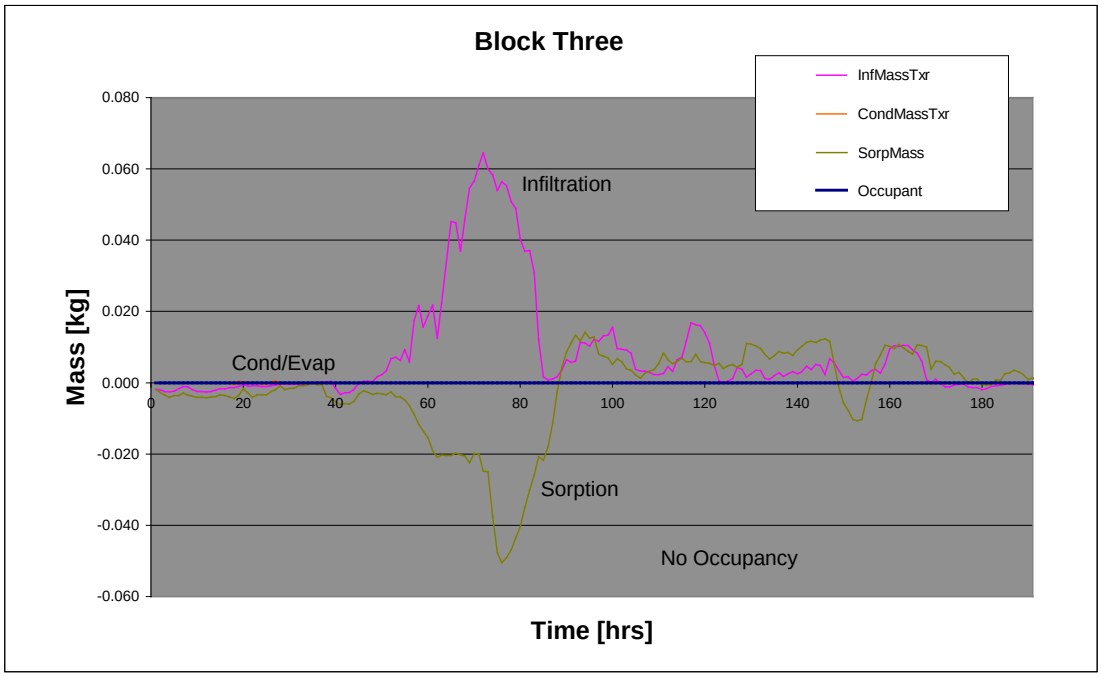

Figure 7.13: The infiltration of moist air adds to the space humidity and is offset by absorption, which later desorbs the moisture back into the space.

7.5.3 Condensation

Condensation was the minor player of all the modelled mechanisms. For condensation to occur, the surface temperature needed to be lower than the dewpoint, and this did not happen too frequently.

Approximately 7g of water was calculated to condense and then re-evaporate following the large visitor group in the Block One data of Figure 7.14. This is a result of the expected scenario where the large moisture gain in such a short time does not allow the hygroscopic materials time to react and quickly condenses out of the air.

Condensation was noted when the room relative humidity was driven high and then followed by a rapid decrease in temperature, such as immediately following a northerly storm. Such an occasion occurred at the end of the Block Four period, but did not contribute greatly to mass transfer.

The condensation model suffered the most from the lack of a simultaneous thermal model, in that all condensate was assumed to be equally ready to evaporate but in fact may be frozen in place requiring a latent heat of sublimation to allow mass transfer directly to the space. The potential effect of this is covered in §7.11.

7.5.4 Occupancy

The occupancy was the most simple model, but the data was sparse and while the influence of visitors in existing data has been shown in Chapter Three, the modelled step to the room air state can be seen in Fig. 7.15. The first peak has been offset with the model boosting the infiltration rate by assuming the door has been left open. Sorption can also be seen responding to the increase in indoor relative humidity. The second peak was not recorded in the log-book and the occupancy was judged by trial and error from the response to be approximately six people with the door closed behind them.

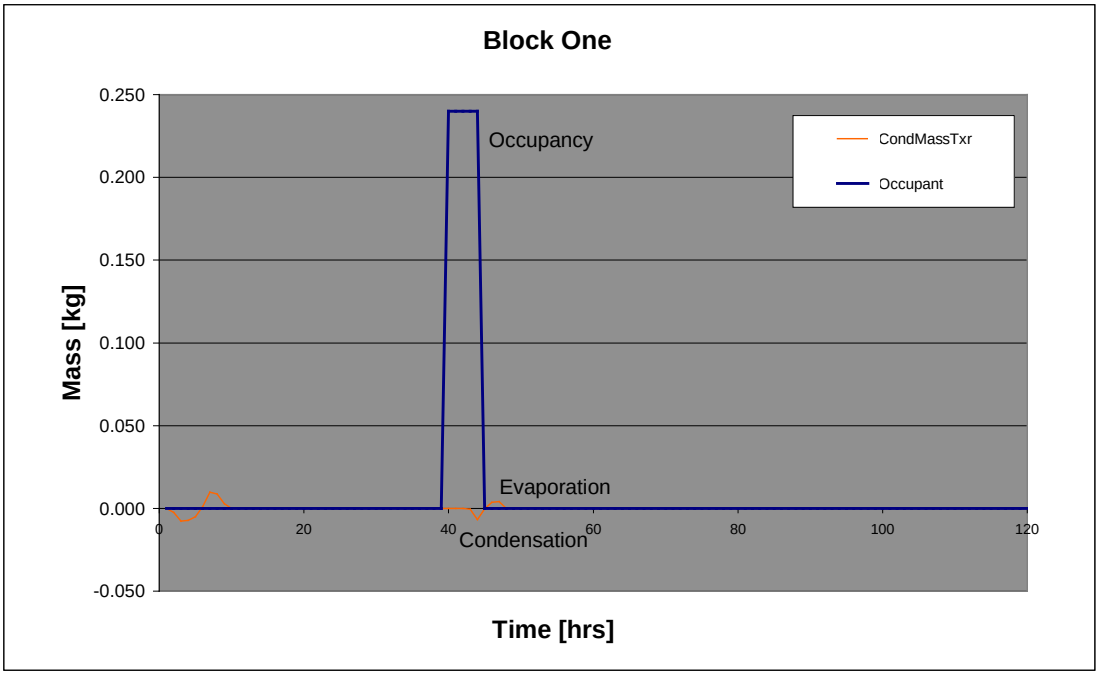

Figure 7.14: Condensation appears at the end of a large group visit. Sorption and infiltration trends have been removed for clarity.

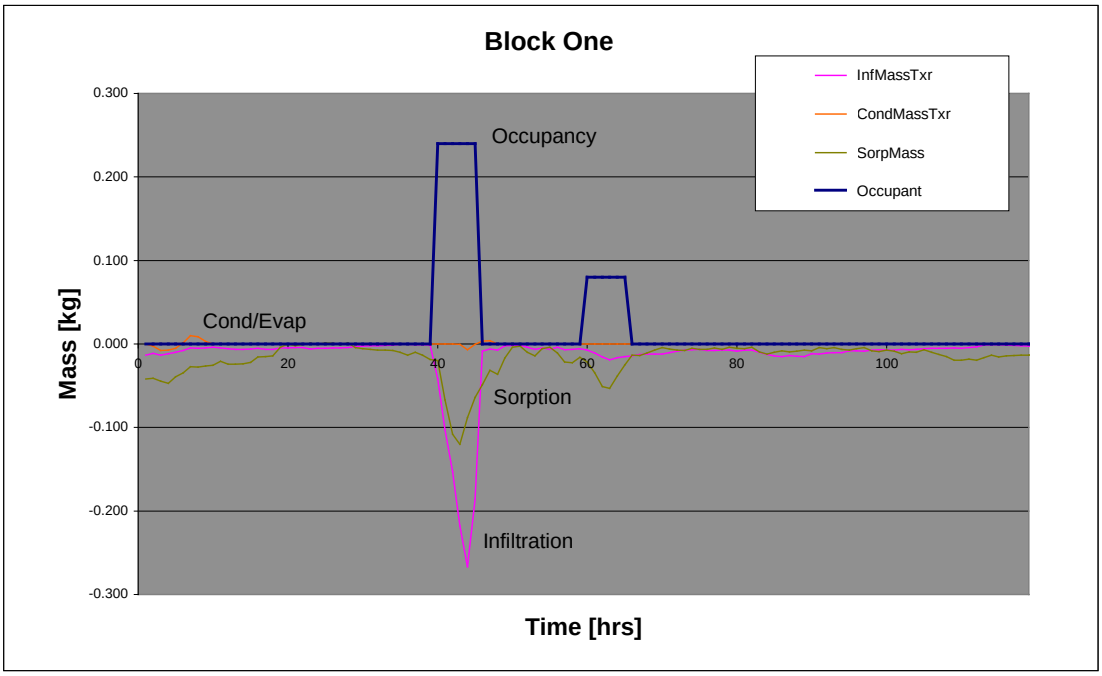

Figure 7.15: Block One data showing two occurrences of visitors to the hut and the response of the model.

7.6 Non-modelled Effects and Underfloor Ice

7.6.1 Analysing Model Error

The saturated patches of wall lining and floor materials, caused by underfloor ice and snow resting against the outside of the building, were thought to be major sources of moisture and the reason for high indoor humidity levels inside the building. The moisture gain to the space from these sources was not modelled, but the error between the modelled and actual results can be examined to shed some light on the subject. The error can be considered as a non-modelled mass exchange with the hut space.

The results of correlating model error against the major external influences are shown in Table 7.6.

Table 7.6: Correlation of model error against external influences

	Solar	External Temperature	Wind
Block One	0.119	0.126	0.022
Block Two	-0.020	0.769	0.274
Block Three	0.000	0.618	0.575
Block Four	0.000	0.161	0.258
Block Five	-0.026	0.408	0.776

The lack of solar radiation in winter denies any correlation with moisture at this time of the year but even in the presence of substantial solar gain, there is little correlation with the effects of the sun. External temperature does track well with the unaccounted mass but, as it does not rise due to solar means, it can be assumed that the temperature increase is a result of the warmer, moist winds from the north. This wind also shows a solid correlation with the mass transfer. This analysis provides modelling support to the earlier data analysis carried out in Chapter Three, which proposed that the major source of moisture was from northerly storms.

This result may appear to give the impression that removing the ice and moisture sources from under and around the hut will have no effect, but that does not take into account the effects of sorption.

Sorption has been shown to be a major factor in the moisture response of the hut, and while the majority of the timber in the hut has been assumed to be in equilibrium with the environment, the constant high moisture content of the wetted timber known to exist in the hut will raise the relative humidity.

7.6.2 Effect of Removing the Moisture Source

The model was adjusted to include $2m^2$ of wetted timber that replaced the same area of material in equilibrium. The addition to the model assumed that the material maintained a constant moisture content of 25% because the material was continuously wetted by capillarity from behind or beneath. The same mass transfer coefficient as the rest of the material area was used.

Assuming that this material was the only possible moisture source not already modelled, the area of this material was arrived at by tuning the modelled relative humidity trend to the actual relative humidity trend. The net influence of the near-saturated material is the difference between these two ‘before and after’ modelled trends.

For representative data Blocks One and Three, removing the moisture source caused an average reduction of room air humidity of 1.7 and 1.4% respectively. Figure 7.16 demonstrates how the trend was effectively shifted down by this amount, using the Block One data.

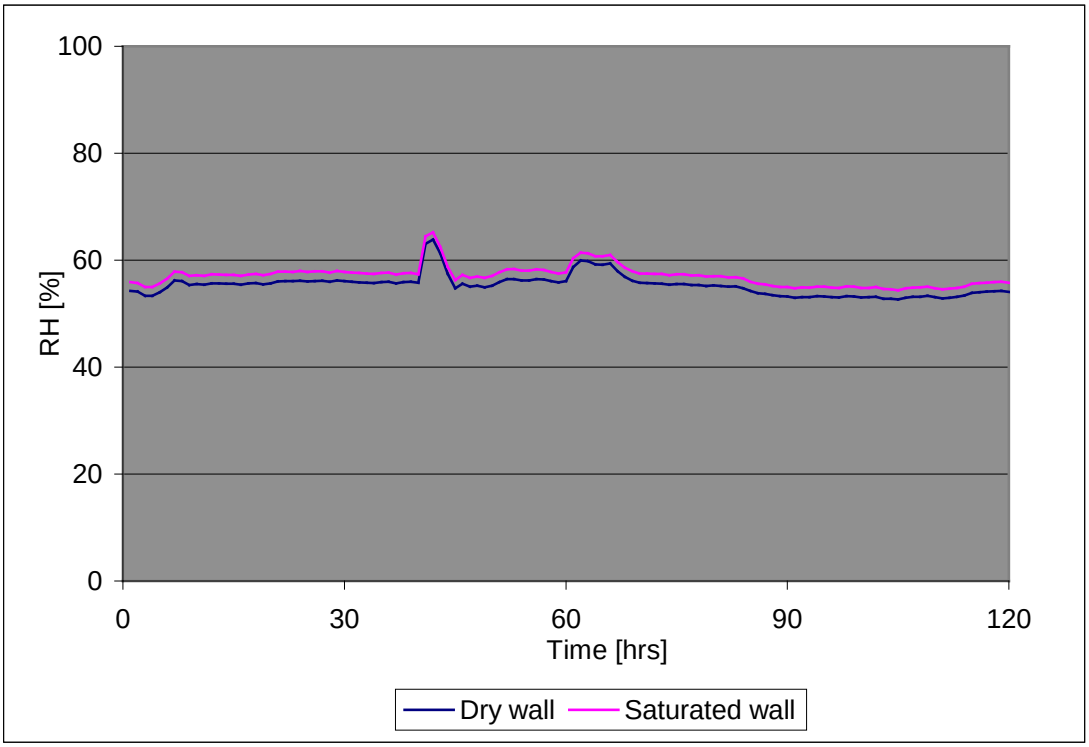

Figure 7.16: Predicted offset in relative humidity by removing capillary moisture sources from the hut at Cape Evans. Block One data used for modelling.

7.7 Investigating Visitor Effects

7.7.1 Gauging the Present Limit

The Heritage Management Plan specifies that a maximum of twelve people at one time are allowed in the Cape Evans hut. Data analysis showed that this number of people would offset the indoor relative humidity for a time, but the level returned to prior conditions soon after the party left. The amount of time that the room state took to return to normal was a function of the time that the party spent in the hut and the number in the group.

After an extended length of time, the equilibrium state of the wall materials will be disturbed and the time taken to return to normal will increase drastically.

The time of the year is also big factor in how visitors influence the room relative humidity. Due to the low quantity of water vapour in the air in winter, a single

person may offset the relative humidity more than a whole group for a comparable period in summer. As mid-winter visits generally are not a problem in Antarctica, this was not covered in detail.

7.7.2 Relative Humidity Disturbance

This analysis used the Block One data as the hut generally has been visited at this time of the year. The model allows the occupancy to be modelled with the door closed or open and a separate analysis is presented in each case for a given six hour total duration of the visit. Opening the door added an effective leakage area (ELA) of 750cm^2.

a) Open door occupancy

Figure 7.17 shows the incremental effect of increasing the number of people. The present limit sees the relative humidity rise by 6% and fall back to starting conditions pretty much coincident with the group leaving due to the sorption response. A group size of 18 people will cause the indoor relative humidity to rise more than 10%.

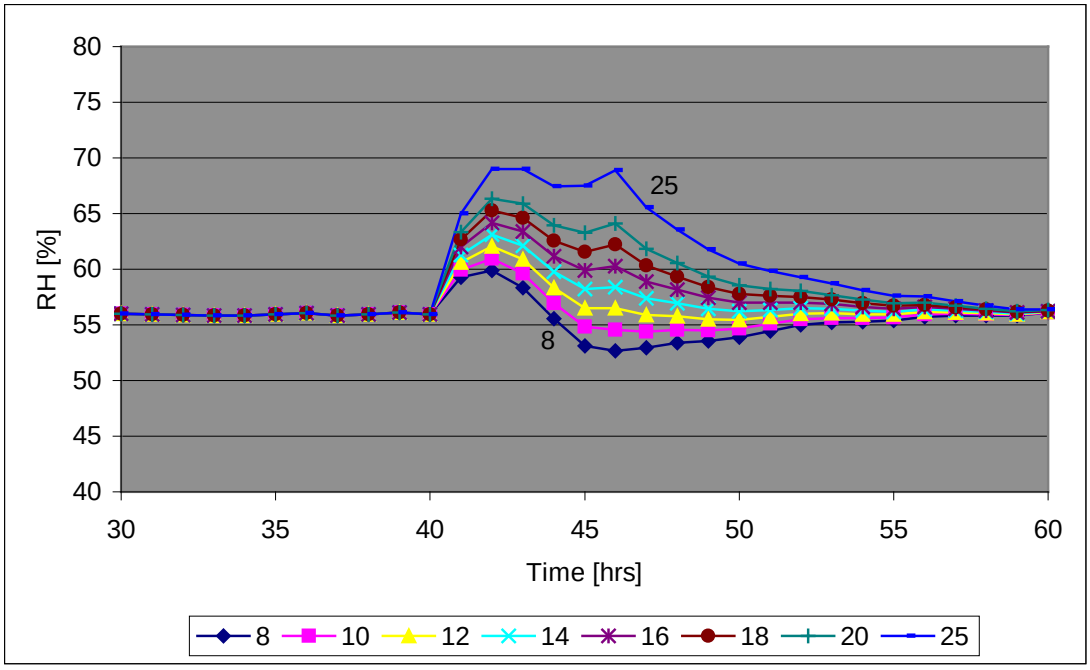

Figure 7.17: Hut relative humidity response to incremental group size, with the door assumed to be left open.

b) Closed door occupancy

Closing the door and removing the infiltration offset to the human latent gain is seen in Fig. 7.18 to be equivalent to approximately 4-6 people. The 10% relative humidity increase occurs with only 14 people in the hut for the same duration of visit.

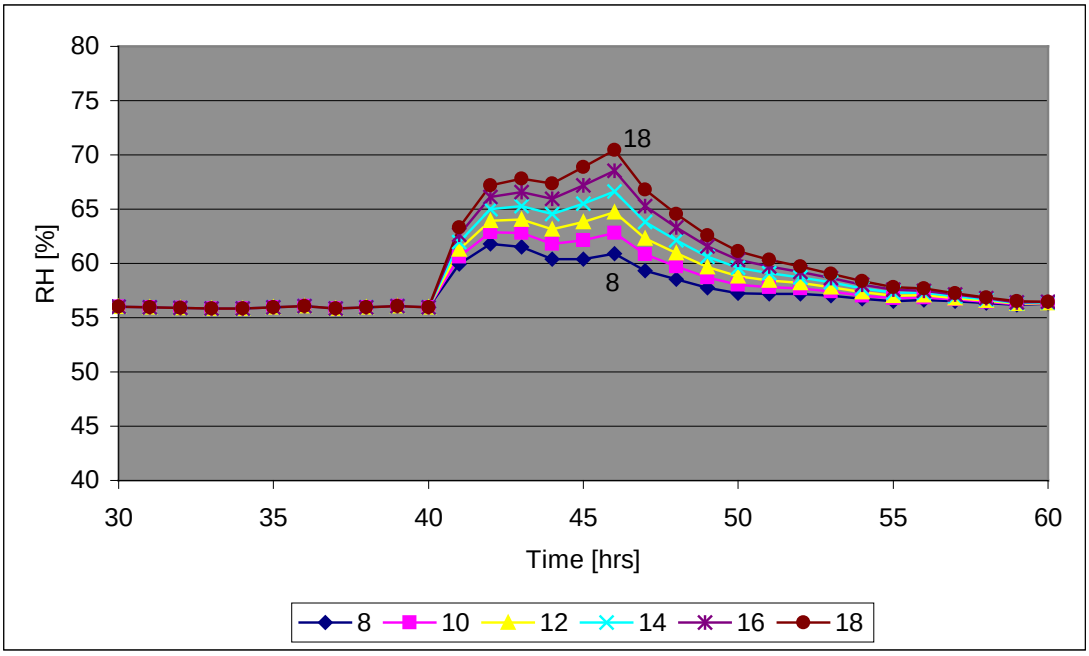

Figure 7.18: Hut relative humidity response with the door closed.

7.8 Ventilation

7.8.1 Is Ventilation Desirable?

For added ventilation to remove moisture, there must be less moisture in the external air state than that it is replacing inside. The absolute humidity data for the whole year indicates that additional ventilation would be desirable only over the summer period. During winter, the humidity ratios are mostly similar except for the northerly storms, where the external values rise dramatically. Any additional ventilation during these times would have an extremely negative effect on the moisture state of the hut.

7.8.2 Effect of Additional Ventilation

As all ventilation was passive, (i.e. only wind and stack effects, not with mechanical fans driving air), additional ventilation was modelled by adding to the effective leakage area of the infiltration model. Figure 7.19 shows the effect of added leakage area to the room relative humidity. The wind was particularly still around the time of the visit, so the infiltration was based only on the stack effect, which explains why the relative humidity trends pack together.

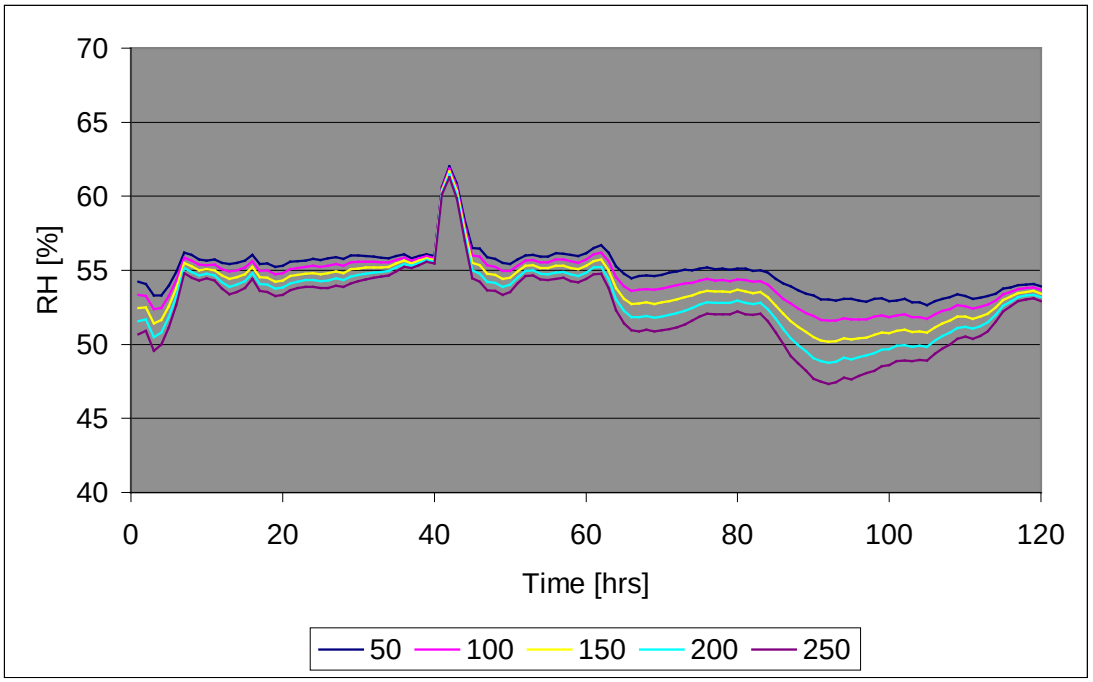

Figure 7.19: Additional ventilation (ELA units of cm^2) effectively reduces the relative humidity of the room for the Block One data.

7.8.3 Approach to Summer Ventilation

The model has shown that there is a case for introducing a passive summer ventilation scheme for Scott's hut at Cape Evans. The model did not, however, account for the temperature drop associated with bringing cooler air inside the building. If the air flow was sufficient to reduce the temperature to outside levels then the relative humidity may actually increase in the room. A basic heat and mass transfer model (considering infiltration only) could be developed to estimate the net effect of mixing the two air states.

Should the device still prove to be worthwhile, such a system would have the following features:

- The ventilator would have a facility to be shut off or removed in winter
- Sufficient flow rate to be effective in low winds
- A wind-vane operated damper or similar mechanism appropriate for shutting off the flue during northerly winds
- A self-draining or collecting snow trap that can be inspected and cleaned out, possibly using solar heating to melt the accumulated snow
- A self-regulating mechanism to restrict high wind air flows
- A diffuser to avoid air blasting into the hut

7.9 Active Layer Depth

7.9.1 Method of Analysis

A 'running' moisture content value was calculated in the model by adding or subtracting the transferred mass from the active volume of timber in every period. This timber had a surface moisture content equated to the time weighted average moisture content. The difference between the values of running moisture content and time-weighted average moisture content was a

function of the volume and therefore, also of the specified active layer depth[10]. For example, with the layer specified too thin, the volume of material (from which the mass was transferred) was less than that effectively modelled and thus the variation in the running moisture content was much greater than that of the time-weighted average moisture content. The incrementally stepped active layer depth was considered to be defined correctly when the running moisture content became just equal to the time-weighted average moisture content.

For consistency in the following analysis, the sorption time constant parameter remained at 8 hours.

7.9.2 Results

Figures 7.20, 7.21 and 7.22 show the effect of increasing the active layer depth and how the running moisture content and the time-weighted average moisture content trends close together. The y-axis scales have been zoomed in for clarity and this must be considered in their interpretation as the actual moisture content fluctuation is minimal.

Included on the plots is the mass transfer trend, which shows the inverse relationship between ‘gain to space’ and material moisture content.

[10] The specification of active layer depth had no effect on the outcome of the mass transfer process.

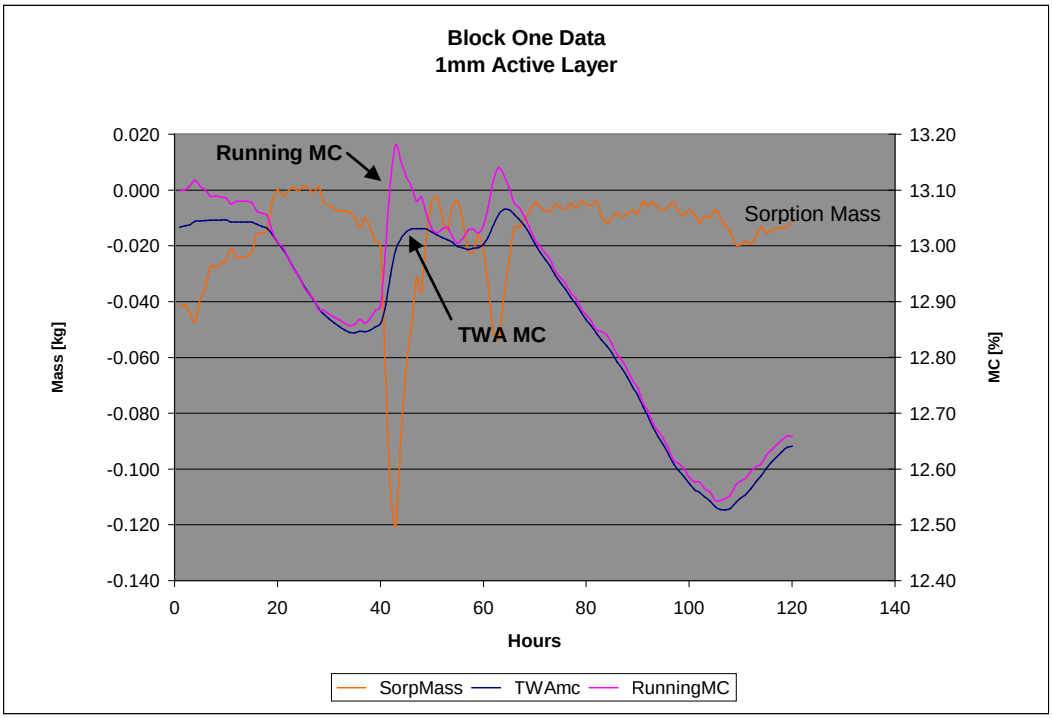

Figure 7.20: Plot showing modelled moisture content variation of hut lining materials. Block One data used with an active layer depth of 1mm.

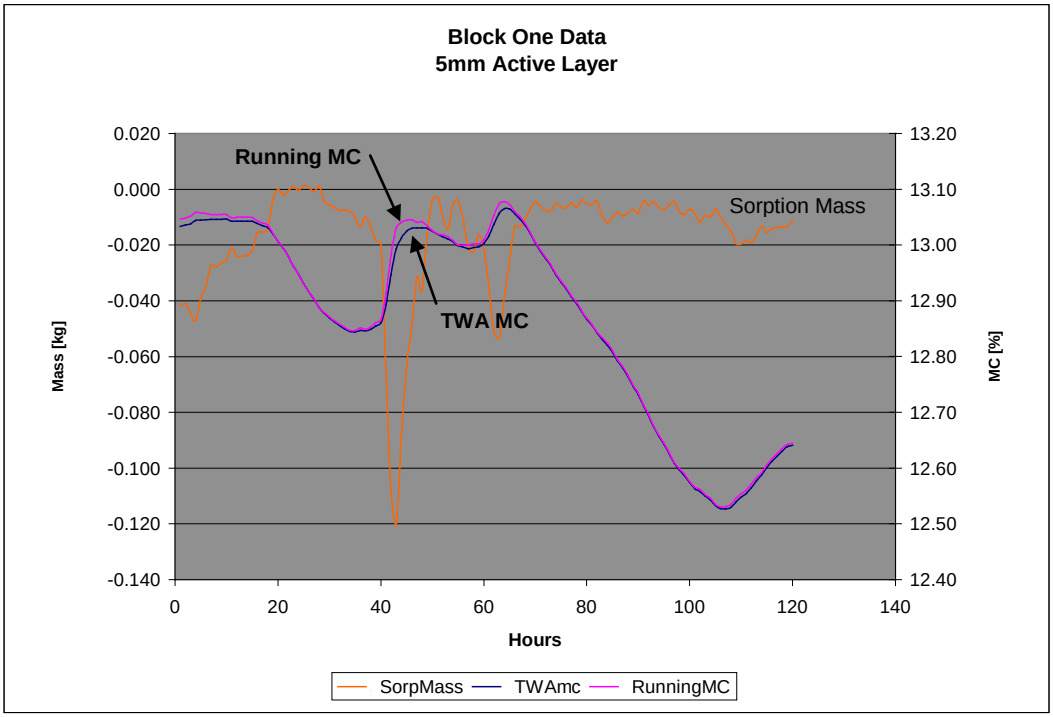

Figure 7.21: The scenario of Fig. 7.20 but with an active layer of 5mm.

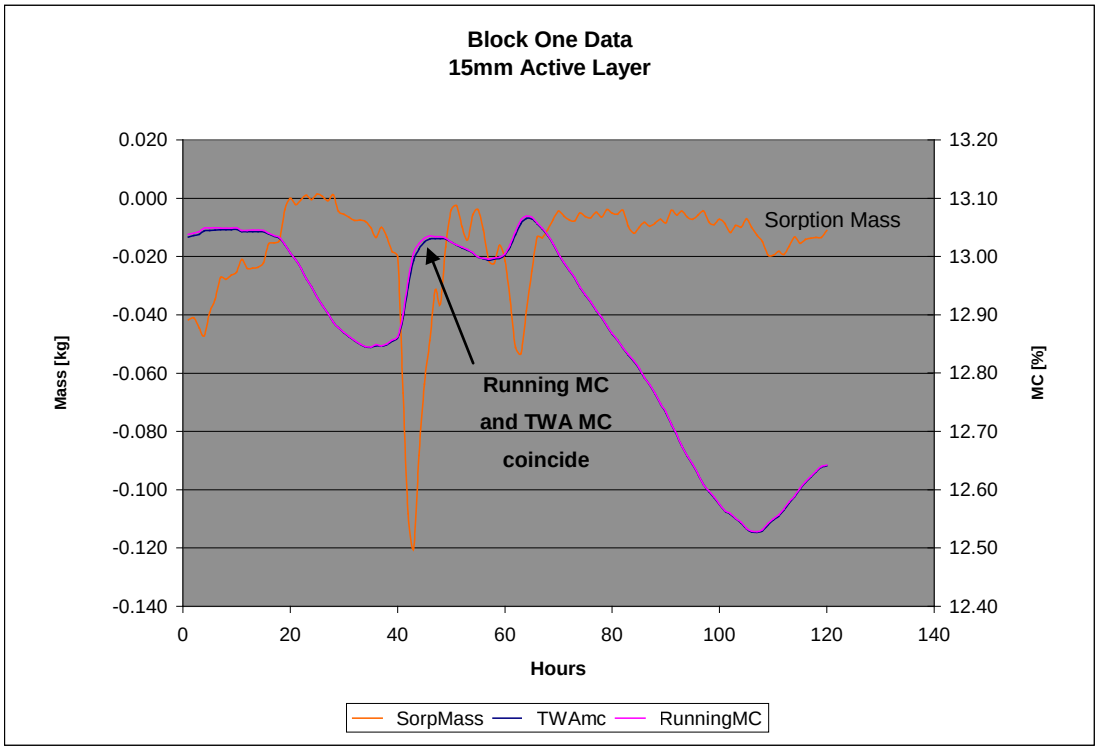

Figure 7.22: The scenario of Fig. 7.20 but with an active layer of 15mm. Both the time weighted average and the running moisture contents virtually coincide.

Data Block One, depicted in the above figures, was found to have an effective layer depth of ~15mm which was significantly greater than that determined for the other four data blocks at < 3mm. The typical volume of material involved was in the region of 0.8 to 0.9m^3.

This difference was also notable in comparing similar moisture gains to the lining during Blocks One and Three, where in Block Three the moisture content of the lining increased substantially more than for Block One. Using the modelled sorption mass gain and the net increase in moisture content, the effective layer depth can be solved through iteration. These results are presented in Table 7.7.

Table 7.7: Modelled effective layer depth for periods in summer and winter.

	Block One	Block Three	
Time period	10	30	*[hrs]*
Additional gain from model	0.7	0.7	*[kg]*
Change in MC noted	0.2	3.4	*[%]*
Effective layer thickness †	**5.50**	**0.32**	*[mm]*

† The effective layer depth indicated is only appropriate for the short term period examined.

This was most likely attributable to the absolute humidity being substantially greater in the summer. For a given relative humidity difference, the driving absolute humidity differential between the room air and the surface was much greater and the mass transfer rates were correspondingly higher in summer.

This 'real' effect steps out from under the assumption of uniform moisture content used in the model. The high mass transfer rate increases the active depth of the surrounding material by rapidly absorbing vapour into the material surface which then diffuses further into the material. As moisture rapidly builds up near the surface of the material, the diffusion rate increases and moisture moves further and further into the material. A slower rate of surface moisture absorption occurs with a lower mass transfer rate and the internal diffusion process slows accordingly, with less penetration into the material.

7.10 Hygroscopic Damping

7.10.1 Definitions

Hygroscopic damping refers to the time-averaging effect the sorption properties of the room material has on the relative humidity of the room. Increasing the volume of hygroscopic material in the room would increase the damping effect. This may possibly be carried out by the provision of rechargeable cartridges of sorptive material. Although the practical feasibility of doing this has not been investigated to any significant degree, in principle such a cartridge could be installed prior to the summer season to buffer the moisture gains, then removed

later in the season to be recharged by heating in an oven. This might be done in conjunction with sealing the hut to lower the moisture load on the cartridge during this time.

7.10.2 Moisture Load

To remove all additional moisture over and above the 76% relative humidity starting point found in Block Five is equivalent to removing the net gain to the space for the entire data block. The modelled positive gain to the air space, for the 300 hours represented by Block Five, sums to approximately 3.5kg of water. Maintaining the relative humidity at 60% would increase this load further still.

Assuming that this system would be required to operate at this moisture load for the entire summer season of about 2000 hours, the total load would be around 25kg.

7.11 Condensation

7.11.1 Condensate Formation

The model was modified to include an option of shutting off evaporation. This provided for the idea that any condensate would become immediately frozen and not readily evaporate, albeit in the extreme case.

Condensation was found to occur in short periods of three to four hours when the conditions allowed, usually following bursts of moisture gain to the hut air space. These conditions also promoted a large absorption component and the rapid reduction of moisture from the micro-climate brought the air state quickly to a level where the formation of condensate was not viable.

a) Evaporation allowed

With the evaporation model activated, the model results indicated that all condensed mass would evaporate immediately after formation on the surface, with a negligible net deposition.

b) Evaporation mechanism shut off

Completely restricting the evaporation of the accumulated condensate caused the build up of ice in the building with a quantity that was ‘ballpark’ consistent with the ice observed during the summer field work.

With Block One (summer) data, the calculated total mass deposition was 174g over the period of 120days. The higher absolute humidity during warmer times of the year will promote a greater accumulation of ice than in winter. The total mass of ice over the mid-winter period described by data Block Four was 91g. This value was considered to be quite high in proportion to the summer condensation mass when the humidity ratio was taken into account, but a much greater disturbance to the air state had happened during the winter data set.

7.11.2 Condensate on Artefacts

Cold metal artefacts in the hut may also attract condensation increasing the area over which approximately the same mass will be deposited. The mass will not increase substantially with modelled area due to the periodic nature of condensation, where once the mass has been deposited the room conditions return to normal and condensation ceases.

The temperature of the thermally-bridged area of the floor is likely to preferentially accumulate condensation rather than the artefacts themselves, so it is unlikely that condensation will form on artefacts in significant quantities.

7.11.3 Treatment of Condensate

The ice that has been seen to form on the edge of the floor does not appear to be causing any great deal of damage. In the interests of removing moisture sources from the building, however, it is better removed than left to potentially re-evaporate or build-up unnecessarily.

7.11.4 Condensate Prevention

Should this amount of condensate formation be considered by conservationists to be excessive, or patches of ice are found appearing on artefacts in the future, it is worth mentioning options for the prevention and collection of condensate:

- To prevent condensation forming on artefacts, the artefact could be moved to a warmer location in the hut, for example, away from a cold surface.
- Insulating a metal artefact from a cold surface may help to reduce the chance of the surface temperature falling below the dewpoint.
- Adding a ‘condensate collector’ to the hut that is thermally bridged to the outdoor temperature, thus preferentially accumulating condensate. The periodic removal of the collected ice would have to be carried out.

7.12 Limitations of the Model

Due to the simple, time-stepped model developed for this project, many assumptions were drawn that were based on what was the best available information. Many of the results drawn from this model were derived from these assumptions. The analysis of the model results was therefore more of a qualitative approach than quantitative, and exact numbers and values were not intended to provide more than a comparison between one result and the next. For more detailed information in the future, improvements to the overall solution method could be made, although the component models would remain much the same.

7.12.1 Simultaneous Thermal Model

The biggest drawback of this model was the lack of a simultaneous thermal model. Assumptions were made on the effects of what would actually occur should the heat balance have been accounted for. The infiltration model could have been improved substantially with consideration to the enthalpy difference between the inside and outside air states. The condensation model would require a much more detailed model (perhaps a finite element model) to judge the impact of heat flow to the condensate in assessing the subsequent evaporation. This level of detail was considered not to be justifiable in this circumstance.

7.12.2 Iterative, Simultaneous, Numerical Solution

This is far beyond the needs of this project, but has been included to help define the scope of what has been achieved.

With a large step in complexity, the improvements offered by an iterative scheme with matrix-based, simultaneous numerical solution would make the model less dependent on the input data and refine the mass calculation at each step. Ideally, only the external data would be required to obtain a fully predictive model of internal conditions.

7.13 Chapter Summary

The input data and parameters have been presented and discussed before passing them into the model for analysis. Once the model had been fine-tuned, a range of input value were tweaked to assess the outcome in the modelled micro-climate inside the hut. Various results have been generated from the model and the implications discussed.

The following chapter summarises the conclusions made from the discussion throughout the body of this thesis and sets out recommendations based on these results.

CHAPTER EIGHT

CONCLUSIONS AND RECOMMENDATIONS

8.1 Introduction

This final chapter serves to complete the thesis by collating all the main findings from throughout the previous chapters and presenting the conclusions drawn from them. The main objectives of the thesis are answered in terms of the determined outcome.

Several recommendations are made as a result of these conclusions, including ideas for future research or development of ideas that have stemmed from this work.

8.2 Main Findings

8.2.1 Data Logging

The continuity of the logger data was found to be sufficient for the needs of this project, but large sections were missing from important periods during summer when most of the influences were maximal. The recent system of downloading the data with a laptop should be continued to avoid gaps like this in the future record.

The operation of the ACR loggers was found to be reliable over the eight years since installation, provided that the calibration plan was adhered to. The calibration of each logger ideally should be performed annually and removed as late in the summer season as is possible so the device could be re-installed before winter.

Stratification in the hut should be reassessed when summer data is returned from the loggers in the new configuration. If no evidence of thermal stratification is encountered, then the loggers could be redistributed around the hut/s as AHT deems appropriate.

The hourly NIWA weather data was crucial and the continued presence of this recording facility at Scott Base should be encouraged.

8.2.2 Groundwater and Ice Heave

The observation-based work showed that the beach location had a propensity to attract the flow of groundwater underneath the building. A method is required of either restricting the groundwater flow and/or removing the ice from underneath the hut and maintaining the air space between the ground and the floor materials. Action in this matter will reduce the high early-summer relative humidity inside the hut by removing a known moisture source and may halt the ice heave deformation of the floor. The moisture content of the floor materials is expected to drop to levels found elsewhere in the hut drastically reducing any

incidence of mould or sweating under artefacts resting on the floor. A regular survey of the hut floor and elevation of the building is advised at intervals not exceeding five years.

8.2.3 Visitor Impact

One of the main objectives of the study was to examine the effects of the visitors on the hut micro-climate and then be able to extrapolate the numbers to obtain an indication of the effects that any variation in the policy might cause.

The current occupancy limit of 12 people was shown to be low enough to not disturb the relative humidity excessively. There is scope to increase the number of visitors by up to two more without significant influence provided the visits are not scheduled for consecutive days, when the disturbance from the previous day might not have dissipated completely. If multi-day visits are intended, then any subsequent party must be scheduled to provide a settling time. A ‘day for a day’ would be sufficient recovery time during mild weather conditions. It is important to note that the effects of any short term visit are not going to remotely compare with that of a typical high external humidity state, but they tend to come later in the year when the absolute humidity is lower.

Leaving the door open should be made policy for those entering the hut, (excepting strong onshore wind conditions where sea-salt may infiltrate) and, to help implement this, a permanent method of holding the door open should be provided. This may also prevent the door becoming unhinged in a gust.

The visitor book should be rebranded as an *occupancy log* with emphasis on signing the book to maintain the records for conservation reasons. The group leader should be made responsible for recording the group details in the log.

8.2.4 Building Air-tightness

The data indicates a moderate to high air-tightness, compared to modern residential buildings, and this was backed up by the experimental CO_2 decay

data collected. This was found to reduce the infiltration air change rate and cause the sorption mechanism to dominate the moisture balance.

Sealing the building completely is not recommended nor is it entirely practical. To improve the air-tightness over current levels, the lining would have to be stripped and an air-barrier installed, which is usually done with a continuous sheet to avoid holes. It is unlikely that any practical barrier would stop long term external conditions from influencing the indoor air state and, would then lengthen the recovery period to return the hut air to normal levels.

8.2.5 Internal Relative Humidity

A significant result from the data analysis was that the main cause of high relative humidity in the hut was found to be driven predominantly by warm, humid storms from the Southern Ocean. Large increases in the relative humidity were maintained for long periods, offsetting the equilibrium state of the building so that the high relative humidity was maintained by moisture from the lining materials long after the storm had passed. These weather patterns seemed to occur from mid-winter through to the end of the year.

Increases in indoor absolute humidity during summer were found to correlate well with the indoor temperature rise due to solar radiation, with the time delay due to thermal capacitance of the building shell taken into account. This was caused by desorption (with a contribution from evaporation), as the moisture capacity of the air rose with temperature. This sorption effect tended to stabilise the relative humidity in the room during mild fluctuations of the external conditions and is a desired outcome of having such an air-tight building.

8.2.6 Corrosive Pollutants

Not surprisingly, the salt deposition rates found at Cape Evans (with the sea-ice inshore) were consistent with a marine environment designation. Salt was found to be windblown into the hut in sufficient quantity to aid the corrosion of metals, but this is thought to be related to door opening by visitors rather than

directly through the shell. The ‘ice-docking’ of ships in the immediate vicinity of the hut is to be discouraged due to opening the sea and the increased potential for aerosol salt. More samples would be necessary to draw any firm conclusions from the salt deposition tests and identify possible correlation to visitor activity. Vacuum removal of the salt from artefacts should continue. No evidence of sulphur dioxide contamination from Mt. Erebus was detected at either Cape Evans or Cape Royds.

8.2.7 The Experimental Programme

The field work generally went to plan, achieving most of the objectives with the principal exception of the blower door test, and many of the results were of sufficient quantity and quality to establish the important parameters necessary for the model.

8.2.8 The Model

The model was shown to agree well with the conditions present inside the hut at Cape Evans and has the versatility to be applied to other huts or buildings if the appropriate building parameters have been determined experimentally. The model allowed qualitative ‘what if?’ analysis with different scenarios to be carried out on mass transfer conditions inside the building. Overall, the model performed well in accordance with the original objectives of the thesis in that it was adaptable and covered all the major mass transfer mechanisms.

8.3 Transferring Findings to Cape Royds

Shackleton's hut at Cape Royds was not considered in the main body of this work, but some of the findings for Cape Evans were considered to be applicable to both huts.

8.3.1 Under-floor Ice

The hut was built level with the sloping ground, providing a cavity that narrowed from the entrance towards the back of the building. Ice build-up under the hut was much less than Cape Evans due to this large cavity and the ventilation it received. Removal of the ice that has formed underneath the building would be advised for the same reasons as Cape Evans.

8.3.2 Indoor Humidity

Observations on the construction and condition of Shackleton's hut suggest that it would not be nearly as air-tight as Cape Evans. This would cause a much greater infiltration rate and hygroscopic damping would not be as effective. The indoor relative humidity would then be much more closely aligned with that of the outdoors.

8.4 Suggestions for Future Work

8.4.1 Data Analysis

A continuation of the data logging programme should concentrate on providing a seamless temperature and relative humidity record of the conditions inside all of the huts. The danger of minimal interpretation of the data in the future can be addressed by developing automated spreadsheets to take the laborious work out of inputting, calculating and presenting this information in a consistent format that can be readily understood. Much of the basic code to achieve this goal has been developed in the course of this project and is included in the

appendices. Such an analysis tool would make use of the data obtained in the other historic huts that have not been explicitly covered in this work.

8.4.2 Ice Removal

The early objective to study the underfloor ice was not fully resolved in that the complete study would involve more structural and soil study than the author was qualified for. Investigation by a geotechnical and structurally qualified person, likely a civil engineer, should be carried out on the removal of ice from under the building and to determine subsidence hazards and potential repercussions for the foundation of the building. Clearing the ice would involve an initial period of mechanical removal run concurrently with a permanent ventilation scheme that would be designed to inhibit further ice formation.

8.4.3 Passive Summer Ventilation

The development of this system would involve further modelling of infiltration with a thermal extension to the mass transfer code used in this project. Should the improved model findings suggest such a system to be appropriate, as was determined by the mass transfer model, then the design and building of a passive ventilator for use over the summer season could continue.

REFERENCES

AHT [1997] Heritage management plan for the historic sites of the Ross Sea region. *Antarctic Heritage Trust, Christchurch, New Zealand.*

AICCM [1998] The Wilkes hut project. *AICCM National Newsletter. Australian Institute for the Conservation of Cultural Material. No. 69, December issue.*

Analar [1984] Analar standards for laboratory chemicals. *BDH Chemicals Ltd. 8th Ed. London, UK.*

ASHRAE [1989a] Handbook of fundamentals. SI Edition. *American Society of Heating, Refrigeration and Air-Conditioning Engineers, Atlanta, USA.*

ASHRAE [1989b] Air leakage performance for detached single-family residential buildings. *ASHRAE Standard 62. American Society of Heating, Refrigeration and Air-Conditioning Engineers, Atlanta.*

ASTM C518 [1991] Standard test method for steady state heat flux measurements and thermal transmission properties by means of the heat flow meter apparatus. *American Society of Testing and Materials, Annual book of standards Vol. 4.07.*

ASTM C871 [1995] Standard test methods for chemical analysis of thermal insulation materials for leachable chloride, fluoride, silicate and sodium ions. *American Society of Testing and Materials, Annual book of standards Vol. 4.06.*

ASTM E1186 [1987] Standard practices for air leakage site detection in building envelopes. *American Society of Testing and Materials, Annual book of standards Vol. 4.07. Re-approved 1992.*

ASTM E741 [1993] Standard test methods for determining air change in a single zone by means of a tracer gas dilution. *American Society of Testing and Materials, Annual book of standards Vol. 4.07.*

ASTM E779 [1987] Standard test method for determining air leakage rate by fan pressurisation. *American Society of Testing and Materials, Annual book of standards Vol. 4.07. Re-approved 1992.*

Barringer, CG and McGugan, CA [1989] Development of a dynamic model for simulating indoor air temperature and humidity. *ASHRAE Transactions Vol. 95 (2). pp 449 – 460.*

Blaisdell, GL, Lang, RM, Crist, G, Kurtti, K, Harbin, RJ and Flora, D [1998] Construction, maintenance and operation of a glacial runway, McMurdo Sound, Antarctica. *Monograph 98-1. US Army Corp of Engineers, Cold regions research and engineering laboratory, Hanover, New Hampshire, USA.*

Burch, DM and Chi, R [1997] MOIST. A PC program for predicting heat and moisture transfer in building envelopes. Release 3.0. *NIST. Special Publication 917. United States Department of Commerce Technology Administration. National Institute of Science and Technology, Gaithersburg, USA.*

Burch, DM and Thomas, WC [1986] MOIST: A PC program for predicting heat and moisture transfer in building envelopes. Release 2.0. *National Institute of Standards and Technology, Gaithersburg, USA.*

Burch, DM and Thomas, WC [1992] An analysis of moisture accumulation in a wood-frame wall subjected to winter climate. *Proc. Conf. Thermal performance of the exterior envelopes of buildings V, Clearwater Beach, Florida, USA*

Cawse, P [1974] A survey of atmospheric trace elements in the UK, 1972-73. *Atomic Energy Research Establishment Report AERE R7669, Harwell, United Kingdom.*

CIBSE [1986] The CIBSE guide. Volume A, Design data. *The Chartered Institution of Building Services Engineers, UK.*

Clayton, MN and King, RJ [1990] Biology of marine plants. *Longman, Cheshire, Melbourne.*

Crall, GCP [1983] Development of the air infiltration model for the energy performance design system. *ASHRAE Transactions Vol. 89 (2B) pp. 201 – 210.*

Cunningham, MJ [1983a] A new analytical approach to the long term behaviour of moisture concentrations in building cavities – I Non-condensing cavity. *Building and Environment. Vol. 18. No. 3. pp. 109 – 116.*

Cunningham, MJ [1983b] A new analytical approach to the long term behaviour of moisture concentrations in building cavities – II Condensing cavity. *Building and Environment. Vol. 18. No. 3. pp. 117 – 124.* (Also published as *BRANZ Reprint Number 31,* Building Research Association of New Zealand, Wellington.)

Cunningham, MJ [1984] Further analytical studies of building cavity moisture concentrations. *Building and Environment*. *Vol. 19. No. 1. pp. 21 – 29.* (Also published as *BRANZ Reprint Number 34,* Building Research Association of New Zealand, Wellington.)

Cunningham, MJ [1987] The use of equivalent electrical circuits to describe the moisture behaviour of structures. *Proceedings, NZ Workshop on Airborne Moisture Transfer, Technical Note AIVC 20, Paper 4.* (Also published as *BRANZ Reprint Number 81,* Building Research Association of New Zealand, Wellington.)

Cunningham, MJ [1988] The moisture performance of framed structures – a mathematical model. *Building and Environment, Vol. 23, No. 2, 1988. pp. 123 – 135.* (Also published as *BRANZ Reprint Number 76,* Building Research Association of New Zealand, Wellington.)

Cunningham, MJ [1992] Moisture diffusion due to periodic moisture and temperature boundary conditions – an approximate steady analytical solution with non-constant diffusion coefficients. *Building and Environment, Vol. 27, No. 3, pp. 367 – 377.* (Also published as *BRANZ Reprint Number 114,* Building Research Association of New Zealand, Wellington.)

Cunningham, MJ [1994] Using hygroscopic damping of relative humidity and vapour pressure fluctuations to measure room ventilation rates. *Building and Environment, Vol. 29, No. 4, pp. 501 – 510.* (Also published as *BRANZ Reprint Number 130,* Building Research Association of New Zealand, Wellington.)

Cunningham, MJ and Sprott, TJ [1984] Sorption properties of New Zealand building materials. *BRANZ Research Report, R43. Building Research Association of New Zealand, Wellington.*

Duncan, JR and Balance, JA [1988] Marine salts contribution to atmospheric corrosion. *Degradation of Metals in the Atmosphere, ASTM Special Technical Publication 965*. *pp. 316 – 326.* (Also published as *BRANZ Reprint Number 77,* Building Research Association of New Zealand, Wellington.)

Easdale, S [1998] Personal communication with Ms. S. Easdale, *AHT conservator*.

El Diasty, R, Fazio, P and Budaiwi, I [1992] Modelling of indoor air humidity: the dynamic behaviour within an enclosure. *Energy and Buildings, Vol. 19, pp.61-73.*

Enzenbacher, D [1992] Tourists in Antarctica: Numbers and trends. *Scott Polar Research Institute, Cambridge, UK. Polar Record 28 (164): pp17 – 22.*

Fairey, PW and Kerestecioglu, A [1985] Dynamic modelling of combined thermal and moisture transport in buildings: Effects on cooling loads and space conditions. *ASHRAE Transactions Vol. 91 (2A) pp. 461 – 472.*

Fontana, MG and Greene, ND [1978] Corrosion engineering. *2nd Ed*. *McGraw Hill, New York.*

Garrecht, H, Hilsdorf, HK and Kropp, J [1990] Hygroscopic salts – Influence on the moisture behaviour of structural elements. *Durability of Building Materials and Components. Proceedings of the Fifth International Conference held in Brighton, UK.. Ed: JM Baker et al. (BRE). E. & F.N. Spon, London. pp. 313 – 324.*

Haberecht, P [1998] Personal communication with Mr. P. Haberecht, *Senior Materials Scientist, Building Research Association of New Zealand, Wellington.*

Harrowfield, DL [1995] Icy heritage: Historic sites of the Ross Sea region. *Antarctic Heritage Trust, Christchurch, New Zealand.*

Harrowfield, DL [1999] Personal communication with Mr. D. Harrowfield, *AHT historian, Antarctic Heritage Trust, Christchurch, New Zealand.*

Hobbs, PV [1974] Ice Physics. *Oxford Clarendon Press, Oxford, UK.*

Hughes, JD, King, GA and O'Brien, DJ [1995] Corrosivity in Antarctica – revelations on the nature of corrosion in the world's coldest, driest, highest and purest continent. *CSIRO Division of Building, Construction and Engineering. 13th ICC Conference, Melbourne, Australia.*

Hyland, RW and Wexler, A [1983] Formulations for the thermodynamic properties of dry air from 173.15K to 473.15K. *ASHRAE Transactions. Vol. 89 (2A)*, *pp. 500 – 513.*

Isaacs, N [1986] Engineering application of heat flux sensors in buildings – Technical note. *ASTM Special Technical Testing Publication 885.* (Also published as *BRANZ Reprint Number 47,* Building Research Association of New Zealand, Wellington.)

ISO 9223 [1992] Corrosion of metals and alloys – Corrosivity of atmospheres – Classification. *International Standards Organisation. Geneva, Switzerland.*

ISO 9225 [1992] Corrosion of metals and alloys – Corrosivity of atmospheres – Measurement of pollution. *International Standards Organisation. Geneva, Switzerland.*

Johnston, GH [1981] Permafrost. Engineering design and construction. *National Research Council of Canada. Associate Committee on Geotechnical Research. Wiley, Toronto.*

Keiper, G, Cammerer, W and Wagner, A [1976] A new diagram to evaluate the performance of building constructions with a view to water vapour diffusion. *C.I.B. W40 Working Commission, London, UK.*

Keresteciogl u, AA and Gu, L [1990] Theoretical and computational investigation of simultaneous heat and moisture transfer in buildings: "evaporation and condensation" theory. *ASHRAE Transactions Vol. 96 (1). pp. 455 – 462.*

Keresteciogl u, AA, Fairey, PW and Chandra, S [1985] Algorithms to predict detailed moisture effects in buildings. *Proc. Conf. Thermal performance of the exterior envelopes of buildings III, Clearwater Beach, Florida. pp. 606 – 619.*

Keresteciogl u, AA, Swami, M and Kamel, A [1990] Theoretical and computational investigation of simultaneous heat and moisture transfer in buildings: "effective penetration depth" theory. *ASHRAE Transactions Vol. 96 (1). pp. 447 – 454.*

Kusuda, T [1983] Indoor humidity calculations. *ASHRAE Transactions Vol. 89 (2). pp. 728 – 740.*

Liddament, MW [1991] A review of building air flow simulation. *Coventry Air Infiltration and Ventilation Centre, UK.*

Liddament, MW and Allen, C [1983] The validation and comparison of mathematical models of air infiltration. *Bracknell, Berks. Air Infiltration Centre, UK.*

Liddament, MW and Thompson, C [1983] Techniques and instrumentation for the measurement of air infiltration in buildings: a brief review and annotated bibliography. *Bracknell, Berks. Air Infiltration Centre, UK.*

Mason, GW [1999] K282 field report 98/99, *Antarctic Heritage Trust field programme. Antarctica New Zealand, Christchurch, New Zealand.*

Miller, JD [1984] Development and validation of a moisture mass balance model for predicting residential cooling energy consumption. *ASHRAE Transactions. Vol. 90 (2B)*. pp. 275 – 293.

OSH [1999] Workplace exposure standards. *http://www.osh.dol.govt.nz/ Occupational Safety and Health Service, Department of Health, New Zealand.*

Schuyler, GD, Swinton, M and Lankin, J [1987] Walldry – A computer model that simulates moisture migration through wood frame walls – comparison to field data. *Proc. Conf. Thermal performance of the exterior envelopes of buildings IV, Orlando, Florida.*

Schweitzer, PA [1987] What every engineer should know about corrosion. *Marcel Dekker, Inc. New York.*

Sherman, MH and Grimsrud, DT [1980] Infiltration – pressurisation correlation: Simplified physical modelling. *ASHRAE Transactions 86 (2):778.*

Smith, WF [1993] Foundations of materials science and engineering. *2nd Ed. McGraw Hill. New York.*

TenWolde, A [1994] Ventilation, humidity, and condensation in manufactured houses during winter. *ASHRAE Transactions. Vol. 100 (1)*. pp. 103 – 115.

Trethowen, HA [1979] The Keiper method for moisture design in buildings. *Paper 12, New Zealand Institute of Engineers Annual Conference, Wellington.* (Also published as *BRANZ Reprint Number 12,* Building Research Association of New Zealand, Wellington.)

Trethowen, HA [1986a] Measurement errors with surface-mounted heat flux sensors. *Building and Environment Vol.21, No.1.* (Also published as *BRANZ Reprint Number 51,* Building Research Association of New Zealand, Wellington.)

Trethowen, HA [1986b] Engineering application of heat flux sensors in buildings – The sensor and its behaviour. *ASTM Special Technical Testing Publication 885.* (Also published as *BRANZ Reprint Number 46,* Building Research Association of New Zealand, Wellington.)

Trethowen, HA [1990] Systematic errors with surface mounted heat flux transducers and how to live with them. *BTECC/CRREL workshop "In-situ flux measurements in buildings", UK.* (Also published as *BRANZ Reprint Number 110,* Building Research Association of New Zealand, Wellington.)

TSI [1999a] Q-Trak 8551 IAQ monitor specifications. *http://www.tsi.com/hsi/homepage/qtrak/qtrkspec.htm TSI Inc.*

TSI [1999b] Non-dispersive infrared sensor for CO_2 concentration. *http://www.tsi.com/hsi/homepage/applnote/ndir_co2.htm TSI Inc.*

Tsongas, G, Burch, D, Roos, C and Cunningham, MJ [1995] A parametric study of wall moisture contents using a revised variable indoor relative humidity version of the 'MOIST' transient heat and moisture transfer model. *ASHRAE, Thermal Performance of Exterior Envelopes of Buildings VI, Clearwater Beach, Florida, USA. pp 307-319.*

Tsuchiya, T [1980] Infiltration and indoor air temperature and moisture variation in a detached residence. *Journal of the Society of Heating, Air-Conditioning and Sanitary Engineers of Japan, Vol. 54, No. 11, pp. 13-19.*

Tucker, AS [1997a] Heat and mass transfer with HVAC applications. 435/455 course notes. *Department of Mechanical Engineering, University of Canterbury, New Zealand.*

Tucker, AS [1997b] Tables of thermodynamic and transport properties of fluids. *Department of Mechanical Engineering, University of Canterbury, New Zealand.*

Vogel, AI [1989] Vogel's textbook of quantitative chemical analysis. 5th ed. *Longman Scientific & Technical, Harlow, Essex, England.*

Walton, G [1983] TARP reference manual. *NBSIR, 83-2655. National Bureau of Standards, Washington, DC..*

BIBLIOGRAPHY

Ailor, WH [1982] Atmospheric corrosion. *John Wiley and Sons. New York.*

AIVC [1987] Airborne moisture transfer, NZ workshop proceedings. *Air Infiltration and Ventilation Centre.*

Anton, H [1992] Calculus, with analytical geometry. 4th ed. *John Wiley and Sons. New York.*

Anton, H [1994] Elementary linear algebra. 7th ed. *John Wiley and Sons. New York.*

ASTM D4444 [1992] Standard test methods for use and calibration of hand-held moisture meters. *Annual book of standards Vol. 4.09. American Society of Testing and Materials, Philadelphia, USA.*

Bassett, M [1985] The infiltration component of ventilation in New Zealand houses. *BRANZ Proceedings, 6th AIC Conference: Ventilation Strategies and Measurement Techniques. Paper 2.* (Also published as *BRANZ Reprint Number 42,* Building Research Association of New Zealand, Wellington.)

Bassett, M [1986] Building site measurements for predicting air infiltration rates. *Measured Air Leakage of Buildings*, *ASTM STP 904, Trechsel and Lagus. American Society for Testing and Materials, Philadelphia, USA. pp. 365 – 383.*

Bootle, KR [1983] Wood in Australia. types, properties and uses. *McGraw Hill. Sydney.*

Bradley, JC and Millspaugh, AC [1998] Programming in visual basic, version 5.0. *Irwin/McGraw-Hill. New York.*

BRANZ [1992] Solar control glass – types and properties. *BRANZ Bulletin Number 297. Building Research Association of New Zealand, Wellington.*

BRANZ [1995] Wind barriers & vapour barriers and building papers. *BRANZ Bulletin Number 336, August. Building Research Association of New Zealand, Wellington.*

BRANZ [1996] Moisture in timber. *BRANZ Bulletin Number 343, April. Building Research Association of New Zealand, Wellington.*

BRANZ [1998] Preventing moisture problems in timber framed skillion roofs. *BRANZ Bulletin Number 368, March. Building Research Association of New Zealand, Wellington.*

BRANZ [1998] Publications catalogue. *Building Research Association of New Zealand, Wellington.*

Brett, D [1990] Keeping track of corrosion. *Ecos no. 64, Winter 1990. Melbourne, Australia.*

Burch, D and TenWolde, A [1993] A computer analysis of moisture accumulation in the walls of manufactured houses. *ASHRAE Transactions 1993, V. 99, Pt. 2. pp 977 - 990*

Chaddock, JB and Todorovic, B [1991] Heat and mass transfer in building materials and structures. *Hemisphere Publishing Corp. New York.*

Chang, R [1991] Chemistry. 4th edition. *McGraw-Hill International Edition. New York.*

Chaplin, P [1998] The historic sites of the Ross Sea region. *Antarctic Heritage Trust, Christchurch, New Zealand.*

Cherry-Garrard, A [1922] The worst journey in the world : Antarctic, 1910-1913. *Chatto & Windus, London.*

Crossley, L [1995] Explore Antarctica. *Australian Antarctic Foundation, Cambridge Press, UK.*

Davis, P [1995] Antarctic visitor behaviour: are guidelines enough? *Scott Polar Research Institute, Cambridge, UK. Polar Record 31 (178). pp327 – 334.*

Duncan, JR [1984] Atmospheric corrosion in New Zealand. *Corrosion Australasia*. *October issue.* (Also published as *BRANZ Reprint Number 38,* Building Research Association of New Zealand, Wellington.)

Enzenbacher, D [1994] Antarctic tourism: an overview of 1992/3 season activity, recent developments, and emerging issues. *Scott Polar Research Institute, Cambridge. Polar Record 30 (173): pp105 – 116. UK*

Griffiths, DV and Smith, IM [1991] Numerical methods for engineers. A programming approach. *Blackwell Scientific Publications, London.*

Harrowfield, DL [1996] The role of the wind in the destruction of an historic hut at Cape Adare in Antarctica. *International Antarctic Centre, NZ. Polar Record 32 (180): pp. 3 – 18. UK*

Hughes, JD [1992] Mawson's Antarctic huts and tourism: a case for on-site preservation. *Institute for Antarctic and Southern Ocean Studies, Tasmania. Polar Record 28 (164): pp37 – 42. UK*

Kendrick, J [1993] An overview of combined modelling of heat transport and air movement. *Coventry Air Infiltration and Ventilation Centre, UK.*

King, GA and Hughes, JD [1993] Measurement of atmospheric corrosion using standard coupons and ATCORR units, and its application in the preservation of outdoor cultural material. *AICCM Bulletin*, *No. 8. Australian Institute for the Conservation of Cultural Material. Melbourne, Australia.*

Kuehn, TH, Ramsey, JW and Threlkeld, JL [1998] Thermal environmental engineering. 3rd edition. *Prentice Hall, New Jersey, USA.*

Liddament, MW [1986] Air infiltration calculation techniques : an applications guide. *Bracknell, Berkshire : Air Infiltration and Ventilation Centre, UK.*

McMullen, R [1992] Environmental science in building. 3rd Edition. *Houndmills, Basingstoke, Hampshire: Macmillan.*

MountEvans, ERGR [1958] South with Scott. *Collins, London, UK.*

Norris, B [undated] Antarctic Reflections: An anthology of Antarctic articles written originally for the Christchurch Press. *New Zealand Antarctic Society, Christchurch, New Zealand.*

Ogle, BM [1998] Understanding Antarctic studies: INCO 103. *Personal Communication with Ms. Ogle.*

Pearson, C [1992] Expedition huts in Antarctica: 1899-1917. *Australian Heritage Commission. Polar Record 28 (167): pp261 – 276. UK.*

Powers, DJ, Colbeck, SC and O'Neill, K [1985] Thermal convection in snow. *CRREL Report 85-9. Cold Regions Research and Engineering Laboratory, US Army Corps of Engineers, Hanover, New Hampshire, USA.*

Rogers, TH [1968] Marine corrosion. *Newnes, London.*

Summitt, R and Fink, FT [1982] The USAF corrosion testing program and a corrosion severity index algorithm. *Atmospheric Corrosion*. *Ed: W.H. Ailor: John Wiley and Sons Inc., New York, pp. 245 - 258*

Van Wylen, GJ, Sonntag, RE and Borgnakke, C [1994] Fundamentals of classical thermodynamics. 4th edition. *John Wiley and Sons, Inc. New York.*

Yin-Chao Yen [1981] Review of thermal properties of snow, ice and sea ice. *CRREL Report 81-10. Cold Regions Research and Engineering Laboratory, US Army Corps of Engineers, Hanover, New Hampshire, USA.*

Yin-Chao Yen [1982] On the temperature distribution in an air-ventilated snow layer. *CRREL Report 82-5. Cold Regions Research and Engineering Laboratory, US Army Corps of Engineers, Hanover, New Hampshire, USA.*

Zeigler, BP [1976] Theory of modelling and simulation. *John Wiley and Sons. New York*

APPENDIX A

DRAWINGS

A.1 Locality and Hut Drawings

A.1.1 Cape Evans Area

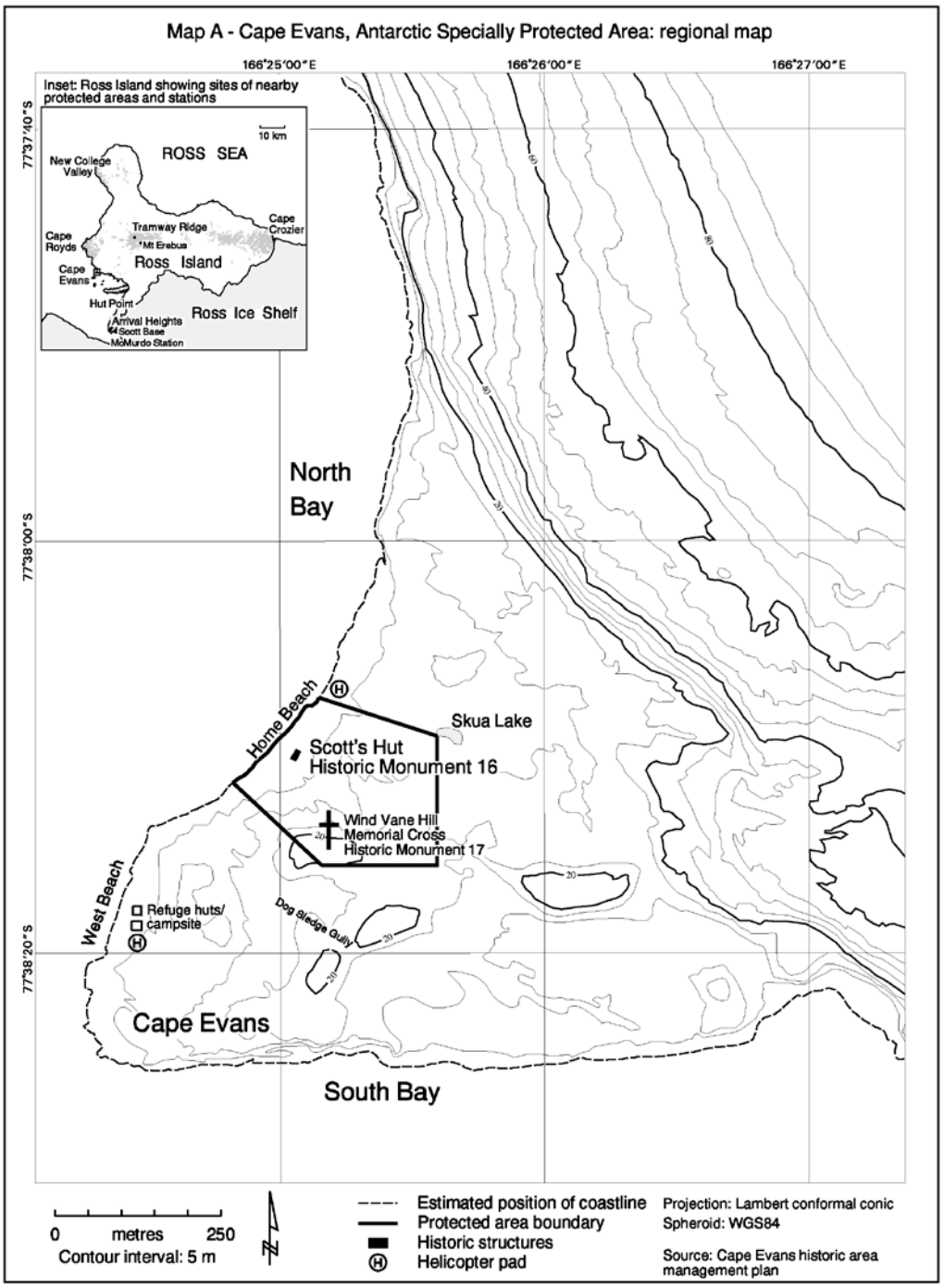

A.1.2 Terra Nova Hut Layout

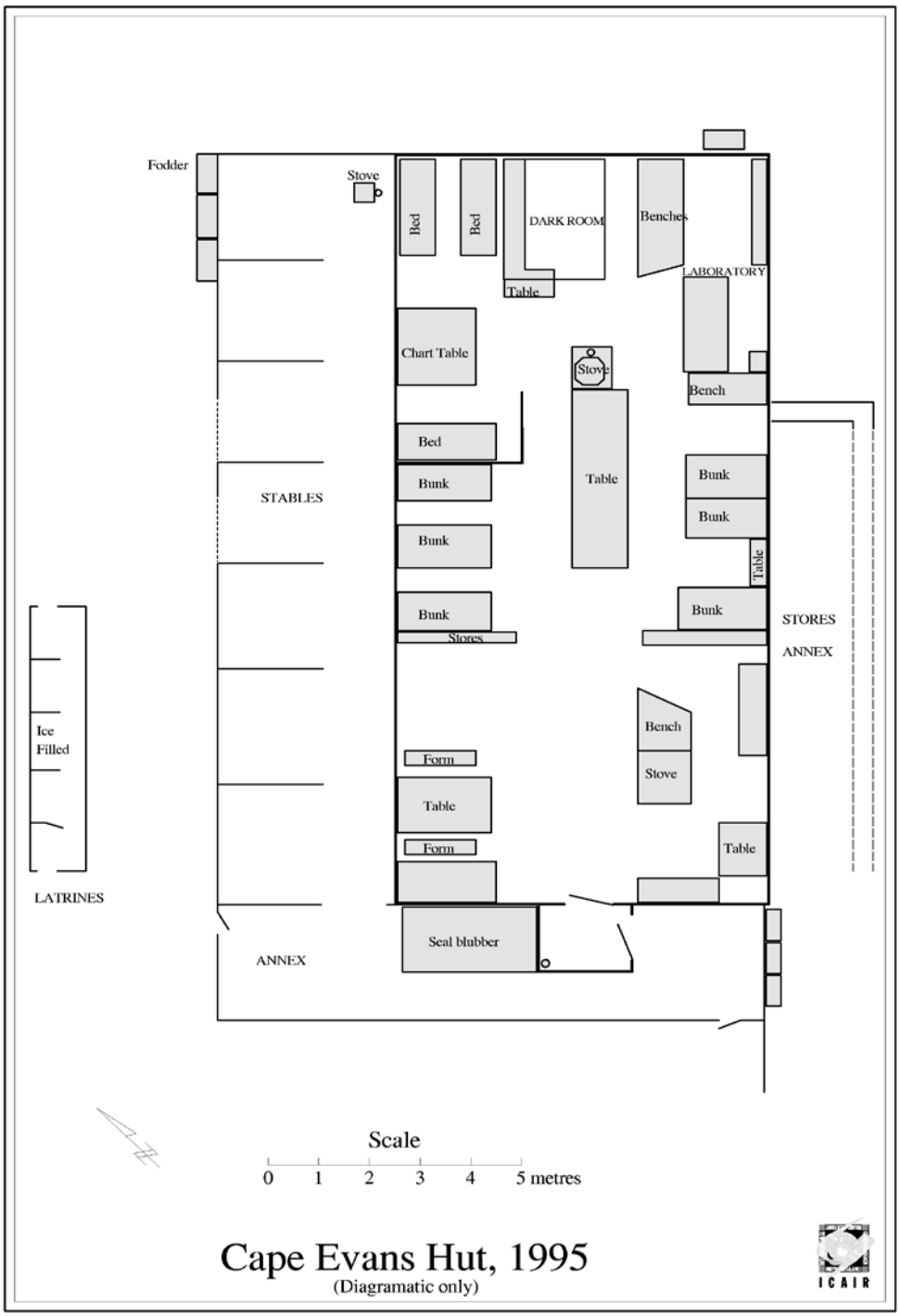

A.1.3 Scott's Hut Orthographic

A.2 Engineering Part Drawings

A.2.1 Hot Box

A.2.2 Salt Collector Bung

A.2.3 Salt Candle End Cap

A.2.4 Salt Candle

A.2.5 Base Locking Pin

A.2.6 Bottle Cage Bracket

A.2.7 Salt Collector Stand

APPENDIX B

PROGRAM LISTINGS AND INPUT SPREADSHEETS

B.1 Program Listings

B.1.1 Command Button Event Assignments

```
Private Sub CommandButton1_Click()
      Application.StatusBar = "Block One Solution Current at " & Time
      Application.Run "ThisWorkbook.BlockOne"
End Sub

Private Sub CommandButton2_Click()
      Application.StatusBar = "Block Two Solution Current at " & Time
      Application.Run "ThisWorkbook.BlockTwo"
End Sub

Private Sub CommandButton3_Click()
      Application.StatusBar = "Block Three Solution Current at " &
      Time
      Application.Run "ThisWorkbook.BlockThree"
End Sub

Private Sub CommandButton4_Click()
      Application.StatusBar = "Block Four Solution Current at " & Time
      Application.Run "ThisWorkbook.BlockFour"
End Sub

Private Sub CommandButton5_Click()
      Application.StatusBar = "Block Five Solution Current at " & Time
      Application.Run "ThisWorkbook.BlockFive"
End Sub

Private Sub CommandButton6_Click()
      Worksheets("Data").Activate
      Range("o5:ac998").Select
      Selection.ClearContents
Range("a1").Select
End Sub
```

B.1.2 Full Model Code with Automated Graphing

```
Option Explicit
'
'*******************************************************
'
'   Cold Climate Mass Transfer Model
'   Glen Mason, 1999
'
'*******************************************************
'
'Define Module level Variables, Constants and Arrays
Dim iRowStart As Integer
Dim iRowEnd As Integer
Dim iBlockNumber As Integer

Dim iRowLoop As Integer  'Specific use looping variables
```

```
Dim iColLoop As Integer
Dim iNumRows As Integer
Dim iTimeConst As Integer

Dim iLoop As Integer     'General use looping variables
Dim iStep As Integer
Dim iHour As Integer

Dim sBlock() As Single   'Main data dynamic array
Dim sOccupant() As Single
Dim sSorpResult() As Single
Dim sCEResults() As Single
Dim sInfilResults() As Single
Dim sModelOutput() As Single
Dim sStack() As Single
Dim sMassTxrVector() As Single
Dim HR() As Single
Dim ErrorValue() As Single

Const cHutVolume As Integer = 358


Sub MainBody()
' Main Body, written by Glen Mason, May 1999
' The intention of this block of code is to organise the sub model
' codes and call them as required.  The data from the flagged block
' is written to the array here.

Application.ScreenUpdating = False

'Write data to Block array
Worksheets("Data").Activate

For iRowLoop = iRowStart To iRowEnd
    For iColLoop = 3 To 10
        sBlock(iRowLoop - iRowStart, iColLoop - 3) = _
        Cells(iRowLoop, iColLoop)
    Next iColLoop
Next iRowLoop

'*****************************************************************
'Run Models
Call MeasuredMassTxr
Call Infiltration
Call Condensation
Call Sorption
Call Occupancy
Call RoomState
Call PlotData
Call ChartHandler

Application.ScreenUpdating = True
End Sub

'Command Button routines
'
' Each block gets a command button to run the model on that
' particular block of data.  This code defines the row limits
' for the block, re dim's the array and then hands over
' to the main body.
```

```
Public Sub BlockOne()
    'Set up and run for Block One data
    iRowStart = 7
    iRowEnd = 126
    iBlockNumber = 1
    iNumRows = iRowEnd - iRowStart
    ReDim sBlock(iNumRows, 7) 'Dimension Dynamic Array
    Call MainBody
End Sub
Public Sub BlockTwo()
    'Set up and run for Block Two data
    iRowStart = 132
    iRowEnd = 323
    iBlockNumber = 2
    iNumRows = iRowEnd - iRowStart
    ReDim sBlock(iNumRows, 7) 'Dimension Dynamic Array
    Call MainBody
End Sub
Public Sub BlockThree()
    'Set up and run for Block Three data
    iRowStart = 329
    iRowEnd = 520
    iBlockNumber = 3
    iNumRows = iRowEnd - iRowStart
    ReDim sBlock(iNumRows, 7) 'Dimension Dynamic Array
    Call MainBody
End Sub
Public Sub BlockFour()
    'Set up and run for Block Four data
    iRowStart = 526
    iRowEnd = 693
    iBlockNumber = 4
    iNumRows = iRowEnd - iRowStart
    ReDim sBlock(iNumRows, 7) 'Dimension Dynamic Array
    Call MainBody
End Sub

Public Sub BlockFive()
    'Set up and run for Block Five data
    iRowStart = 699
    iRowEnd = 998
    iBlockNumber = 5
    iNumRows = iRowEnd - iRowStart
    ReDim sBlock(iNumRows, 7) 'Dimension Dynamic Array
    Call MainBody
End Sub


Sub PlotData()
'Calculates the humidity ratio data needed for the plots
'And also the difference between the model and actual mass txr

Dim sIntTemp As Single
Dim sExtTemp As Single

ReDim HR(iNumRows, 1) As Single
ReDim ErrorValue(iNumRows) As Single


For iLoop = 0 To iNumRows
    sIntTemp = sBlock(iLoop, 0)
```

```
    sExtTemp = sBlock(iLoop, 3)
    HR(iLoop, 0) = sSatHR(sIntTemp) * sBlock(iLoop, 1)
    HR(iLoop, 1) = sSatHR(sExtTemp) * sBlock(iLoop, 4)
    'The difference between model  and actual
    ErrorValue(iLoop)      =      sModelOutput(iLoop,      0)      -
sMassTxrVector(iNumRows)
Next iLoop

'dump to Data sheet, col's 25, 26, 27
Cells(iRowStart - 1, 25) = "sIntHR"
Cells(iRowStart - 2, 25) = "[kgw/kga]"
Cells(iRowStart - 1, 26) = "sExtHR"
Cells(iRowStart - 2, 26) = "[kgw/kga]"
Cells(iRowStart - 1, 27) = "Error"
Cells(iRowStart - 2, 27) = "[kg]"

For iRowLoop = 0 To iNumRows
    For iColLoop = 0 To 1
        Cells(iRowLoop  +  iRowStart,  iColLoop  +  25)  =  HR(iRowLoop,
iColLoop)
    Next iColLoop
    Cells(iRowLoop + iRowStart, 27) = ErrorValue(iRowLoop)
Next iRowLoop

End Sub


Sub Infiltration()
' This module calculates the infiltration rate into the hut
' based on inside/outside temperature differential and wind
' speed.  The LBL infiltration model is used for this purpose.
'

'Define local variables
Dim iLeakArea As Integer
Dim sStackCoeff As Single
Dim sWindCoeff As Single

Dim sIntTemp As Single
Dim sIntRH As Single
Dim sExtTemp As Single
Dim sWindSpeed As Single
Dim sWindDir As Single
Dim sIntHR As Single
Dim sExtHR As Single

Dim sFlowRate As Single
Dim sAirChanges As Single
Dim sInfMassTxr As Single

'Read in fixed data from sheet
Worksheets("Infiltration").Activate


sStackCoeff = Range("d7")
'sWindCoeff = Range("d8") see direction adjustment later in code


'Set Infiltration Array size
ReDim sInfilResults(iNumRows, 2)
```

```
'Start data-churning loop
For iLoop = 0 To iNumRows

'Check for occupancy and open the door
'note that negative values can be used which will
'keep the door closed.  Abs function in occupancy model.
If sBlock(iLoop, 7) > 0 Then
    iLeakArea = Range("g6") + Range("d6") 'open door = +800cm2
Else
    iLeakArea = Range("d6") 'close door 50cm2
End If

 'read in hourly data from data array
    sIntTemp = sBlock(iLoop, 0)
    sExtTemp = sBlock(iLoop, 3)
    sIntHR = sSatHR(sIntTemp) * sBlock(iLoop, 1) / 100
    sExtHR = sSatHR(sExtTemp) * sBlock(iLoop, 4) / 100
    sWindSpeed = sBlock(iLoop, 5)
    sWindDir = sBlock(iLoop, 6)

    'Wind Direction adjustment
    'adjusts the coefficient.

    If sWindDir < 90 Or sWindDir > 270 Then
        sWindCoeff = Range("e8")
    Else: sWindCoeff = Range("d8")
    End If

    If (sIntTemp - sExtTemp) < 0 Then sIntTemp = 0: sExtTemp = 0
    ' Infiltration Calculations
    sFlowRate = iLeakArea * Sqr(sStackCoeff * (sIntTemp - sExtTemp) _
        + sWindCoeff * sWindSpeed ^ 2) * (3600 / 1000) ' in m^3/hr


    sAirChanges = sFlowRate / cHutVolume
    sInfMassTxr = sFlowRate * sAirDens(sExtTemp) * (sExtHR - sIntHR)


    'output the data to the InfilResults array
    sInfilResults(iLoop, 0) = sFlowRate
    sInfilResults(iLoop, 1) = sAirChanges
    sInfilResults(iLoop, 2) = sInfMassTxr

Next iLoop

' Dump infiltration data into Data sheet
Worksheets("Data").Activate
Cells(iRowStart - 1, 15) = "sInfMassTxr"
Cells(iRowStart - 2, 15) = "[kg]"
For iLoop = 0 To iNumRows
    Cells(iLoop + iRowStart, 15) = sInfilResults(iLoop, 2)
    'Cells(iLoop + iRowStart, 28) = sInfilResults(iLoop, 0)
Next iLoop

End Sub

Sub MeasuredMassTxr()
' This routine calculates the internal mass transfer taken place
' between each consecutive time period (1hr).
' This data will be used to compare the different model rates.
```

```
'Procedure level
Dim sIntTemp As Single
Dim sIntRH As Single
Dim sIntHR As Single
Dim sLastIntHR As Single
Dim sMassTxr As Single


'Calculate
ReDim sMassTxrVector(iNumRows)

For iLoop = 0 To iNumRows
    sIntTemp = sBlock(iLoop, 0)
    sIntRH = sBlock(iLoop, 1)
    sIntHR = sSatHR(sIntTemp) * sIntRH / 100
    If iLoop > 0 Then
        sMassTxr  =  sAirDens(sIntTemp)  *  cHutVolume  *  (sIntHR  -
sLastIntHR)
    End If
    sMassTxrVector(iLoop) = sMassTxr
    sLastIntHR = sIntHR

Next iLoop

'Dump to sheet to view
Worksheets("Data").Activate
Cells(iRowStart - 1, 19) = "sMassTxr"
Cells(iRowStart - 2, 19) = "[kg]"
Cells(iRowStart, 19) = ""

For iLoop = 0 To iNumRows
    Cells(iLoop + iRowStart, 19) = sMassTxrVector(iLoop)
Next iLoop

End Sub

Sub Condensation()

'References the condensation worksheet for parameters
'Calculates the total mass of moisture transfer from the room air
'per hourly period.

'dimension local variables
Dim sIntHR As Single
Dim sMassTxrCoeff As Single
Dim sFMassTxrCoeff As Single
Dim sCEArea As Single
Dim sFArea As Single
Dim sTempPercent As Single
Dim sFTempPercent As Single
Dim sSurfaceTemp As Single
Dim sIntTemp As Single
Dim sExtTemp As Single
Dim sMass As Single
Dim iFlag As Integer
Dim sCondensate As Single

ReDim sCEResults(iNumRows)

'Activate parameter input sheet
Worksheets("Cond Evap").Activate
```

```
'Input parameters, glass
sMassTxrCoeff = Cells(15, 3)
sCEArea = Cells(16, 3)
sTempPercent = Cells(17, 3) / 100

'Input parameters, floor
sFMassTxrCoeff = Cells(15, 7)
sFArea = Cells(16, 7)
sFTempPercent = Cells(17, 7) / 100


'Start looping through rows
For iLoop = 0 To iNumRows

    'Yes or no to dewpoint check?
    iFlag = Cells(18, 3)

    'read values from array
    sIntTemp = sBlock(iLoop, 0)
    sIntHR = sSatHR(sIntTemp) * sBlock(iLoop, 1) / 100
    sExtTemp = sBlock(iLoop, 3)



    '*************************************************************
    'Run through calculation process for the windows

    'Calculate the surface temp of the glass
    sSurfaceTemp = (sIntTemp - sExtTemp) * sTempPercent + sExtTemp

    'using the function for the surface hum. ratio
    'calculate the hourly mass transfer
    sCEResults(iLoop) = sMassTxrCoeff * sCEArea * _
        (sSatHR(sSurfaceTemp) - sIntHR) * 3600 'seconds/hr

    ' Dewpoint check only if flag = 1
    ' If dpt < surface temp then null condensation
    If sSurfaceTemp > sBlock(iLoop, 2) And iFlag = 1 _
        And sCEResults(iLoop) < 0 Then sCEResults(iLoop) = 0

    '*************************************************************
    'Repeat calculation process for the floor

    'Calculate the surface temp of the floor
    sSurfaceTemp = (sIntTemp - sExtTemp) * sFTempPercent + sExtTemp

    'using the function for the surface hum. ratio
    'calculate the hourly mass transfer
    sMass = sFMassTxrCoeff * sFArea * _
            (sSatHR(sSurfaceTemp) - sIntHR) * 3600 'seconds/hr

    ' Dewpoint check only if flag = 1
    ' If dpt < surface temp then null condensation
    If sSurfaceTemp >= sBlock(iLoop, 2) And iFlag = 1 _
        And sMass < 0 Then sMass = 0

    '*************************************************************
    'Stop any evaporation from occurring
    'Block this code out during normal modelling
'    If sCEResults(iLoop) > 0 Then sCEResults(iLoop) = 0
```

```
'    If sMass > 0 Then sMass = 0

    'Sum the window and floor masses together
    sCEResults(iLoop) = sCEResults(iLoop) + sMass

    'Running sum of condensate and only allow evap from
    'cond already accumulated.  See notes 30/6, book 4
    If sCEResults(iLoop) < 0 Then sCondensate = sCondensate +
Abs(sCEResults(iLoop))
    If sCondensate <= 0 And sCEResults(iLoop) > 0 Then
sCEResults(iLoop) = 0
    If sCondensate > 0 And sCEResults(iLoop) > 0 Then
        If sCEResults(iLoop) > sCondensate Then
            sCEResults(iLoop) = sCondensate
            sCondensate = 0
        Else
            sCondensate = sCondensate - sCEResults(iLoop)
        End If
    End If
Next iLoop

'Punch data out into the data sheet
Worksheets("Data").Activate
Cells(iRowStart - 1, 16) = "sCondMassTxr"
Cells(iRowStart - 2, 16) = "[kg]"
For iLoop = 0 To iNumRows
    Cells(iLoop + iRowStart, 16) = sCEResults(iLoop)
Next iLoop

End Sub

Sub Sorption()
'This routine calculates the mass transfer due to sorption in
'and out of the timber contained in the room.

'local variables
Dim sIntTemp As Single
Dim sIntHR As Single
Dim sIntRH As Single
Dim sExtTemp As Single
Dim sTWArh As Single
Dim sRunningRH As Single
Dim sRunningMC As Single

Dim sArea As Single
Dim sMassTxrCoeff As Single
Dim sSurfaceRH As Single
Dim sSurfaceHR As Single
Dim sSurfaceTemp As Single
Dim sTempPercent As Single
Dim sDryTimberMass As Single
Dim sTimberMoisture As Single
Dim sWetWoodHR As Single


Dim sSum As Single
Dim sTWAmc As Single


Const cSorpA As Single = 2.97
Const cSorpB As Single = -0.17
```

```
Const cSorpC As Single = 4.48

ReDim sSorpResult(iNumRows, 0 To 3)

'read in input data from Sorption sheet
Worksheets("Sorption").Activate

sArea = Cells(17, 3)
sMassTxrCoeff = Cells(18, 3)
sDryTimberMass = Cells(19, 3)
sTempPercent = Cells(20, 3) / 100
iTimeConst = Cells(21, 3)

'Initialise Stack
ReDim sStack(1 To 4 * iTimeConst, 0 To 1) As Single
'this has been complicated by the back filling of the stack
'required when the time constant is variable, modified 18/8/99
For iHour = 4 * iTimeConst To 1 Step -1
    sStack(iHour,  0)  =  Cells(-iHour  +  4  *  iTimeConst  +  18,
iBlockNumber + 9)
    sStack(iHour,  1)  =  Exp((-((4  *  iTimeConst  +  1)  -  iHour))  /
iTimeConst)
Next iHour

'Renew actual data from sheet
Worksheets("Data").Activate
For iRowLoop = iRowStart To iRowEnd
    For iColLoop = 3 To 4
        sBlock(iRowLoop - iRowStart, iColLoop - 3) = _
        Cells(iRowLoop, iColLoop)
    Next iColLoop
Next iRowLoop

'Start loop and define transient variables
For iLoop = 0 To iNumRows

    'get the values from the array
    sIntTemp = sBlock(iLoop, 0)
    sIntRH = sBlock(iLoop, 1)
    sIntHR = sSatHR(sIntTemp) * sIntRH / 100
    sExtTemp = sBlock(iLoop, 3)

    'Here I want to roll the stack and add the new value to the end
    For iHour = 1 To (4 * iTimeConst - 1)
        sStack(iHour, 0) = sStack(iHour + 1, 0)
    Next iHour
    sStack(4 * iTimeConst, 0) = sIntRH


'*****************************************************************
    '  Stage One, Calculate the TWArh from the rolling stack, and
    '             therefore mass transfer occurring from the material

'*****************************************************************

    'define the surface conditions
    sSurfaceTemp = (sIntTemp - sExtTemp) * sTempPercent + sExtTemp

    'Evaluate the sTWArh based on the history
    sTWArh = 0
    sSum = 0
```

```
    For iHour = 1 To 4 * iTimeConst
        sTWArh = sTWArh + (sStack(iHour, 0) * sStack(iHour, 1))
        sSum = sSum + sStack(iHour, 1)
    Next iHour
    sTWArh = sTWArh / sSum

    sSurfaceRH = sTWArh   'equate to TWA based RH

    sSurfaceHR = sSatHR(sSurfaceTemp) * sSurfaceRH / 100

    'calc the mass txr based on TWA, store in array
    sSorpResult(iLoop, 0) = sMassTxrCoeff * sArea * _
    (sSurfaceHR - sIntHR) * 3600 'seconds/hr

'
'*****************************************************************
'      'Additional code for modelling high MC timber, emc = 25% =
95.5%rh
'     'Area = 10m2 with the normal area reduced to 100m2
'     sWetWoodHR = sSatHR(sSurfaceTemp) * 0.955
'
'     sSorpResult(iLoop, 0) = sSorpResult(iLoop, 0) + sMassTxrCoeff * 2
* (sWetWoodHR - sIntHR) * 3600


'*****************************************************************
    '  Stage Two, Translate into MC terms and calculate RunningMC
    '             from TWAmc

'*****************************************************************

    'Time weighted average moisture content
    sTWAmc = Exp(cSorpA + cSorpB * Log((sTWArh * 0.01) ^ (-cSorpC) -
1))

    sSorpResult(iLoop, 1) = sTWAmc

    'Calc the moisture mass present in the timber
    sTimberMoisture = sDryTimberMass * (sTWAmc / 100) _
    / (1 - sTWAmc / 100)

    'Calculate the moisture content of the timber after
    'the mass transfer occurs
    sRunningMC = (sTimberMoisture - sSorpResult(iLoop, 0)) _
    / ((sTimberMoisture - sSorpResult(iLoop, 0) + sDryTimberMass)) *
100

    sSorpResult(iLoop, 2) = sRunningMC

    'Running RH calculation serves no purpose
    'sRunningRH = (1 + Exp((Log(sRunningMC) - cSorpA) / cSorpB)) ^ (-1
/ cSorpC) * 100

Next iLoop

' dump the data to the data sheet for a looksee

Cells(iRowStart - 1, 17) = "sSorpMass"
Cells(iRowStart - 2, 17) = "[kg]"
Cells(iRowStart - 1, 22) = "sTWAmc"
Cells(iRowStart - 2, 22) = "[%]"
```

```
Cells(iRowStart - 1, 23) = "sRunningMC"
Cells(iRowStart - 2, 23) = "[%]"
'Cells(iRowStart - 1, 29) = "sWetWood Mass"
'Cells(iRowStart - 2, 29) = "[kg]"


For iLoop = 0 To iNumRows
    Cells(iLoop + iRowStart, 17) = sSorpResult(iLoop, 0)
    Cells(iLoop + iRowStart, 22) = sSorpResult(iLoop, 1)
    Cells(iLoop + iRowStart, 23) = sSorpResult(iLoop, 2)
Next iLoop

End Sub
Private Function sAirDens(sTemp As Single)
'This function calculates the air density for a given temp
'based on a linear approximation.
'Accurate over the range +/-50degC

sAirDens = -0.0049 * sTemp + 1.3061

End Function


Private Function sSatHR(sTemp As Single)
'This function calculates the Saturated humidity ratio
'for a given temperature.
'Only for (negative) temperatures between 0 and -40degC
'Hyland and Wexler formulation
'
Dim step As Integer
Dim sPws As Single
Dim sSum As Single
Dim sAbsTemp As Single
Dim sMArray(7) As Single

sMArray(0) = -5674.5359
sMArray(1) = 6.3925247
sMArray(2) = -0.009677843
sMArray(3) = 0.00000062215701
sMArray(4) = 2.0747825E-09
sMArray(5) = -9.484024E-13
sMArray(6) = 4.1635019

sAbsTemp = sTemp + 273.15

For step = 0 To 5
    sSum = sSum + sMArray(step) * sAbsTemp ^ (step - 1)
Next step
sSum = sSum + sMArray(6) * Log(sAbsTemp) 'natural log
sPws = Exp(sSum) / 1000 'answer in kPa
sSatHR = 0.622 * (sPws / (101.325 - sPws))


End Function

Sub Occupancy()
'This subroutine calculates the moisture gain based on
'the occupancy of the building over the hour.

Dim sMoistureRate As Single
Dim iPeople As Integer
```

```
'read input from sheet
Worksheets("Internal Gain").Activate
sMoistureRate = Cells(6, 3)
iPeople = Cells(5, 3)



'Set up array
Worksheets("Data").Activate
ReDim sOccupant(iNumRows) As Single

'Calculate
For iRowLoop = 0 To iNumRows - 1
'The absolute value function allows the occupancy to be set
'negative to allow the door to remain closed if wanted
'see the infiltration model for this decision.
    sOccupant(iRowLoop) = Abs(sBlock(iRowLoop, 7)) * sMoistureRate *
iPeople
Next iRowLoop

'Dump to sheet

Cells(iRowStart - 1, 18) = "sOccupant"
Cells(iRowStart - 2, 18) = "[kg]"
For iLoop = 0 To iNumRows
    Cells(iLoop + iRowStart, 18) = sOccupant(iLoop)
Next iLoop
End Sub

Sub RoomState()
'This ties up all the loose ends by calculating the room RH
'as defined by the mass transfer into and out of the room.
'Works on assumption that RH = Degree of Saturation

'sModelOutput array: col 0 = period mass, col 1 = RH by model


Dim sRunHR As Single
Dim sIntTemp As Single
Dim sTWAMass As Single
Dim sSumStack As Single

ReDim sModelOutput(iNumRows, 1) As Single

'Total all models into one array
For iLoop = 0 To iNumRows
    sModelOutput(iLoop,    0)    =    sInfilResults(iLoop,    2)    +
sCEResults(iLoop) _
    + sSorpResult(iLoop, 0) + sOccupant(iLoop) '+ sSorpResult(iLoop,
3) 'wetwood addition
Next iLoop

'Set up stack for rh moderation
iTimeConst = 4

ReDim sStack(0 To 4 * iTimeConst) As Single
For iHour = 0 To 4 * iTimeConst - 1
    sStack(iHour) = Exp((-((4 * iTimeConst) - iHour)) / iTimeConst)
    sSumStack = sSumStack + sStack(iHour)
```

```
Next iHour


'Calc RH based on this data
For iLoop = 0 To iNumRows

    'Calc exp time weighted average
    If iLoop < 4 * iTimeConst Then
'            I shouldn 't require this code section with low time
constants
        For iStep = 0 To iLoop
            sTWAMass = sTWAMass + sModelOutput(iLoop - iStep, 0) _
            * sStack(4 * iTimeConst - iStep - 1)
        Next iStep
        sTWAMass = sTWAMass / sSumStack
        sTWAMass = sModelOutput(iLoop, 0)   'no change until 4*Time
const elapses
    Else:
        sTWAMass = 0
        For iStep = 1 To 4 * iTimeConst
            sTWAMass = sTWAMass + sModelOutput(iLoop - iStep, 0) _
            * sStack(4 * iTimeConst - iStep)
        Next iStep
        sTWAMass = sTWAMass / sSumStack
    End If

    sIntTemp = sBlock(iLoop, 0)
    sRunHR = sSatHR(sIntTemp) * sBlock(iLoop, 1) / 100 'Starting HR

    'sTWAMass = sModelOutput(iLoop, 0)  'bypass above code
    sRunHR = sRunHR + sTWAMass / (sAirDens(sIntTemp) * cHutVolume)
    'RH approximated as the degree of saturation

    sModelOutput(iLoop, 1) = sRunHR / sSatHR(sIntTemp) * 100
Next iLoop

'Output to sheet
Cells(iRowStart - 1, 20) = "sModelOutput - Mass"
Cells(iRowStart - 2, 20) = "[kg]"

Cells(iRowStart - 1, 21) = "sModelOutput - RH"
Cells(iRowStart - 2, 21) = "[%]"

For iLoop = 0 To iNumRows
    Cells(iLoop + iRowStart, 20) = sModelOutput(iLoop, 0)
    Cells(iLoop + iRowStart, 21) = sModelOutput(iLoop, 1)
Next iLoop

End Sub

Sub ChartHandler()
' Sources the current block data for the charts
' 5.7.99 GM

Select Case iBlockNumber

Case 1
    Charts(1).SetSourceData
Source:=Sheets("Data").Range("a6:a126,s6:s126,t6:t126")
```

```
    Charts(2).SetSourceData
Source:=Sheets("Data").Range("a6:a126,o6:o126,p6:p126,q6:q126,r6:r126"
)
    Charts(3).SetSourceData
Source:=Sheets("Data").Range("a6:a126,q6:q126,v6:v126,w6:w126")
    Charts(4).SetSourceData
Source:=Sheets("Data").Range("a6:a126,u6:u126,d6:d126,g6:g126")
    Application.StatusBar = Charts.Count & " charts modified to Block
One data"

Case 2
    Charts(1).SetSourceData
Source:=Sheets("Data").Range("a131:a323,s131:s323,t131:t323")
    Charts(2).SetSourceData
Source:=Sheets("Data").Range("a131:a323,o131:o323,p131:p323,q131:q323,
r131:r323")
    Charts(3).SetSourceData
Source:=Sheets("Data").Range("a131:a323,q131:q323,v131:v323,w131:w323"
)
    Charts(4).SetSourceData
Source:=Sheets("Data").Range("a131:a323,u131:u323,d131:d323,g131:g323"
)
Application.StatusBar = Charts.Count & " charts modified to Block Two
data"

Case 3
    Charts(1).SetSourceData
Source:=Sheets("Data").Range("a328:a520,s328:s520,t328:t520")
    Charts(2).SetSourceData
Source:=Sheets("Data").Range("a328:a520,o328:o520,p328:p520,q328:q520,
r328:r520")
    Charts(3).SetSourceData
Source:=Sheets("Data").Range("a328:a520,q328:q520,v328:v520,w328:w520"
)
    Charts(4).SetSourceData
Source:=Sheets("Data").Range("a328:a520,u328:u520,d328:d520,g328:g520"
)
Application.StatusBar = Charts.Count & " charts modified to Block
Three data"

Case 4
    Charts(1).SetSourceData
Source:=Sheets("Data").Range("a525:a693,s525:s693,t525:t693")
    Charts(2).SetSourceData
Source:=Sheets("Data").Range("a525:a693,o525:o693,p525:p693,q525:q693,
r525:r693")
    Charts(3).SetSourceData
Source:=Sheets("Data").Range("a525:a693,q525:q693,v525:v693,w525:w693"
)
    Charts(4).SetSourceData
Source:=Sheets("Data").Range("a525:a693,u525:u693,d525:d693,g525:g693"
)
Application.StatusBar = Charts.Count & " charts modified to Block Four
data"

Case 5
    Charts(1).SetSourceData
Source:=Sheets("Data").Range("a698:a998,s698:s998,t698:t998")
    Charts(2).SetSourceData
Source:=Sheets("Data").Range("a698:a998,o698:o998,p698:p998,q698:q998,
r698:r998")
```

```
    Charts(3).SetSourceData
Source:=Sheets("Data").Range("a698:a998,q698:q998,v698:v998,w698:w998"
)
    Charts(4).SetSourceData
Source:=Sheets("Data").Range("a698:a998,u698:u998,d698:d998,g698:g998"
)
Application.StatusBar = Charts.Count & " charts modified to Block Five
data"

Case Else
Application.StatusBar = "ChartHandler not configured to data source"

End Select
End Sub
```

B.1.3 Psychrometric Calculation Program – 'AutoCalc'

```
Option Explicit


' Dimension module level variables and constants
Dim msRelHumid As Single
Dim msDewpoint As Single
Dim msStatePw As Single
Dim msHumidRatio As Single
Dim msCurrentPws As Single
Dim msCurrentTemp As Single
Dim msTemp As Single
Const msA As Single = 42.6776
Const msB As Single = -3892.7
Const msC As Single = -9.48654

Sub FormulaMethod()
' This programme calculates the state properties for
' the standard form logger files using the formula method.
' Written by Glen Mason, June 1998.
' AHT Project
' Quick Key CTRL-A

Dim iSteps As Integer
Dim iDatapoints As Integer
Const cFirstRow As Integer = 11 ' first row that data appears
Dim iRows As Integer

'inform user of what they are doing
Application.StatusBar = "Calculating the state properties, takes a
minute or so"

'find the last row number, works fine but slow
'can in future find a faster way to do this.
iRows = 10
Do
    iRows = iRows + 1
Loop Until Cells(iRows, 1) = ""
iRows = iRows - 1
'Range("c1") = iRows  'so that the charting routine can find it
```

```
'fill in some column headings
Range("e10") = "Saturated Vapour Pressure [kPa]"
Range("f10") = "State Vapour Pressure [kPa]"
Range("g10") = "Humidity Ratio [kgw/kga]"
Range("h10") = "Dewpoint [degC]"



For iSteps = cFirstRow To iRows
    msTemp = Cells(iSteps, 2)
    msRelHumid = Cells(iSteps, 3) / 100
    Call CalcEngine
    Cells(iSteps, 5) = msCurrentPws 'paste them in
    Cells(iSteps, 6) = msStatePw
    Cells(iSteps, 7) = msHumidRatio
    Cells(iSteps, 8) = msDewpoint
Next iSteps


End Sub

Private Sub CalcEngine()

'find the sat vapour pressure with calculate routine
' using twin formula for above and below zero degC
msCurrentTemp = msTemp
If msCurrentTemp < 0 Then
    Call CalcPwsBelow
Else
    Call CalcPwsAbove
End If


' from this and the rh, find the state vapour pressure
msStatePw = msRelHumid * msCurrentPws


' Calculate the Humidity ratio
msHumidRatio = 0.622 * msStatePw / (101.325 - msStatePw)
'msHumidRatio = msHumidRatio * 1000 'convert to g/kg

'now using the iterate routine, find the dewpoint
Call DPTIterateBelow

'as the above zero dpt formula is inaccurate below zero
'test this condition upon return and recalc if necessary
'using the below temp iteration
If msCurrentTemp > 0 Then
    msCurrentTemp = msTemp
    Call DPTCalculateAbove
End If

msDewpoint = msCurrentTemp

' thats all the calculation work done, now we have to fill
' down the entries for the entire file

End Sub

Private Sub CalcPwsAbove()
```

```
' This is the main formula for getting pws from t
' for temperatures above zero deg C

' dimension local variables
Dim sSum As Single
Dim sAbsTemp As Single
Dim iStep As Integer

sAbsTemp = msCurrentTemp + 273.15
msCurrentPws = Exp(msB / (sAbsTemp - msA) - msC)
msCurrentPws = msCurrentPws * 1000  'convert from MPa to kPa


End Sub
Private Sub CalcPwsBelow()
' This is the main formula for getting pws from t
' for temperatures below zero deg C

' dimension local variables
Dim sSum As Single
Dim sAbsTemp As Single
Dim iStep As Integer
Dim sMArray(7) As Single

sMArray(0) = -5674.5359
sMArray(1) = 6.3925247
sMArray(2) = -0.009677843
sMArray(3) = 0.00000062215701
sMArray(4) = 2.0747825E-09
sMArray(5) = -9.484024E-13
sMArray(6) = 4.1635019

sAbsTemp = msCurrentTemp + 273.15

For iStep = 0 To 5
    sSum = sSum + sMArray(iStep) * sAbsTemp ^ (iStep - 1)
Next iStep
sSum = sSum + sMArray(6) * Log(sAbsTemp)
msCurrentPws = Exp(sSum) / 1000 'answer in kPa


End Sub

Private Sub DPTCalculateAbove()
'this is the routine for calculating dewpoint temp above zero degrees

msStatePw = msStatePw / 1000 ' convert to MPa

msCurrentTemp = msA + (msB / _
(Application.WorksheetFunction.Ln(msStatePw) + msC))

msCurrentTemp = msCurrentTemp - 273.15 'Back to degC


End Sub
Private Sub DPTIterateBelow()
'This is the iteration procedure for obtaining the dewpoint temp from
'the state vapour pressure

Dim sDiffPws As Single
Dim sLastPws As Single
```

```
'Note: The theory for maximising the efficiency of this step
' relates to the total number of steps

'Start reducing by 1 degree steps
Do
    msCurrentTemp = msCurrentTemp - 1
    Call CalcPwsBelow
    sDiffPws = msCurrentPws - msStatePw
Loop Until sDiffPws < 0

'Back up, increasing in 0.1 degree steps
Do
    msCurrentTemp = msCurrentTemp + 0.1
    Call CalcPwsBelow
    sDiffPws = msCurrentPws - msStatePw
Loop Until sDiffPws > 0

'and back down again for the second decimal place
Do
    msCurrentTemp = msCurrentTemp - 0.01
    Call CalcPwsBelow
    sDiffPws = msCurrentPws - msStatePw
Loop Until sDiffPws < 0


End Sub
```

B.2 Input Spreadsheets

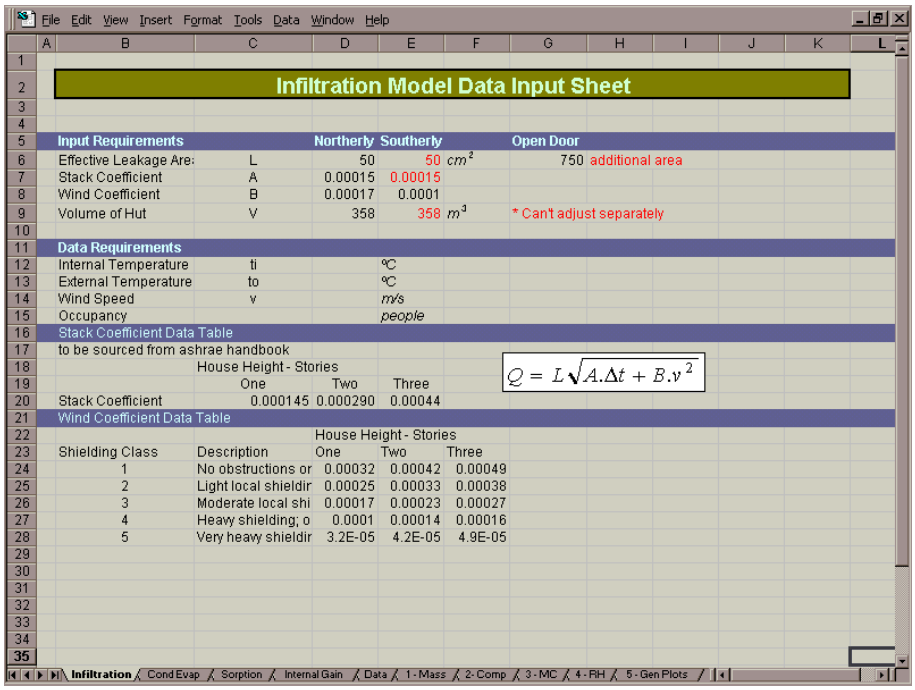

Figure B.1: Infiltration model input sheet

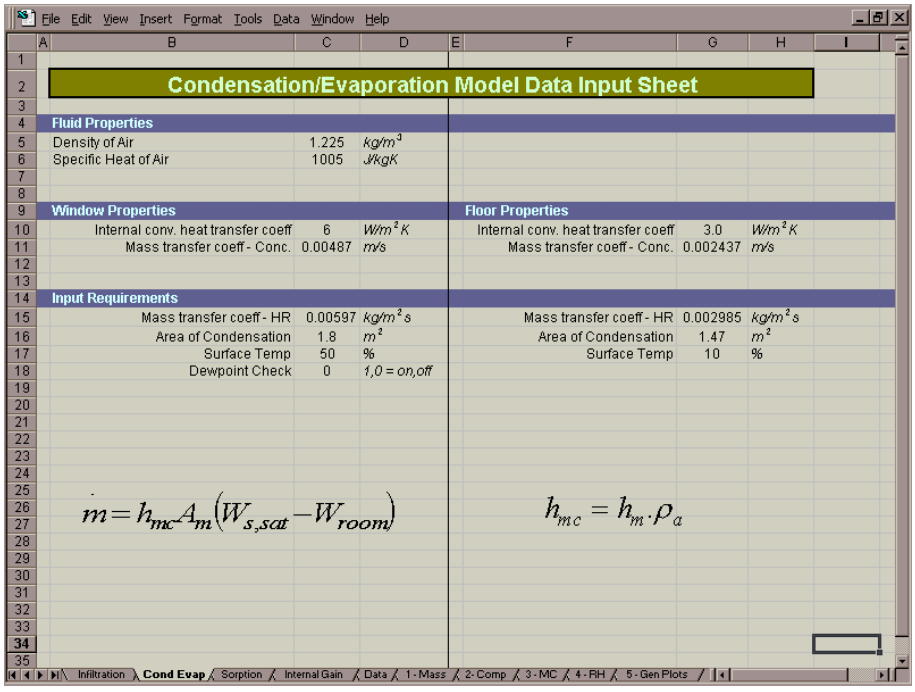

Figure B.2: Condensation and evaporation model input sheet

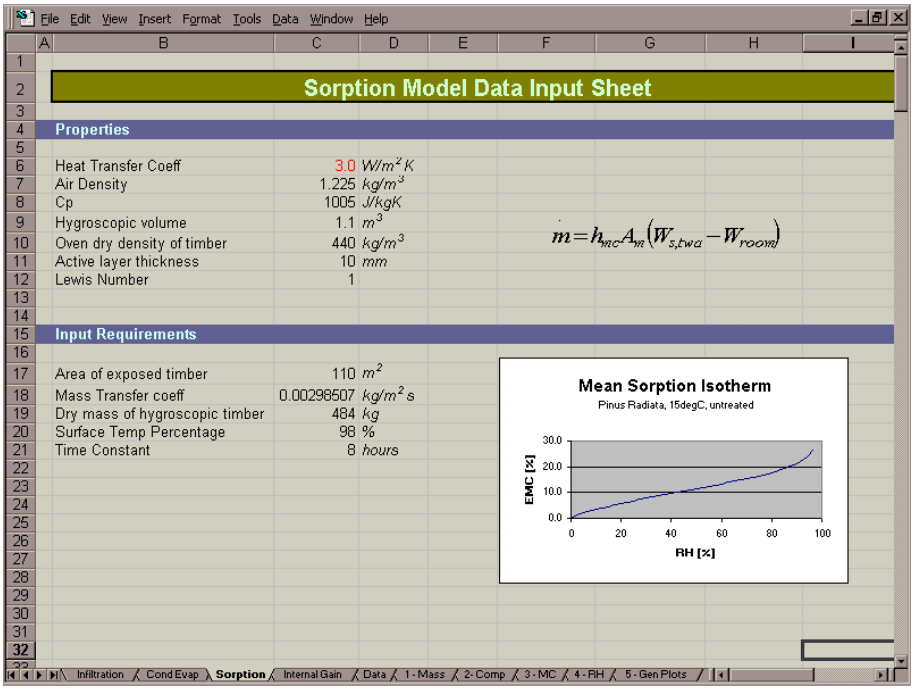

Figure B.3: Sorption model input sheet

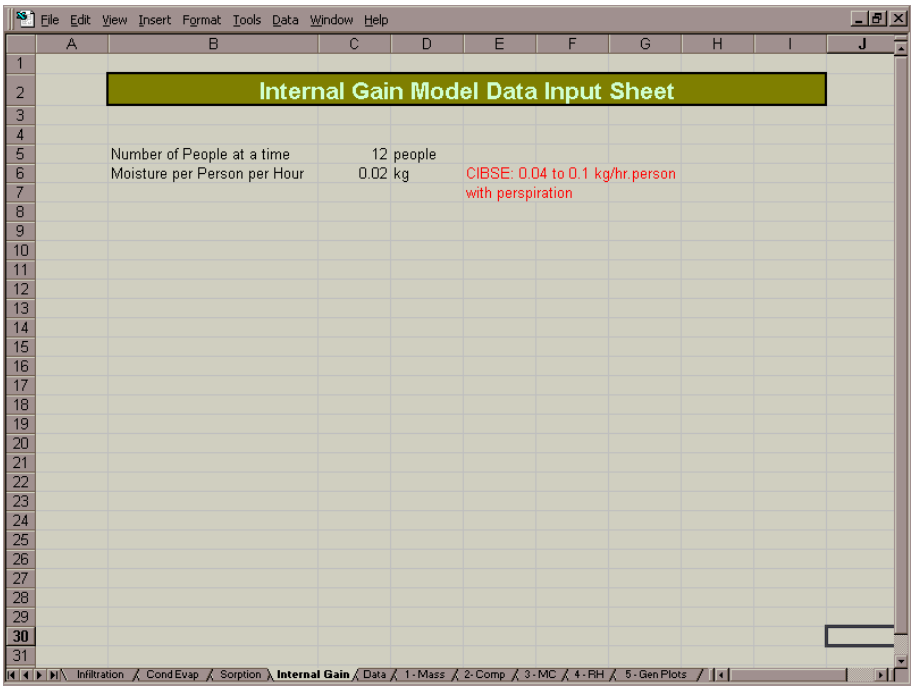

Figure B.4: Occupancy model input sheet

APPENDIX C

DATA, CALIBRATIONS AND RESULTS

C.1 Logger Data Chronological Listing

Table C.1: Logger files with the data time span

Filename (.stk file)	Start Date	End Date
Greenpeace Data	1/03/89	31/12/90
	1/03/89	31/12/90
EVANS910	9/01/91	14/10/91
EVANS911	9/01/91	14/10/91
EVANS92930	5/01/92	13/11/92
EVANS92931	5/01/92	13/11/92
EVANS930	14/11/92	25/01/93
EVANS931	14/11/92	25/01/93
CE93WIN0	25/01/93	21/11/93
EV94950	26/02/94	2/02/95
EV94951	26/02/94	2/02/95
EVANS950	11/01/95	22/10/95
EVANS951	11/01/95	22/10/95
CEJAN960	2/01/96	8/12/96
CEJAN961	2/01/96	8/12/96
EFEB97A0	8/02/97	22/09/97
EFEB97A1	8/02/97	22/09/97
EFEB97A2	8/02/97	22/09/97
EFEB97B0	8/02/97	22/09/97
EFEB97B1	8/02/97	22/09/97
EFEB97B2	8/02/97	22/09/97
EFEB97C0	8/02/97	22/09/97
EFEB97C1	8/02/97	22/09/97
EFEB97C2	8/02/97	22/09/97
EJAN98B0	27/09/97	9/01/98
EJAN97B1	27/09/97	9/01/98
EJAN97B2	27/09/97	9/01/98
EJAN97C0	27/09/97	9/01/98
EJAN97C1	27/09/97	9/01/98
EJAN97C2	27/09/97	9/01/98

C.2 Full Data Correlation Results

Tables C.2 to 7 contain the correlation coefficients between the various input data types.

Table C.2: Whole data set correlation

	Int. Temp	Int. RH	Int. Pv	Ext. Temp	Ext. RH	Ext. Pv	Windspeed	Wind Dir.
Int. Temp	1							
Int. RH	0.573	1						
Int. Pv	0.896	0.754	1					
Ext. Temp	0.810	0.615	0.742	1				
Ext. RH	0.277	0.233	0.269	0.293	1			
Ext. Pv	0.711	0.672	0.798	0.881	0.424	1		
Windspeed	0.002	0.070	-0.048	0.079	0.151	0.075	1	
Wind Dir.	0.001	0.171	0.044	0.161	0.182	0.182	0.311	1
Direct Solar	0.164	-0.129	0.064	0.050	-0.137	-0.032	-0.044	-0.111

Table C.3: Block One data correlation

	Int. Temp	Int. RH	Int. Pv	Ext. Temp	Ext. RH	Ext. Pv	Windspeed	Wind Dir.
Int. Temp	1							
Int. RH	0.930	1						
Int. Pv	0.994	0.925	1					
Ext. Temp	0.727	0.775	0.701	1				
Ext. RH	-0.025	-0.058	-0.038	-0.412	1			
Ext. Pv	0.760	0.781	0.727	0.891	0.026	1		
Windspeed	-0.488	-0.582	-0.500	-0.636	0.118	-0.621	1	
Wind Dir.	0.046	-0.037	0.037	0.196	-0.026	0.306	-0.024	1
Direct Solar	0.381	0.408	0.424	0.326	-0.178	0.282	-0.395	-0.093

Table C.4: Block Two data correlation

	Int. Temp	Int. RH	Int. Pv	Ext. Temp	Ext. RH	Ext. Pv	Windspeed	Wind Dir.
Int. Temp	1							
Int. RH	0.845	1						
Int. Pv	0.999	0.865	1					
Ext. Temp	0.186	0.284	0.202	1				
Ext. RH	-0.121	-0.169	-0.135	-0.531	1			
Ext. Pv	0.152	0.251	0.163	0.842	-0.005	1		
Windspeed	0.062	0.101	0.073	0.399	-0.641	0.104	1	
Wind Dir.	-0.124	-0.014	-0.101	0.492	-0.437	0.328	0.533	1
Direct Solar	0.088	0.048	0.090	0.022	-0.092	-0.036	-0.044	-0.013

Table C.5: Block Three correlation data

	Int. Temp	Int. RH	Int. Pv	Ext. Temp	Ext. RH	Ext. Pv	Windspeed	Wind Dir.
Int. Temp	1							
Int. RH	0.985	1						
Int. Pv	0.988	0.992	1					
Ext. Temp	0.925	0.894	0.897	1				
Ext. RH	0.510	0.502	0.488	0.552	1			
Ext. Pv	0.837	0.811	0.826	0.920	0.689	1		
Windspeed	0.330	0.307	0.312	0.368	0.564	0.490	1	
Wind Dir.	0.290	0.258	0.271	0.355	0.532	0.425	0.574	1
Direct Solar	0.000	0.000	0.000	0.000	0.000	0.000	0.000	0.000

Table C.6: Block Four correlation data

	Int. Temp	Int. RH	Int. Pv	Ext. Temp	Ext. RH	Ext. Pv	Windspeed	Wind Dir.
Int. Temp	1							
Int. RH	0.951	1						
Int. Pv	0.987	0.948	1					
Ext. Temp	0.710	0.722	0.685	1				
Ext. RH	-0.337	-0.249	-0.392	-0.077	1			
Ext. Pv	0.422	0.480	0.372	0.837	0.414	1		
Windspeed	-0.148	-0.065	-0.215	0.180	0.471	0.338	1	
Wind Dir.	-0.210	-0.176	-0.241	0.170	0.425	0.371	0.431	1
Direct Solar	0.000	0.000	0.000	0.000	0.000	0.000	0.000	0.000

Table C.7: Block Five correlation data

	Int. Temp	Int. RH	Int. Pv	Ext. Temp	Ext. RH	Ext. Pv	Windspeed	Wind Dir.
Int. Temp	1							
Int. RH	0.988	1						
Int. Pv	0.992	0.986	1					
Ext. Temp	0.881	0.854	0.837	1				
Ext. RH	-0.244	-0.256	-0.320	0.037	1			
Ext. Pv	0.512	0.487	0.440	0.763	0.637	1		
Windspeed	-0.053	-0.068	-0.109	0.198	0.746	0.606	1	
Wind Dir.	-0.014	-0.029	-0.075	0.244	0.644	0.576	0.728	1
Direct Solar	0.104	0.107	0.116	0.104	-0.160	-0.021	-0.098	-0.094

C.3 Correlation of Humidity Ratio with Solar Radiation

Comparison of the trends for solar radiation and humidity ratio (during summer months) showed periods of similar peaks that were offset by a number of hours. This time-shifted correlation was thought to be caused by the heat capacity of the building. Although a thermal model was not included in this project, the results of a statistical analysis are included here. The humidity ratio inside the hut was found to follow solar gains reasonably well with an eight hour delay.

Table C.8: Correlation of humidity ratio with solar radiation

HR Time shift	Correlation Coefficient
-2	0.467
-4	0.577
-6	0.66
-7	0.676
-8	0.679
-9	0.666
-10	0.64
-12	0.549
[hrs]	**0<R<1**

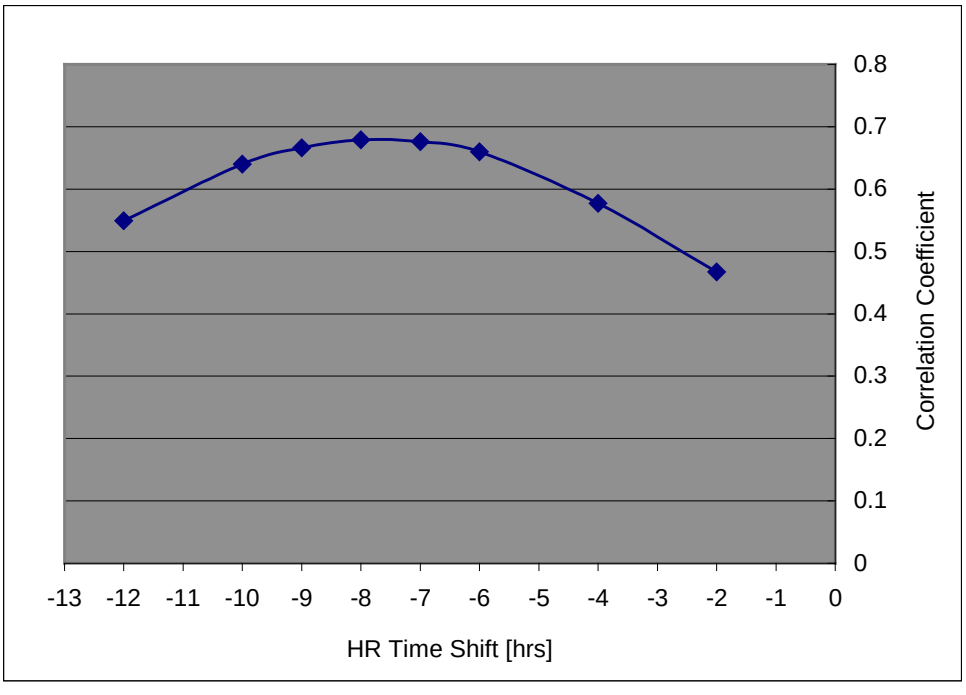

Figure C.1: Correlation peaks, showing a nominal 8 hour delay

C.4 Visitor Book Entries

Figures C.2 to 6 indicate visitor numbers and the time of the year the visit had taken place for the years 1994 through 1997.

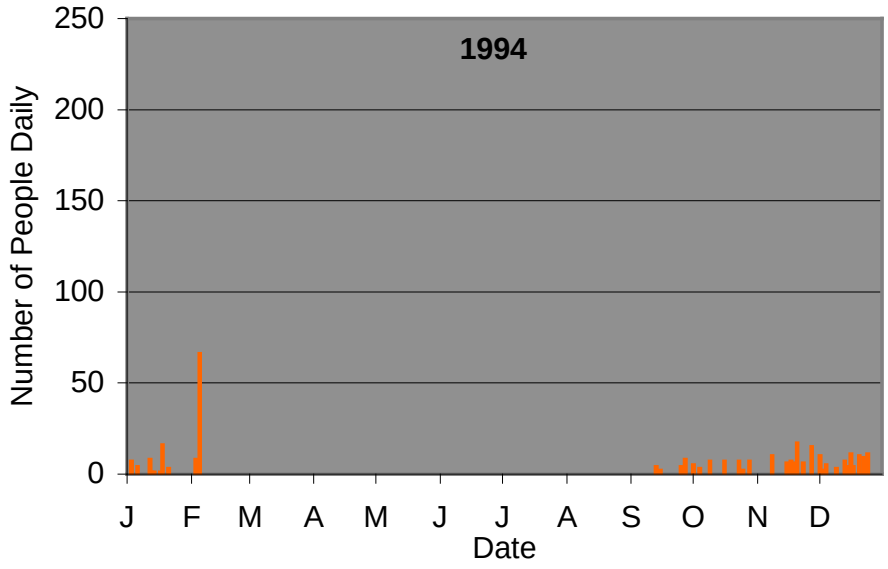

Figure C.2: Visitor book signings in 1994

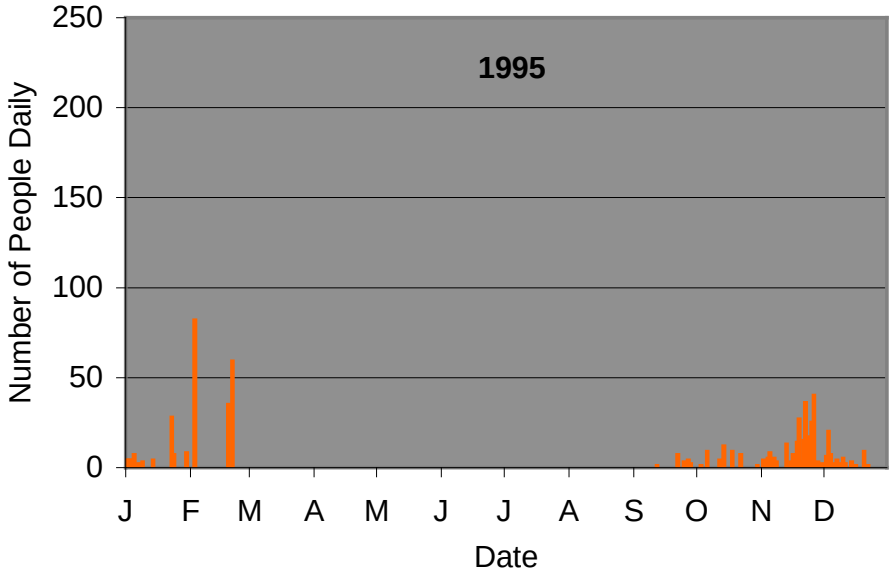

Figure C.3: Visitor book signings in 1995

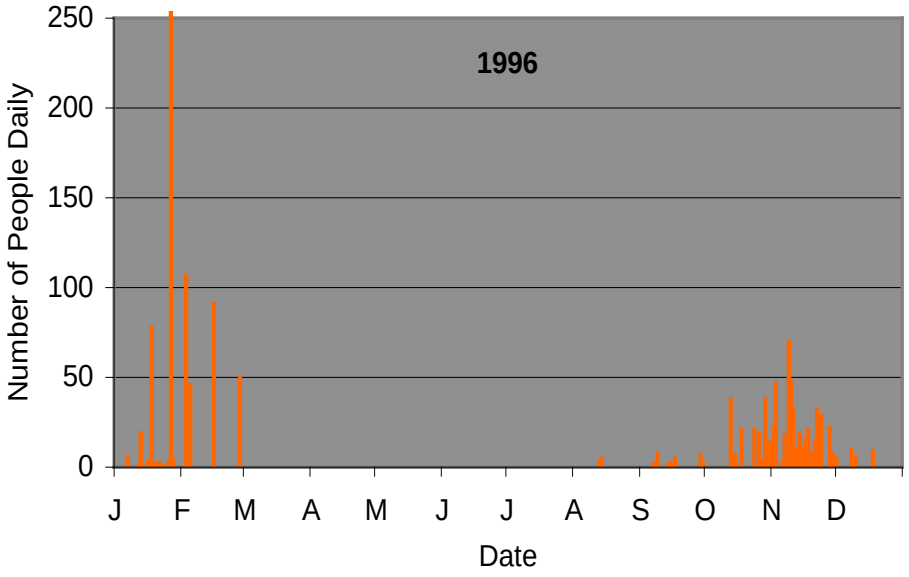

Figure C.4: Visitor book signings in 1996

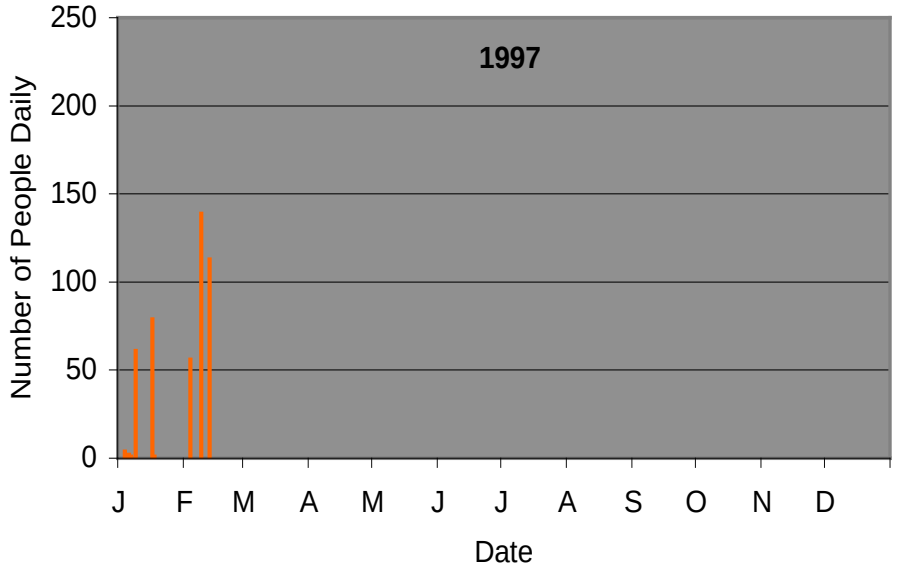

Figure C.5: Visitor book signings for beginning of 1997

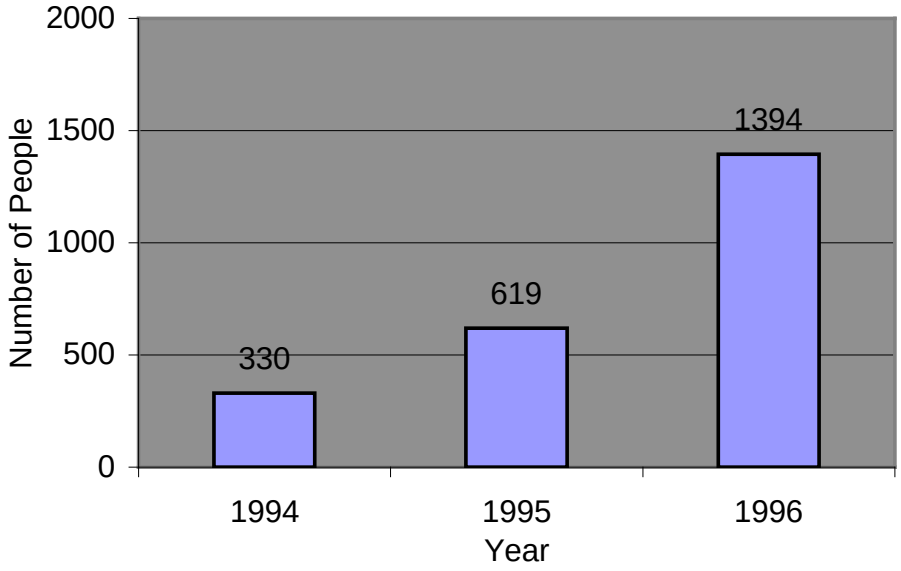

Figure C.6: Visitor numbers trend for 1994 - 1996

C.5 Heat Flux Transducer Calibration Results

Table C.9: HFT calibration test one results

Sample Number	1	2	3	4	5	6	7	Units
Approximate elapsed time	1	5	10	15	20	30	40	*minutes*
Inside surface temp	38.1	53.1	63.5	64.9	67.4	62.7	62	*deg C*
Outside surface temp	27.1	27.1	27.1	27.4	28.1	28.3	28.8	*deg C*
HFT output	1	4.2	3.7	3.3	2.5	1.3	1.2	*mV*
Calculations								
Heat flux	23.5	98.7	86.95	77.55	58.75	30.55	28.2	W/m^2
Material r - value	0.468	0.263	0.419	0.484	0.669	1.126	1.177	m^2K/W
Variation		-0.205	0.155	0.065	0.185	0.457	0.051	m^2K/W
% Variation		-77.7	37.1	13.4	27.7	40.6	4.4	%

Table C.10a: HFT calibration test two results (continues)

Sample Number	1	2	3	4	5	6	Units
Approximate elapsed time	5	10	15	20	25	30	*minutes*
Inside surface temp	51.1	60.3	61.5	62.9	63.4	64.6	*deg C*
Outside surface temp	22.4	26.1	26.6	27.2	27.6	28	*deg C*
HFT output	2.5	2.8	2.2	1.9	1.6	1.5	*mV*
Calculations							
Heat flux	58.75	65.8	51.7	44.65	37.6	35.25	W/m^2
Material r - value	0.489	0.520	0.675	0.800	0.952	1.038	m^2K/W
Variation		0.031	0.155	0.125	0.153	0.086	m^2K/W
% Variation		6.0	23.0	15.6	16.0	8.3	%

Table C.10b: HFT calibration test two results (continued)

Sample Number	7	8	9	10	11	Units
Approximate elapsed time	35	40	45	50	60	*minutes*
Inside surface temp	64.4	63.4	65	65.2	65.3	*deg C*
Outside surface temp	27.3	28.2	28.5	28.7	28.8	*deg C*
HFT output	1.4	1.3	1.4	1.3	1.3	*mV*
Calculations						
Heat flux	32.9	30.55	32.9	30.55	30.55	W/m^2
Material r - value	1.128	1.152	1.109	1.195	1.195	m^2K/W
Variation	0.089	0.025	-0.043	0.085	0.000	m^2K/W
% Variation	7.9	2.1	-3.9	7.1	0.0	%

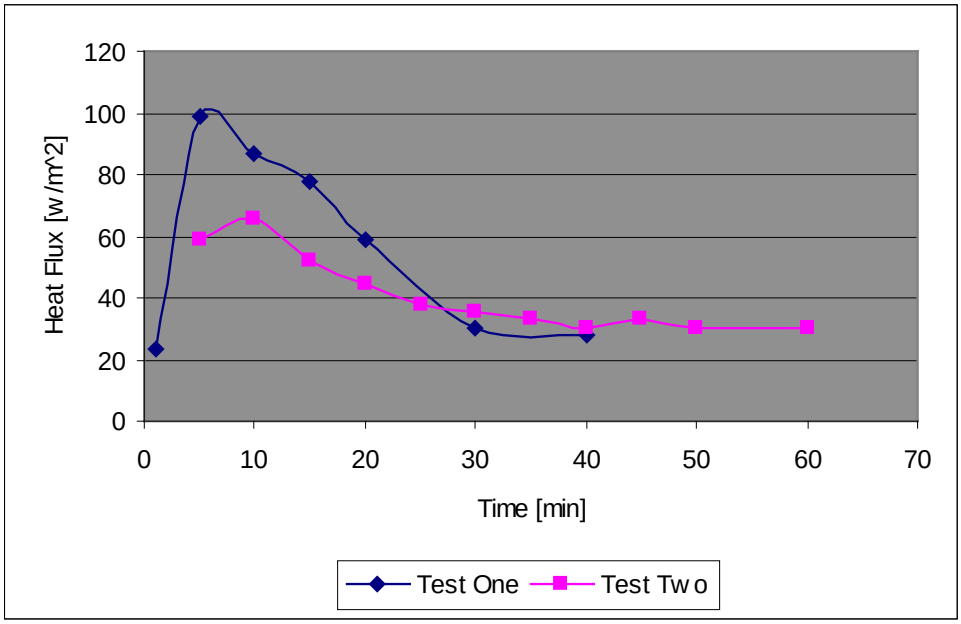

Figure C.7: Transient response of HFT calibration tests one and two

The wall was deduced to have reached steady state conditions after 30 minutes of heating time had elapsed. The average calculated r-value from both tests was 1.19 m^2K/W. This was within a reasonable ±20% error band of the 1.43 m^2K/W theoretical r-value. The 0.1 mV resolution of the voltmeter meant a ±7.7% error per least significant digit.

C.5.1 Terra Nova Insulation Test Results

Table C.11a: Terra Nova hut wall insulation test one (continues)

Sample Number	1	2	3	4	5	6	7	8	Units
Time	16:49	16:52	16:53	16:54	16:57	17:00	17:03	17:06	
Time elapsed [min]	0	00:03	00:04	00:05	00:08	00:11	00:14	00:17	*min*
Inside surface temp	1.9	3.1	4.8	6.8	9.2	11.2	13.3	14.7	*deg C*
Outside surface temp	2.3	2.3	2.3	2.3	2.3	2.4	2.6	2.7	*deg C*
HFT output	0.1	1.4	3.7	4.5	5	4.9	4.9	4.9	*mV*
Calculations									
Heat Flux	2.35	32.9	86.95	105.7	117.5	115.1	115.1	115.1	W/m^2
Material r - Value	0	0.024	0.029	0.043	0.059	0.076	0.093	0.104	m^2K/W
variation in r		0	0.004	0.014	0.016	0.018	0.017	0.011	m^2K/W
% variation in r			15.4	32.4	27.5	23.2	17.8	10.8	%

Table C.11b: Terra Nova hut wall insulation test one (continued)

Sample Number	9	10	11	12	13	14	15	16	Units
Time	17:10	17:13	17:16	17:20	17:24	17:28	17:31	17:34	
Time elapsed [min]	00:21	00:24	00:27	00:31	00:35	00:39	00:42	00:45	*min*
Inside surface temp	16.2	17.4	18.3	19.5	20.4	21.1	21.7	22.2	*deg C*
Outside surface temp	2.9	2.8	2.8	2.9	2.9	2.9	2.8	2.6	*deg C*
HFT output	4.5	4.5	4.2	4.1	3.9	3.6	3.5	3.4	*mV*
Calculations									
Heat Flux	105.75	105.75	98.7	96.35	91.65	84.6	82.25	79.9	W/m^2
Material r - Value	0.126	0.138	0.157	0.172	0.191	0.215	0.230	0.245	m^2K/W
variation in r	0.022	0.012	0.019	0.015	0.019	0.024	0.015	0.016	m^2K/W
% variation in r	17.1	8.9	12.1	8.8	9.8	11.2	6.4	6.3	%

Table C.12a: Terra Nova hut wall insulation test two (continues)

Sample Number	1	2	3	4	5	6	7	Units
Time	16:33	16:36	16:37	16:44	16:48	16:54	16:58	
Time elapsed [min]	0	00:03	00:04	00:11	00:15	00:21	00:25	*min*
Inside surface temp	0.5	5.6	6.8	11.3	12.9	15.3	16.5	*deg C*
Outside surface temp	-0.5	-0.5	-0.5	-0.5	-0.4	-0.4	-0.2	*deg C*
HFT output	0.1	4.7	5	4.7	4.7	4.3	4.1	*mV*
Calculations								
Heat Flux	2.35	110.45	117.5	110.45	110.45	101.05	96.35	W/m^2
Material r - Value	0	0.055	0.062	0.107	0.120	0.155	0.173	m^2K/W
variation in r		0	0.007	0.045	0.014	0.035	0.018	m^2K/W
% variation in r			11.1	41.8	11.3	22.5	10.4	*%*

Table C.12b: Terra Nova hut wall insulation test two (continued)

Sample Number	1	2	3	4	5	6	7	Units
Time	16:33	16:36	16:37	16:44	16:48	16:54	16:58	
Time elapsed [min]	0	00:03	00:04	00:11	00:15	00:21	00:25	*min*
Inside surface temp	0.5	5.6	6.8	11.3	12.9	15.3	16.5	*deg C*
Outside surface temp	-0.5	-0.5	-0.5	-0.5	-0.4	-0.4	-0.2	*deg C*
HFT output	0.1	4.7	5	4.7	4.7	4.3	4.1	*mV*
Calculations								
Heat Flux	2.35	110.45	117.5	110.45	110.45	101.05	96.35	W/m^2
Material r - Value	0	0.055	0.062	0.107	0.120	0.155	0.173	m^2K/W
variation in r		0	0.007	0.045	0.014	0.035	0.018	m^2K/W
% variation in r			11.1	41.8	11.3	22.5	10.4	*%*

Table C.13: Terra Nova hut roof insulation test

Sample Number	1	2	3	4	5	Units
Time	17:24	17:27	17:30	17:34	17:40	
Time elapsed [min]	0	00:03	00:06	00:10	00:16	*min*
Inside surface temp	31.1	30.9	31	31.3	31.3	*deg C*
Outside surface temp	10.6	10.2	9.9	9.6	9.3	*deg C*
HFT output	1.1	1	1	0.9	0.8	*mV*
Calculations						
Heat Flux	25.85	23.5	23.5	21.15	18.8	W/m^2
Material r - Value	1	0.8809	0.8979	1.0260	1.1702	m^2K/W
variation in r		0	0.017	0.128	0.144	m^2K/W
% variation in r		1.0E+01	1.9	12.5	12.3	*%*

C.6 Cup Anemometer Calibration

The windspeed needed to be specified with several of the tests undertaken at Cape Evans. A cup anemometer was obtained from a redundant experiment and calibrated in a wind-tunnel against a pitot micro-manometer. The cup anemometer produced a frequency output that was measured with a Fluke 87 multimeter.

The air-speed calibration for the wind-tunnel was;

$$C = 7.5034\sqrt{\frac{A(273+t)}{kP}} \qquad [C.1]$$

where;

C = air speed, m/s

A = pitot pressure, mmH_2O

k = 1.0185

P = 1014mb, on the day

t = 20ºC, on the day

The anemometer was then fitted to the linear function;

$$u = C.f + k \qquad [C.2]$$

using the wind-tunnel wind-speed data. Two separate tests were carried out, from which the average was obtained.

Table C.14: Sample results for anemometer calibration

Pressure [mmWG]	Frequency [Hz]	Air Speed [m/s]
0.10	1.18	1.26
0.20	1.70	1.79
0.30	2.15	2.19
0.40	2.63	2.53
0.50	3.00	2.83
0.60	3.43	3.10
0.70	3.70	3.34
0.80	4.00	3.57
0.90	4.25	3.79
1.00	4.50	4.00
1.60	5.80	5.06
2.05	6.75	5.72
2.85	7.80	6.75
3.40	8.70	7.37
4.00	9.50	7.99
4.30	10.00	8.29
5.60	11.40	9.46
6.55	12.40	10.23
7.35	13.30	10.84
9.50	15.00	12.32

Figure C.8 shows the linear fit and the function obtained.

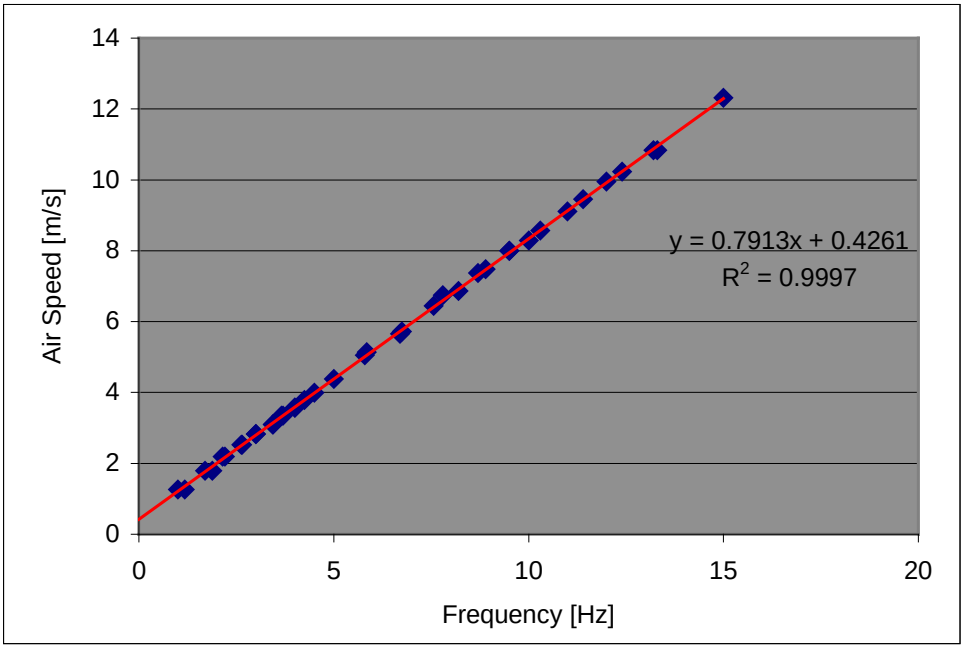

Figure C.8: Calibration plot of cup anemometer

C.7 Salt Deposition Test Titration Solutions

a) Mixed indicator

- 0.5g Diphenylcarbazone
- 0.5g Bromophenol Blue
- Diluted to 100ml with ethanol.

b) Acidifier, nitric acid

- 3ml of 2M HNO3
- Diluted to 1000ml with distilled water
- c[HNO3]=0.05M

c) Sodium chloride standard solution

- Dry NaCl in oven for 1h at 300degC.
- 1.4613g very accurately weighed and diluted to 1000ml with distilled water
- Actual mass of NaCl weighed = 1.4615g.
- Assumed to be exact concentration; c[NaCl solution] = 0.025M

d) Titrating solution, mercury (II) nitrate

- 4.283g of Mercury (II) nitrate dissolved in 1000ml of distilled water
- Actual mass of Mercury (II) nitrate weighed = 4.2930g
- Acidified with 0.5ml HNO3

APPENDIX D

THEORETICAL AND ANALYTICAL EXTENSION

D.1 Relative Humidity and the Degree of Saturation

The sorption and condensation/evaporation models both used the assumption that at the low temperatures encountered, the relative humidity, ϕ, and degree of saturation, μ, are equal. These values are defined as;

$$\phi = \frac{p_v}{p_{v,sat}} \quad [D.1]$$

$$\mu = \frac{W}{W_{sat}} \quad [D.2]$$

The vapour pressure, p_v, and saturation vapour pressure, $p_{v,sat}$, are both obtained from;

$$p_v = \frac{p_{atm} W}{(W + 0.622)} \quad [D.3]$$

Substituting the formulation for p_v and $p_{v,sat}$ into Eqn. D.1, we get;

$$\phi = \frac{W}{W_{sat}} . \frac{(W_{sat} + 0.622)}{(W + 0.622)}$$

Substituting Eqn. D.2 to highlight the degree of saturation term;

$$\phi = \mu . \frac{(W_{sat} + 0.622)}{(W + 0.622)} \quad [D.4]$$

Although $W \leq W_{sat}$ by definition, $t \to -\infty$, $W, W_{sat} \to 0$ as

Therefore;

$$\frac{(W_{sat} + 0.622)}{(W + 0.622)} \to 1 \quad \text{and} \quad \mu \to \phi$$

In practice, the two terms are sufficiently close for most purposes at normal ambient temperatures, and errors become insignificant below 0ºC.

D.2 Fixed Ratio Assumption for Surface Temperatures

In calculating the surface temperature of the walls, floor and windows areas, an assumption was made that the surface would remain at a fixed ratio of the internal and external temperatures. This assumption is derived from Fourier's law [Tucker 1997a: 2].

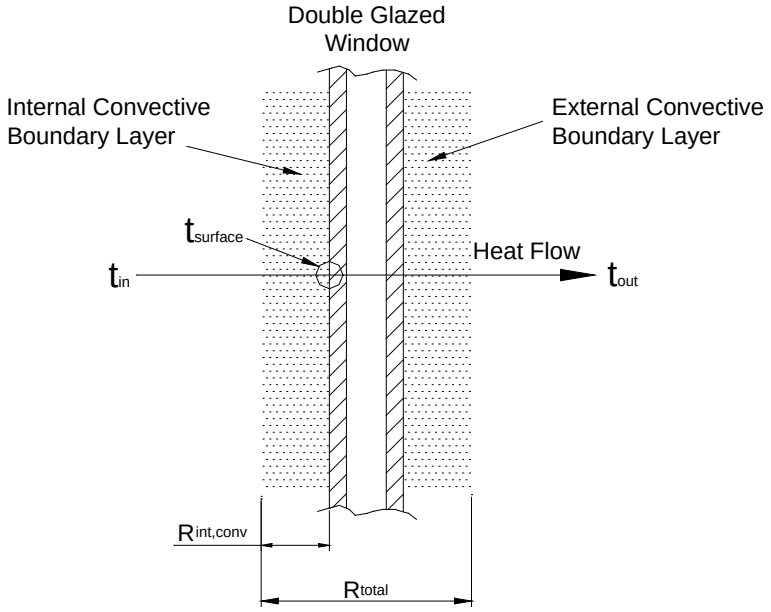

Figure D.1: Convective boundary layers and thermal resistances applied to a double-glazed window

The heat flow, q, through all layers of the window is assumed constant so that;

$$\dot{q} = \frac{A(t_{in} - t_{out})}{R_{total}} = \frac{A(t_{in} - t_s)}{R_{\text{int}.conv}} \qquad [D.5]$$

Solving Eqn. D.5 for surface temperature, we get;

$$t_s = t_{in} - \left[(t_{in} - t_{out}) \left(\frac{R_{\text{int}.conv}}{R_{total}} \right) \right] \qquad [D.6]$$

It is apparent in Eqn. D.6 that the surface temperature is a function of the ratio between the thermal resistances of the convective layer and the total window. These values are constant for a given window, floor or wall section and can be represented by a predetermined ratio to simplify the code and reduce computation time.

D.3 Wood Moisture Mass Calculation

Equation 6.9 was derived from the basic principles;

$$m_{wood,wet} = \frac{m_{wood,dry}}{(1 - U_{wood})} \qquad [D.7]$$

and;

$$m_w = m_{wood,wet} - m_{wood,dry} \qquad [D.8]$$

Combining Equations D.7 and D.8 gives us the final form;

$$m_w = \frac{m_{wood,dry}.U_{wood}}{(1 - U_{wood})} \qquad [6.9]$$

APPENDIX E

RESEARCH PROPOSAL

E.1 Post Graduate Research Proposal for Master of Engineering by Thesis

Title:

Investigation of indoor air conditions to aid preservation of Antarctic huts and their artefacts.

Supervisor:

Dr Alan S. Tucker, Dept of Mechanical Engineering, University of Canterbury

Associate Supervisor:

Assoc. Prof. W.B. Earl, Dept of Chemical and Process Engineering, University of Canterbury

Background:

The Antarctic Heritage Trust (AHT) is concerned at the deterioration of artefacts in the three historic huts on Ross Island, Antarctica, and at Cape Evans in particular. This is believed to be due, at least in part, to moisture and temperature variations. AHT has collected some data records on the relative humidity and temperatures at locations within the huts, and some data on external conditions is also available.

AHT would like a better understanding of;

- The states and dynamics of air circulation within the huts.
- The dynamics of air and moisture transmission through the fabric of the huts.
- The deposition of salts.
- The effect on relative humidity of visits by tourists, considering exhaled air and ventilation factors.
- Such other aspects or findings arising from the research which might contribute to the understanding of the historic hut environments.

Improved understanding of these factors would enable AHT to make better informed decisions regarding the preservations of the huts and their contents.

This research has been made possible by a bequest to AHT by the Estate of the late Dr Trevor Hatherton OBE, Polar Medal, BSc, PhD, DIC, DSc, FRSNZ (1924-1992)

Objective:

To develop a model for indoor air conditions that can be adapted to specific huts and can be used by AHT and its conservators to advise on preservation options. The mass transfer component of this model may be verified with the use of mass transfer finite element software developed and verified for this purpose by the National Institute of Standards and Technology (NIST) in the USA.

Methods will be developed to adapt and implement standard building envelope tests in the special cold climate conditions experienced in Antarctica. This will help determine the special requirements of the building to shelter the artefacts.

Psychrometric processes will be studied in depth to gain a better understanding of moisture transport and ice formation in cold climate conditions, helping to define the mechanisms responsible for underfloor ice accumulation and the resulting heaving of the floor.

To apply a more scientific approach to calculating the load of visitors on the environment of the hut, and determine the impact of tourism on the deterioration of the huts and the artefacts within them.

Outline of Methods:

- Review theories for indoor moisture and air circulation
- Develop a general model for moisture and air circulation using theory and existing data.
- Evaluate requirements for additional data needed to effectively validate the model

- Collect additional data as appropriate from the huts.
- Refine the model with the use of new data.
- Demonstrate how the model can be used to improve decisions related to preservation.

Tentative Timetable:

February 1998	Brief Candidate.
Feb - June 1998	Review relevant theories, identify and analyse existing data.
July - Sept 1998	Evaluation of further data needs, prepare for field data gathering exercise.
Oct - Dec 1998	Development of general model.
January 1999	Field data collection and 'in situ' assessment of huts.
Feb – March	Evaluation of data, refinement of model.
April – July 1999	Implications of finding with regard to preservation options, Thesis preparation.
August 1999	Thesis submission, Oral presentation to AHT.

Resources:

- AHT will be responsible for transport, accommodation and other support costs necessary for agreed data collection in Antarctica.
- The Dept. of Mechanical Engineering will provide principle supervision, office space, laboratory facilities, computing facilities, and technician support for the student.
- Where practicable, use will be made of existing equipment for data collection, wither through AHT of the Dept. of Mechanical Engineering.
- If AHT agrees to a need for consumable supplies or special equipment needs, then they would provide any necessary funds (up to $3000).

THE END